STUDY OF PLASMA SPRAY ALUMINA - ALUMINIDE COMPOSITE COATING ON METALS

THE THESIS SUBMITTED
IN PARTIAL FULFILMENT OF THE REQUIREMENT FOR THE DEGREE OF

Doctor of Philosophy

in

Physics

By

Satrughna Das

Department of Physics

National Institute of Technology

Rourkela, India

March' 2007

STUDY OF PLASMA SPRAY ALUMINA - ALUMINIDE COMPOSITE COATING ON METALS

The Thesis Submitted to
National Institute of Technology, Rourkela
(Deemed University)
In partial fulfilment of the requirement for the degree of
Doctor of Philosophy
in
Physics

By

Satrughna Das

Under the guidance and supervision of

Dr. Subash Chandra Mishra

Department of Metallurgical & Materials Engineering

National Institute of Technology, Rourkela

&

Dr. P.V. Ananthapadmanabhan

Laser & Plasma Technology Division

Bhabha Atomic Research Center, Mumbai

Department of Physics

National Institute of Technology
Rourkela, India

March' 2007

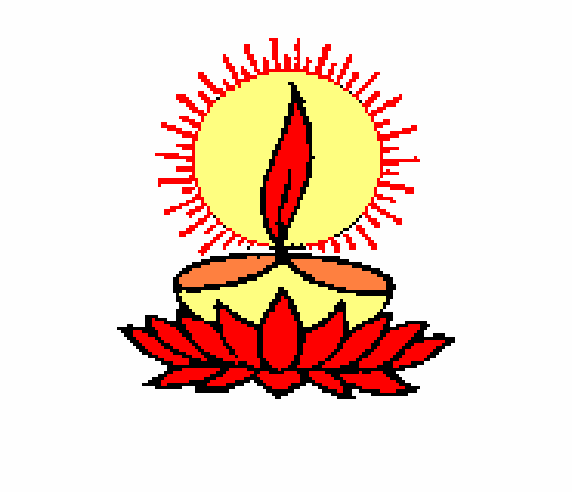

Dedicated to My Parents

Late Gangadhar Das
and
Late Kundalini Devi
(Kuna)

NATOINAL INSTITUTE OF TECHNOLOGY
ROURKELA

CERTIFICATE

This is to certify that the thesis entitled **" Study of Plasma Spray Alumina - Aluminide Composite Coating on Metals "** being submitted by **Sri Satrughna Das** to the National Institute of Technology, Rourkela (India), for the award of the degree of **Doctor of Philosophy** in Physics, is an authentic record of research work carried out by him under my supervision and guidance and the work incorporated in this thesis has not been, to the best of my knowledge, submitted to any other University or Institute for the award of a degree or diploma.

Rourkela
Date:

Dr. Subash Chandra Mishra
(Guide)

Government of India
Bhabha Atomic Research Centre
Laser & Plasma Technology Division
Mumbai-400085

Dr.P.V.Ananthapadmanabhan, SO(H)
Head, Plasma Spray Technologies Section

Tel: 91-22-25595107
Fax: 91-22-25505151
Email: pvananth@barc.gov.in

CERTIFICATE

This is to certify that the thesis entitled **" Study Of Plasma Spray Alumina - Aluminide Composite Coating On Metals "** being submitted by **Sri Satrughna Das** to the National Institute of Technology, Rourkela (India), for the award of the degree of **Doctor of Philosophy** in Physics, is an authentic record of research work carried out by him under my supervision and guidance. To the best of my knowledge, the work incorporated in this thesis has not been submitted to any other University or Institute for the award of a degree or diploma.

Mumbai

Dr.P.V.Ananthapadmanabhan
(Co-guide)

Acknowledgement

The author, Sri Satrughna Das wishes to express his deep sense of gratitude to his guide and supervisor, **Dr. Subash Chandra Mishra**, Assistant Professor, Metallurgical & Materials Engineering Department of National Institute of Technology (N.I.T.), Rourkela and **Dr. P. V. Ananthapadmanabhan**, Scientific Officer (H+) of Laser and Plasma Technology Division, Bhabha Atomic Research Center (B.A.R.C), Mumbai for their invaluable guidance, motivation, untiring efforts and meticulous attention at all stages of this research work.

He also expresses his sincere gratitude to the **Management of Gulf Oil Corporation Limited** for allowing him to undergo this course.

He appreciates the co-operation extended by the scientists at the Laser and Plasma Technology Division, B.A.R.C, Mumbai in carrying out the experimental work. He is extremely thankful to the scientific officers **Mr. K. P. Sreekumar** and **Mr. R. U. Satpute** of this division for all the technical help and advice rendered by them throughout the course of this work. He is also extremely thankful to **Dr. Alok Satapathy**, Mechanical Department of N.I.T. Rourkela, for the concerted support and timely help rendered during the course of this work.

The author is grateful to **Professor Sunil Kumar Sarangi**, Director, National Institute of Technology, Rourkela who has been a constant source of inspiration for the young generations. He is also grateful to **Professor S. Panigrahi**, Head of the Department of Physics for his help and cooperation.

He also wishes to acknowledge with gratitude the endless inspiration and sacrifice that came from his family members, friends and relatives to see the completion of this work.

N.I.T. Rourkela **(Satrughna Das)**

Bio-data in Brief

The author, Sri Satrughna Das was born on 24th April 1964 in the village Raipur in the state of Orissa (India). He obtained his B.Sc. (Honours) degree in Physics with Distinction in Chemistry & Mathematics from Utkal University, Bhubaneswar in the year 1985. In 1987, he got his Masters Degree (M.Sc.) in Physics with specialization in Plasma Physics from Ravenshaw College (presently an Autonomous college), Cuttack of Utkal University; Bhubaneswar. He did his Post Graduate Diploma in Operations Management from IGNOU, Delhi in the year 1996.

The author started his professional carrier from small scale industries (Film extrusion of polyethylene materials, Blow moulding of polyethylene materials & Kraft paper and board products used in Packaging). He has also undergone short term courses from Central Institute of Plastic Engineering & Technology, Bhubaneswar and Indian Institute of Packaging, Calcutta. In 1989, he joined in the Explosive Division, GULF OIL Corporation Limited (Formerly known as IDL Industries Limited); Hyderabad. He has been working in various responsible positions in the Quality Control Department and in the Production Department of its Rourkela Unit. At present, he is working as the Senior Assistant Manager in the Production Department of its Rourkela Unit.

The author is equally interested in research in the area of thermal plasma processing of materials since 1997. He has been associated with the Metallurgical & Materials Engineering Department of National Institute of Technology, Rourkela (Formerly known as Regional Engineering College) and with the Laser & Plasma Technology Division of Bhaba Atomic Research Centre, Mumbai. He is a life member of the Plasma Science Society of India, Ahmedabad, India

*****

C O N T E N T S

List of Figures

4.15 (a) XRD of Plasma Spherodised Fe-Al Powder at 16 KW Power

4.15 (b) XRD of Plasma Spherodised Ni-Al Powder at 16 KW Power

4.16 (a) Surface morphology (SEM micrograph) of Fe-Al powders, after ball milling

4.16 (b) Surface morphology (SEM micrograph) of Fe-Al spheroidised powders, processed at 10kW power level,100mm TBD

4.16 (c) Surface morphology (SEM micrograph) of Fe-Al spheroidised powders, processed at 10kW power level, 400mm TBD

4.16 (d) Surface morphology (SEM micrograph) of Fe-Al spheroidised powders, processed at 16kW power level, 100mm TBD

4.16 (e) Surface morphology (SEM micrograph) of Fe-Al spheroidised powders, processed at 16kW power level, 400mm TBD

4.17 (a) Surface morphology (SEM micrograph) of Ni-Al powders, after ball milling

4.17 (b) Surface morphology (SEM micrograph) of Ni-Al spheroidised powders, processed at 10kW power level, 100mm TBD

4.17 (c) Surface morphology (SEM micrograph) of Ni-Al spheroidised powders, processed at 10kW power level, 400mm TBD

4.17 (d) Surface morphology (SEM micrograph) of Ni-Al spheroidised powders, processed at 10kW power level, 100mm TBD but with higher magnification(x1, 500)

4.17 (e) Surface morphology (SEM micrograph) of Ni-Al spheroidised powders, processed at 16kW power level, 400mm TBD

4.17 (f) Surface morphology (SEM micrograph) of Ni-Al spheroidised powders, processed at 16kW power level, 400mm TBD but with higher magnification(x1, 500)

4.17 (g) Surface morphology (SEM micrograph) of Ni-Al spheroidised powders, processed at 16kW power level, 100mm TBD but with higher magnification

4.18 (a) Surface morphology (SEM micrograph) of Fe-Al bond coat, deposited at 10kW power level, 100mm TBD

*****

List of Tables

*****

Abstract

The investigation is devoted to development of nickel aluminide and iron aluminide coatings on various metal substrates viz. aluminium, mild steel, stainless steel and copper, using locally available and commercial grade aluminum, nickel and iron powders. Duplex structures involving aluminium oxide (alumina) coating over these aluminide bond coatings have also been developed and characterized. Plasma spraying was carried out using the 40kW atmospheric plasma spray system. Input DC power to the plasma torch was varied from 10 kW to 20 kW by controlling the arc current. In order to study the in-flight reaction nickel/iron and aluminium, a set of spheroidization experiments is carried out under identical conditions.

Nickel and iron aluminides are used as bond coat material, where their function is two fold: to minimize the thermo-mechanical stresses at the substrate-coating interface arising out of the thermal expansion mismatch of the metal substrates and the ceramic (alumina) top layer and secondly, to promote coating adhesion. Microstructural and mechanical properties etc. of these coatings as well as the processed powders have been studied. Deposition efficiency is evaluated as the important factor that determines the techno-economics of the process. Thickness of the coatings is measured using a vernier calipers and an optical microscope fitted with a screw gauge arrangement. Evaluation of coating interface bond strengths of bond coat and top alumina coating is measured using coating pull out method, conforming to ASTM C-633 standard. Particle size distribution of raw and processes powders have done using Laser particle size analyzer of Malvern Instruments make. Microhardness measurement is made on the polished cross section of the samples on optically distinguishable phases, using Leitz Microhardness Tester. To ascertain the phases present and phase

changes/transformation taking place during plasma spraying, X-ray diffractograms are taken on the raw materials (Fe-Al & Ni-Al powders), some selected spheroidized powders and coatings using a Philips X-Ray Diffractometer. Scanning electron microscope (JEOL T330) is used to study the surface and interface morphologies of all coatings. This analysis has also been carried out on plasma processed powder samples to ascertain spheroidisation phenomena during the in-flight traverse through plasma jet. Measurement of porosity is done using the image analysis technique. With an appropriate choice of processing conditions a sound and improve adherent ceramic coating is achievable using iron aluminide and nickel aluminide as bond coat.

The results of the present investigation i.e. the variation of coating properties are well supported by previous research evidences.

*****

Chapter 1

Introduction

- Background
- Scope of the thesis

Chapter I

INTRODUCTION

1.1 BACKGROUND

Plasma spray deposition or plasma spraying is a process that combines particle melting, quenching and consolidation in a single operation. The process involves injection of powder particles (metallic, ceramic or cermet powders) into the plasma jet created by heating an inert gas in an electric arc confined within a water-cooled nozzle. The temperature at the core of the plasma jet is 10,000-15,000 K. The particles injected into the plasma jet undergo rapid melting and at the same time are accelerated. These molten droplets moving at high velocities (exceeding 100 meters/second) impact on the surface of the substrate forming adherent coating [1,2]. The coating is incrementally built up by impact of successive particles by the process of flattening, cooling and solidification. By virtue of the high cooling rates, typically 10^5 to 10^6 K/sec., the resulting microstructures are fine-grained and homogeneous. An overview of plasma spray process including some of the important applications would be given in this article.

Plasma spraying has certain unique advantages over other competing surface engineering techniques. By virtue of the high temperature (10,000-15,000K) and high enthalpy available in the thermal plasma jet, any powder, which melts without decomposition or sublimation, can be coated keeping the substrate temperature as low as 50^0C. The coating process is fast and the thickness can go from a few tens of microns to a few mm. Plasma spraying is extensively used in hi-tech industries like aerospace, nuclear energy as well as conventional industries like textiles, chemicals, plastics and paper mainly as wear resistant coatings in crucial components.

Thermal plasma for plasma spray deposition is generated using plasma spray gun or plasma spray torch. The spray system also includes DC power supplies, cooling water system, gas feeding system, powder feeder and control console. The plasma torch consists of a cathode, made of thoriated tungsten and a nozzle shaped copper anode. Both the electrodes are water-cooled. The electrodes are separated by an insulating block made of nylon that has provision for gas injection. Powder to be spray deposited is injected through an injection port located at the nozzle exit.

A DC arc is struck between the anode and the cathode and the arc energy is extracted by the plasma gas, usually argon, which issues out of the nozzle with high temperature (10,000-15,000K) and high velocity. The material can be introduced in the form of wires or rods (Arc wire spraying and rod spraying) or powders, which is the most widely used variant of the process. Metal or ceramic powder is injected into the plasma jet, where the powder particles melt and the molten droplets are accelerated towards the substrate and get deposited. This results in a typical lamellar structure (Fig.1.1).

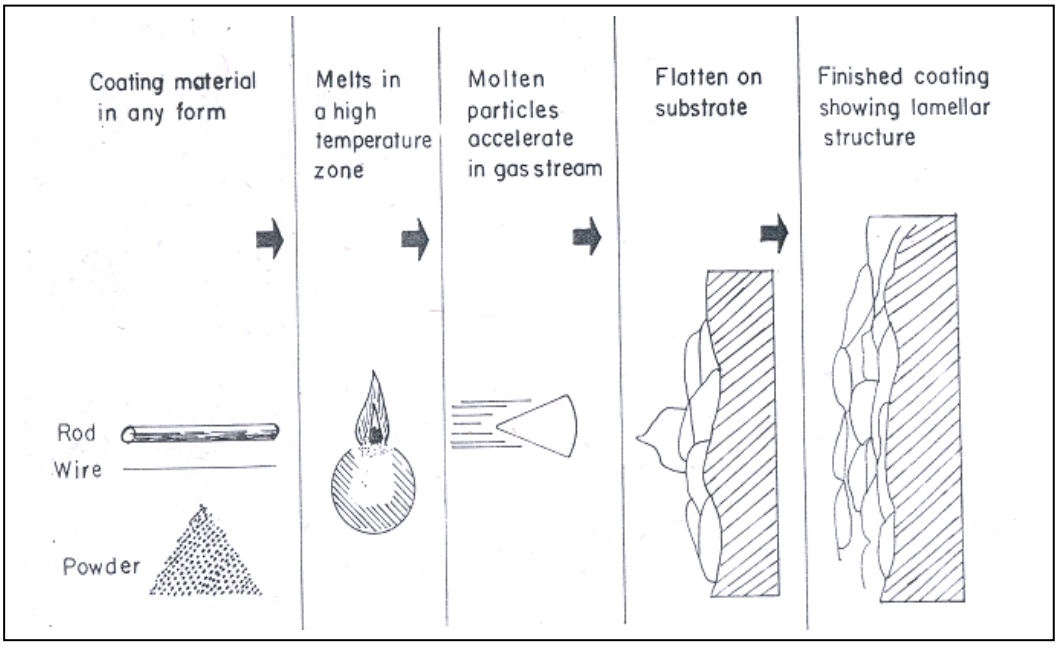

Fig. 1.1 Schematic Diagram Showing Steps for Coating Process

The coating-substrate interface bond mechanism is purely mechanical. Plasma spray deposits typically have lamellar structure with fine-grained microstructure within the lamellae. Atmospheric plasma sprayed coatings also contain varying amounts of retained porosity and inclusions depending on the deposition parameters.

There has been a steady growth in the number of applications of thermally sprayed coatings. Availability of hardware and adaptability of the technique are the most important factors for this growth. Plasma spraying has been successfully applied to a wide range of industrial technologies. Automotive industry, aerospace industry, nuclear industry, textile industry, paper industry and iron and steel industry are some of the sectors that have successfully exploited thermal plasma spray technology [2,3].

Plasma spraying has replaced the classical technologies of chrome plating, anodizing and chemical surface hardening of textile machinery parts, such as thread guiding & distribution rollers, tension rollers, thread brake caps, etc, which are in contact with synthetic fibers. For this purpose Al_2O_3 + 3% TiO_2, Al_2O_3 + 13% TiO_2, and Cr_2O_3, WC + Co are applied. Detail studies have been carried out on alumina-Titania coating deposition [4,5].The machinery parts with plasma sprayed coatings last 10 to 20 times longer than parts coated by chrome plating or other classical technique [6]. Plasma spraying reduces the idle time of the textile machinery, replacement of worn out parts is minimized, which add to the quality and quantity of textile production, including the life of the textile machinery. In the Paper and printing industry, plasma sprayed coatings of alumina, alumina-titania, or, chromia, are applied on the paper drying rolls, sieves, & filters, roll pins etc. to enhance their lifetime [7,8].

Automotive industries of many industrially advanced countries employ diverse plasma sprayed coatings to improve wear resistance, thermal resistance, resistance to cavitations and corrosion of car parts. It is common to spray

friction surface of steel piston rings with molybdenum or other alloys of type Mo+Chromium carbide + NiCr, Al_2O_3+TiO_2 [9,10]. One of these materials is selected based on the speed of the engine.

Thermal barrier coating (TBC) systems are extensively used in aerospace industry and diesel engines to enhance the life span of critical components. In the aerospace industry, austenitic super alloy blades and vanes of gas turbine engines, combustor cans and turbine shrouds require ceramic coatings to protect them from various degrading forces including hot corrosion, thermal fatigue and oxidation. Experimental and theoretical basis calculations are also studied by Padmanabhan et.al [11] on dependency of operating parameters on ceramic coating deposition. The second area of application is in diesel engines. The primary goals are to insulate components such as pistons, valves, intake and exhaust ports and to protect moving parts from wear and corrosion.

A TBC system, usually, consists of two layers - a metallic bond coat and top ceramic coat. The function of the bond coat is to protect the substrate from oxidation and provide sufficient bonding of the top ceramic coat to the substrate. The insulating ceramic layer provides a reduction of the temperature of the metallic substrate, which leads to improved component durability. Thermal barrier coating system currently employs a duplex design consisting of a bond coat and top ceramic layer. The function of the bond coat is to minimize substrate-coating interface stresses. Bond coat materials that are widely used are MCrAlY(M=Co,Ni) or Pt modified aluminide. Vacuum plasma spraying (VPS) is used for depositing the bond coat. Alternatively, electron beam physical vapor deposition (EB-PVD) can also be used, although the process is more expensive. The standard TBC top layer is YSZ containing 7-8 wt % of yttrium oxide. Since its discovery in 1957, the technology has undergone rapid growth and many innovations have been introduced in the process. In particular, with the developments in VPS and reactive plasma spraying, plasma

spray technology has become a versatile Surface Engineering tool with unique processing capabilities.Recently, TiN coatings have been developed using reactive plasma spraying technique [12].

1.2 SCOPE OF THE THESIS

The basic aim of the present work is to study the formation of Ni-Al and Fe-Al coatings and characterize them. Plasma spheroidization experiments to study the (in-flight) formation of nickel aluminide and iron aluminide have also been carried out. A top layer aluminium oxide coating over these aluminide coatings have also been developed and characterized.

The thesis has been divided into five chapters. Chapter 2 contains literature survey relevant to the work and Chapter 3 describes plasma spray equipment and process details. Spray deposition and coating characterization form the contents of Chapter 4. Conclusions and scope for future work are presented in Chapter 5.

References

1. R.B. Hieman, Plasma Spray Coating-Principles and Applications, VCH Publishers Inc., New York, USA, **1996**.
2. D. Matejka and B. Benko Plasma Spraying of Metallic and Ceramic Materials, John Wiley & Sons Ltd., Chichester, U.K, **1989**.
3. L. Pauloski, The Science and Engineering of Thermal Spray Coatings, John Wiley & Sons Ltd., Chichester, U.K, **1995.**
4. P.V. Ananthapadmanabhan, T.K. Thiyagarajan, K.P. Sreekumar, R.U. Satpute, N. Venkatramani and K. Ramachandran, Surface and Coatings Technology 168, 231, **2003**.
5. E. Pfender and Y.C. Lee, Plasma Chem. Plasma Process, 5, 211, **1985.**

6. Y.C. Lee, Y.P. Chyou and E. Pfender Plasma Chem. Plasma Process, 5, 391, **1985.**
7. A. Vardelle, P. Fauchais, B. Dussoubs and N.J. Themelis, Plasma Chem. Plasma Process, 18, 551, **1998**.
8. R. Westhoff, G. Trapaga and J. Szekely, Metal Trans. B 23, 683, **1992.**
9. C.B. Ang, H.W. Ng, S.C.M. Yu and Y.C. Lam, Plasma Chem. Plasma Process, 20, 325, **2000.**
10 A. Notomi and N. Hisatome, Pure and Appl. Chem., 68, 1101, **1996.**
11. P.V. Ananthapadmanabhan, T.K. Thiyagarajan, K.P. Sreekumar, and N. Venkatramani, Scripta Materialia, 50, 143, **2004.**
12. P.V. Ananthapadmanabhan, and P.R. Taylor, J. Alloys and Cpds, 287, 437, **1999**.

*****

Chapter 2

Literature Survey

- Preamble
- Surface Modification
- Thermal Plasma Generation
- Plasma Spraying and Process Conditions
- Industrial Applications of Plasma Spraying
- Wear and Corrosion Resistance Coatings
- Thermal Barrier Coatings
- Bio-Ceramic Coatings
- Bond Coat
- Nickel Aluminide
- Iron Aluminide
- Applications of Alumina Coating
- Plasma Spheroidization
- References

Chapter II

LITERATURE SURVEY

2.1 PREAMBLE

This chapter deals with survey of literature relevant to the work, namely the development of bond coatings for thermal barrier applications. It embraces on the industrial application of various coating techniques with special reference to plasma spraying, the coating materials and their characteristics. The spheroidal formations of plasma processed powders have also been reviewed.

2.2 SURFACE MODIFICATION: the key to obtain optimum performance

The past decade has seen a rapid development in the range of techniques which are available to modify the surfaces of engineering components. In the last two decades this in turn has led to the emergence to the new field of surface modification. It describes the interdisciplinary activities aimed at tailoring the surface properties of engineering materials. Surface Engineering is the name of the discipline and surface modification is the philosophy behind it. The object of surface engineering is to up grade their functional capabilities keeping the economic factors in mind [1,2]. It is usually necessary to apply a surface treatment or coating on a base component (substrate) in order to design a composite system, which has a performance, which cannot be achieved by either of the base component or the surface layer alone [1]. Thus, through a surface modification process, we assemble two (or more) materials by the

appropriate method and exploit the qualities of both [3, 4]. The concept can be elucidated with few examples.

Aero-engines: In the parts of modern aero engines-*turbine blades/vanes, stator blades, combustion cans/vanes* etc., the base alloys have been designed primarily for high temperature strength and these advanced materials may not provide optimal corrosion or oxidation resistance, especially to satisfy the requirements for a service life. In such cases the only option is to rely on effective surface coating to prevent or minimize the degradation processes. Oxidation and corrosion resistance coatings are typically M-Cr-Al-X alloys (VPS) (M=Ni,Co,Co-Ni and X=Y,Si,Ta etc.).This concept is also now applied to adiabatic diesel engines. A thermal barrier coating that includes ZrO_2+Y_2O_3 with a bond coating CoCrAlY is applied onto its critical components-*piston crown and cylinder head*. The engine efficiency is increased up to 50% [5].

Cutting tools: Cutting tools are subjected to a high degree of abrasion.WC-Co composite is a very popular cutting tool material, and is well known for his high hardness and wear resistance. If a thin coating of TiN (CVD) is applied on to the WC-Co insert, its capability increases considerably [6]. TiN is more capable of combating abrasion. On the other hand, TiN is extremely brittle, but the relatively tough core of WC-Co composite protects it from fracture.

Surface modification is a versatile tool for technological development provided it is applied judiciously keeping in mind the following issues.

- The coating-surface treatment should not impair the properties of the bulk material.
- The choice of technique must be capable of coating the component, in terms of both size and shape.
- The technological value addition should justify the cost.

A suitable classification system for surface modification is given in Fig.2.1. It can be seen that the advanced technologies can be subdivided into gaseous, molten or semi-molten state processes [7], which are dominated by

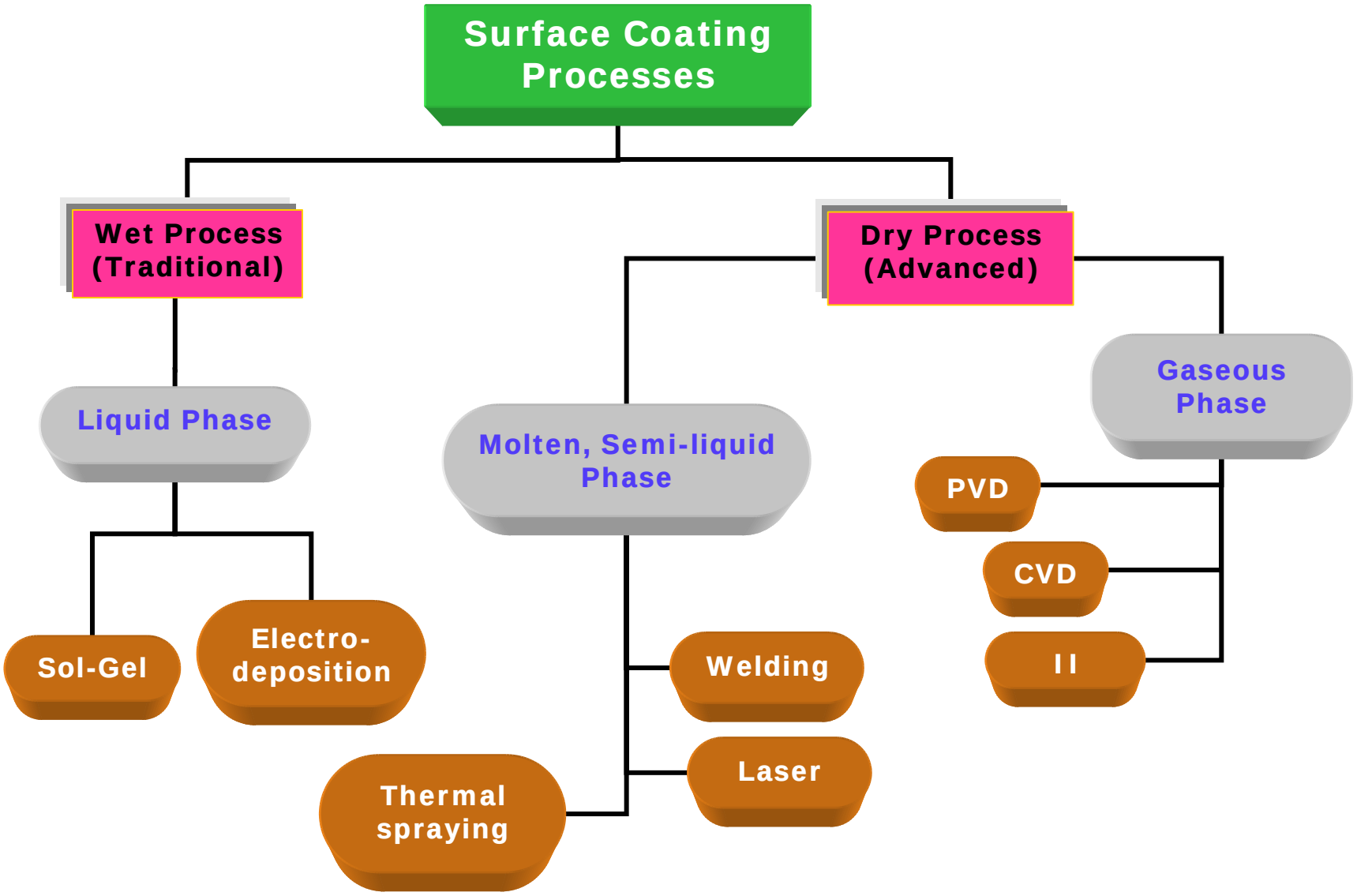

Fig.2.1 Classification of deposition technologies for surface modification.

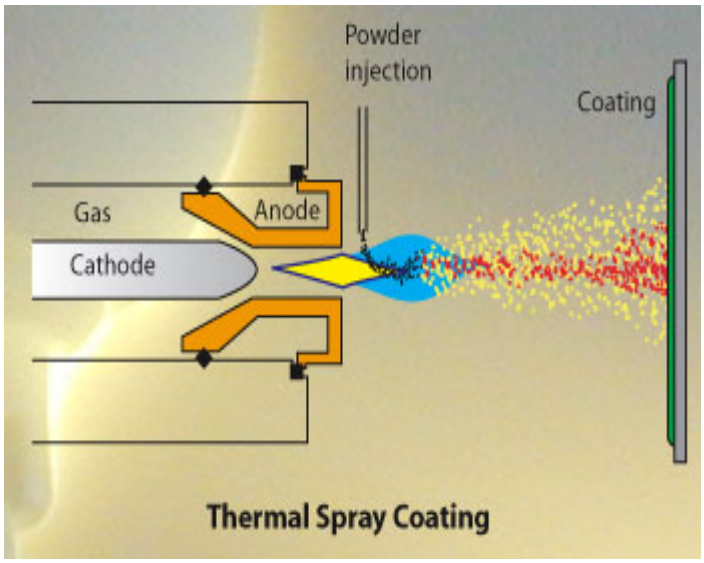

Fig.2.2 Schematic diagram of Thermal Spray Coating process

"dry" methods. These "dry" coating methods are recognized as having less environmental impact than the traditional "wet" processes such as electroplating and salt bath nitriding.Of all advanced coatings techniques, thermal spraying has gradually emerged as the one of the most industrially useful and versatile because of the wide range of coating materials and substrates that can be processed, ranging from gas turbine technology (heat engines) to the electronics industry (tape recording heads). Thermal spraying has been practiced since the early part of 20^{th} century when the first oxy-acetylene torches were modified to deposit powders and wires [8]. Processes available for thermal spraying have been developed specifically for a purpose and fall into two categories-high and low energy processes. The key processes and their energy sources are summarized in table 2.1 [9]. The processes are also named differently according to the atmosphere in which the spray operation is performed.

Processes		Energy sources	Different nomenclature
Low energy processes	Flame spraying	Chemical	Oxyfuel gas-powder spraying
			Oxyfuel gas-wire spraying
			Metallizing
	Arc spraying	Electrical	Electric arc spraying
			Twin-wire arc spraying
			Metallizing
High energy processes	**Plasma spraying**	Electrical	Air plasma spraying (APS)
			Vacuum plasma spraying (VPS)
			Low pressure plasma spraying (LPPS)
			Water stabilized plasma spraying (UWS)
			Reactive plasma spraying (RPS)
	Detonation flame spraying	Chemical	D-gun
	High velocity oxyfuel spraying	Chemical	HVOF spraying
			High velocity oxygen fuel spraying
			High velocity flame spraying (HVFS)
			High velocity air fuel

Table 2.1 Thermal-spraying processes

2.3 THERMAL PLASMA GENERATION

Classification of Plasma: Plasmas of technological interest can be classified into two categories, namely, Non-equilibrium plasmas and Thermal plasmas [10,11].

Non-equilibrium plasma or *cold plasmas*, more popularly known as *glow-discharge plasmas*, are low-pressure plasmas characterized by high electron temperatures (T_e) and low ion and neutral particle temperatures (T_i). They are widely used in lighting, surface cleaning, etching, film deposition and polymerization. *Thermal plasmas* or *hot plasmas* are characterized by the electron temperature being approximately equal to the gas temperature (T_g)

and the plasma is said to be in local thermal equilibrium. Normally, plasmas in the temperature range of 2,000 – 30,000 K and with charged particle density of 10^{19}-10^{21} m^{-3} are termed thermal plasmas. Thermal plasma processing has been successfully applied to develop advanced ceramic coatings, synthesis of nanocrystalline materials, processing of minerals and ores, and treatment of hazardous wastes. The different categories of plasmas and their applications are listed in Table 2.2.

Category of plasma	Applications
Low-pressure plasmas (10^{-4} - 10^{-2} torr) & ($T_e > T_i > T_g$)	Sputtering and surface modification processes, plasma source for ion implantation
Medium pressure plasmas (10^{-2} - 1 torr) & ($T_e > T_i = T_g$)	Etching, microelectronic processing
Sub atmospheric pressure plasmas (1- 100 torr) & ($T_e > \sim T_i = T_g$)	Plasma chemistry, plasma polymerization
Atmospheric plasmas (100+ torr) & ($T_e = T_i = T_g$)	**Plasma spraying**, plasma melting, material synthesis

Table 2.2 Plasmas of technological interest

Plasma retains many of the properties of gases, and behaves in conformance with the physical laws valid for the gases. The specific properties of plasma that distinguish it from a gas become apparent in the presence of a strong magnetic field, when the plasma acquires non-isotropic property. Thus, the fundamental difference between plasma and non-ionized gas lies in their response to electro-magnetic forces. The electrically charged particles present in a plasma are effected by externally applied magnetic and electric fields and also interact with one another .The electric field which they setup is so extensive that every particle is effected by a multitude of other particle.

Consequently, the energy bonds between the particles are much stronger in plasma than in a non-ionized gas.

The classical plasma is a fully ionized gas consisting of electrons and ions that interact with each other only through Coulomb forces [12]. This model is valid only for astrophysical or fusion plasmas; it does not hold good for industrial plasmas, which are partially ionized gases and dominated by atomic and molecular processes. Thermal plasma is a viscous, electrically and thermally conducting fluid. The unique feature of the thermal plasma jet that distinguishes it from other heat resources is its high power density. The energy density of thermal plasma devices is of the order of several GW/m^2, which is 10-100 times the power density of conventional oxy-fuel flames. Although higher power densities are obtainable with electron and laser beams, the source strengths available with these devices, especially laser devices, are not high enough for large-scale material processing applications.

DC Plasma Torch: Laboratory thermal plasmas are produced in devices known as *plasma torches* or *plasma-guns* or *plasmatrons* [13]. Plasma torches are electro-thermal devices, which convert the electrical input energy to thermal energy of the plasma. Depending on the primary source, which can be direct current (DC), alternating current (AC) at main frequency, or at radio frequency (RF), they are known as DC, AC or RF torches. There are also combinations of torches known as hybrid devices.

The most commonly used plasma device for material processing applications is the DC arc plasma torch. The DC plasma torch can be operated in a transferred or non-transferred mode, depending on whether the arc is electrically transferred to the work piece or not, as illustrated in Fig.2.3 (a) and 2.3 (b). The transferred arc mode is mainly used for cutting metal sheets, refining and remelting operations. The non-transferred arc mode is used in plasma-spraying and other material processing operations.

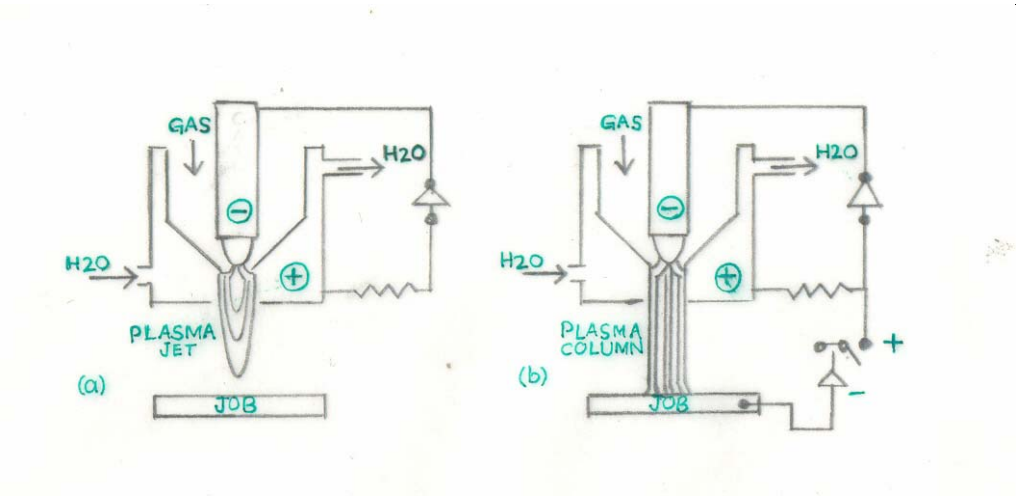

Fig.2.3 Schematic of DC Plasma Torches :(a) non-transferred arc mode type; (b) transferred arc mode type.

The design of a typical DC plasma torch is based on a rod type cathode and nozzle shaped anode (both are strongly water cooled) with tangential gas entry through the insulator module. When a gas is injected into the electrode gap and a high intensity current is passed, a DC arc is established between the electrodes. The plasma gas extracts energy from the arc and emerges out of the nozzle (due to forced flow of gas) as a high temperature, high velocity jet. The temperature at the core of the plasma jet ranges between 15,000 K and 20,000 K [14].

The typical operating parameters of a low power, laboratory DC plasma torch (non-transferred arc mode) are:

Arc voltage (40V)	Water inlet temp.(33.2 ^{o}C)
Arc current(250A)	Water out let temp.(36.3 ^{o}C)
Arc gas(Argon)	Cooling water flow rate (15 l/min)
Torch input power(10kW)	Flow rate of Argon (1.19 g /s)
Enthalpy of plasma (5.71kJ/g)	Cold gas flow velocity (13.27m/s)
Thermal energy of emerging plasma (6.8 kW)	
Power loss at the electrodes (3.2 kW)	
Plasma temperature at the nozzle exit (10,600 K, calculated)	
Plasma exit velocity (468.9 m/s, calculated)	

A thermal pinch effect is produced by the joint action of the cold wall arc channel and the cold gas sheath around a very high-temperature conducting core (the arc column).Improper gas flow may lead to blowing out of the flame or fail to create the necessary thermal pinch effect to force the arc down the nozzle.

The DC arc in a plasma torch needs to be stabilized, i.e. it should be remain stationary against fluctuation. This is often done by constricting the arc to a well-adjusted narrow high-temperature, highly conducting arc column. Various torch configurations are possible depending upon the stabilization mode: tangential vortex gas input in the arc channel, axial gas input along the cathode, segmented anode arc and magnetic stabilization [10]. The magnetic field can be self-induced (by an arc current greater than 8000 A), or externally generated. The electric arc is stabilized by using a constricted anode nozzle and by the resultant aerodynamic effects in the streaming plasma gas. Stabilizing action of the vortex gas flow provides a cold boundary layer near the anode wall so that heat loss to the wall is reduced. This results in the thermal energy being highly concentrated with improved torch stability and efficiency.

Electrodes (cathode and anode) are chosen depending upon the desired performance for a particular application. The material for electrodes may be consumable (graphite) or non-consumable (copper, tungsten or molybdenum). The obvious choice of material for the anode is copper although molybdenum and graphite are also used. The cathode can be of thermionic type such as tungsten, carbon or molybdenum, which obviously, must be used in non-oxidizing atmosphere. Under certain conditions of oxidizing atmosphere, one can use zirconium or hafnium cathodes. Non-thermionic cathodes are normally made of copper. The cathodes are usually made of tungsten enriched by 2% ThO_2.Thorium in tungsten serves predominantly for lowering the electron emission potential and hindering of cathode wear due to impurities in the plasma gas [15]. Depending upon the nature of the gas and the working parameters, the anode losses range between 8 and 10 % of the energy input in the arc. The anode losses are proportional to the current density and are a

function of the arc voltage. Heat losses at the cathode are generally quite low (less than 10% of the input power) [16].

The shape of the electrodes is another aspect depending upon the application for the plasma torch. Anodes are usually in the shape of tubes, disks, nozzles or rings. Nozzle shaped anodes are the standard design, where they serve as both an electrode and an arc constrictor (increasing the enthalpy level of the emanating plasma jet).The shape of the cathode is mainly determined by the range of operating arc current. Cathodes consisting of a rod with either a sharp pointed or conical tip; are useful for currents up to about 1,000 amperes and button type cathodes may be useful up to around 5,000 amperes.

Extending electrode life time is a very important aspect of thermal plasma research. In order to reduce electrode wear electrodes are protected by efficient cooling systems. Electrode erosion is reduced by rapid motion of the arc attachment by means of gas flow or magnetic fields. Cathode erosion can be a severe problem if reactive gases are used in the arc.

Advantages for Thermal Plasma Torches: As a heat source the major advantages are:

a. A very concentrated enthalpy and the resultant high temperature, much greater than achievable with fossil fuels,
b. A clean and adjustable reaction atmosphere (reducing, oxidizing or inert),
c. Smaller amounts of off gas to recycle or treat,
d. Capable of small portable reactor design,
e. Electricity based technology that may lead to easier control and instrumentation.

2.4 PLASMA SPRAYING AND PROCESS CONDITIONS

Plasma spraying is a material processing technique which uses the energy of an electric arc and gases to generate a plasma beam capable of melting and depositing metallic and non-metallic materials on a substrate. This technique has been used to develop protective coatings of ceramics, alloys, and composites to enhance the surface properties of critical components operating in severe environment [14,17]. In conventional plasma spraying, an arc is created between a rod/stick type thoriated tungsten cathode and an nozzle type copper anode (both water cooled). Plasma generating gas is forced to pass through the annular space between the electrodes. While passing through the arc, the gas undergoes dissociation and/or ionization in the high temperature environment resulting plasma. The ionization is achieved by collision of electrons of the arc with the neutral molecules of the gas. The plasma protrudes out of the electrode encasement in the form of a jet. The material to be coated is introduced into the plasma jet in powder form in metered quantity by means of a carrier gas. The powder particles, as they enter the plasma jet, are heated and melted and the molten droplets absorb the momentum of the expanding gas and are accelerated to a very high velocities (exceeding 100 m/s).As these molten droplets strike the substrate surface, they flatten and get anchored to the surface irregularities to form an adherent coating. The coating builds up layer by layer [2,3,17,18].

Plasma spraying has certain unique advantages over other competing surface engineering techniques. By virtue of the high temperature (10,000-15,000K) and high enthalpy available in the thermal plasma jet, any powder, which melts without decomposition or sublimation, can be coated keeping the substrate temperature as low as 50^0C. The coating process is fast and the thickness can go from a few tens of microns to a few mm. The spraying technique does not impose any restriction on the work piece dimensions and large samples can be coated.

In plasma spraying one has to deal with a lot of process parameters. An elaborate listing of these parameters and their effects are reported in the

literature [19-22]. Some important process parameters and their roles are listed below.

- ⇨ Roughness of the substrate surface
- ⇨ Cleanliness of the substrate
- ⇨ Cooling water
- ⇨ Arc power
- ⇨ Plasma gas
- ⇨ Carrier gas
- ⇨ Mass flow rate of powder
- ⇨ Standoff distance (TBD)
- ⇨ Spraying angle
- ⇨ Substrate cooling
- ⇨ Powder related variables
- ⇨ Preheating of the substrate
- ⇨ Angle of powder injection

Roughness of the substrate surface: A rough surface provides a good coating adhesion. A rough surface provides enough room for anchorage of the splats facilitating bonding through mechanical interlocking. A rough surface is generally created by shot blasting technique. The shorts are kept inside a hopper, and compressed air is supplied at the bottom of the hopper. The shorts are taken afloat by the compressed air stream into a hose and ultimately directed to an object kept in front of the exit nozzle of the hose. The shorts used for this purpose are irregular in shape, highly angular in nature, and made up of hard material like alumina, silicon carbide, etc. Upon impact they create small craters on the surface by localized plastic deformation, and finally yield a very rough and highly worked surface. The roughness obtained is determined by shot blasting parameters, i.e., shot size, shape and material, air pressure, standoff distance between nozzle and the job, angle of impact, substrate material etc.[23]. The effect of shot blasting parameters on the adhesion of

plasma sprayed alumina has been studied [24,25]. Mild steel serves as the substrate material. The adhesion increases proportionally with surface roughness and the parameters listed above are of importance. A significant time lapse between shot blasting and plasma spraying causes a marked decrease in bond strength [26].

Cleanliness of the substrates: The substrate to be sprayed on must be free from any dirt or grease or any other material that might prevent intimate contact of the splat and the substrate. For this purpose the substrate must be thoroughly cleaned (ultrasonically, if possible) with a solvent before spraying. Spraying must be conducted immediately after shot blasting and cleaning. Otherwise on the nascent surfaces, oxide layers tend to grow quickly and moisture may also affect the surface. These factors deteriorate the coating quality drastically [26].

Cooling water: For cooling purpose distilled water should be used, whenever possible. Normally a small volume of distilled water is recirculated into the gun and it is cooled by an external water supply from a large tank. Sometime water from a large external tank is pumped directly into the gun [27].

Arc power: It is the electrical power drawn by the arc. The power is injected in to the plasma gas, which in turn heats the plasma stream. Part of the power is dissipated as radiation and also by the gun cooling water. Arc power determines the mass flow rate of a given powder that can be effectively melted by the arc. Deposition efficiency improves to a certain extent with an increase in arc power, since it is associated with an enhanced particle melting [20,27,28]. However, increasing power beyond a certain limit may not cause a significant improvement. On the contrary, once a complete particle melting is achieved, a higher gas temperature may prove to be harmful. In the case of steel, at some point vaporization may take place lowering the deposition efficiency.

Plasma gas: The most commonly used gases for plasma generation are argon, nitrogen, helium, hydrogen and air. Plasma gas flow rate and the electric power to the plasma torch must be properly balanced in order to get a stable arc. The choice of plasma gas depends on many factors, such as the design features of the torch, in particular the electrode materials [29].In the case of plasma torches employing tungsten cathode, the choice of plasma gas is limited to inert gases and non-oxidizing gases. Gas enthalpy is another important factor deciding the choice of the gas [30].

The major constituent of the gas mixture is known as primary gas and the minor is known as the secondary gas. The neutral molecules are subjected to the electron bombardment resulting in their ionization. Both temperature and enthalpy of the gas increase as it absorbs energy. Since nitrogen and hydrogen are diatomic gases, they first undergo dissociation followed by ionization. Thus they need higher energy input to enter the plasma state. This extra energy increases the enthalpy of the plasma. The heat transfer coefficient is also higher, enabling efficient plasma-particle heat transfer.

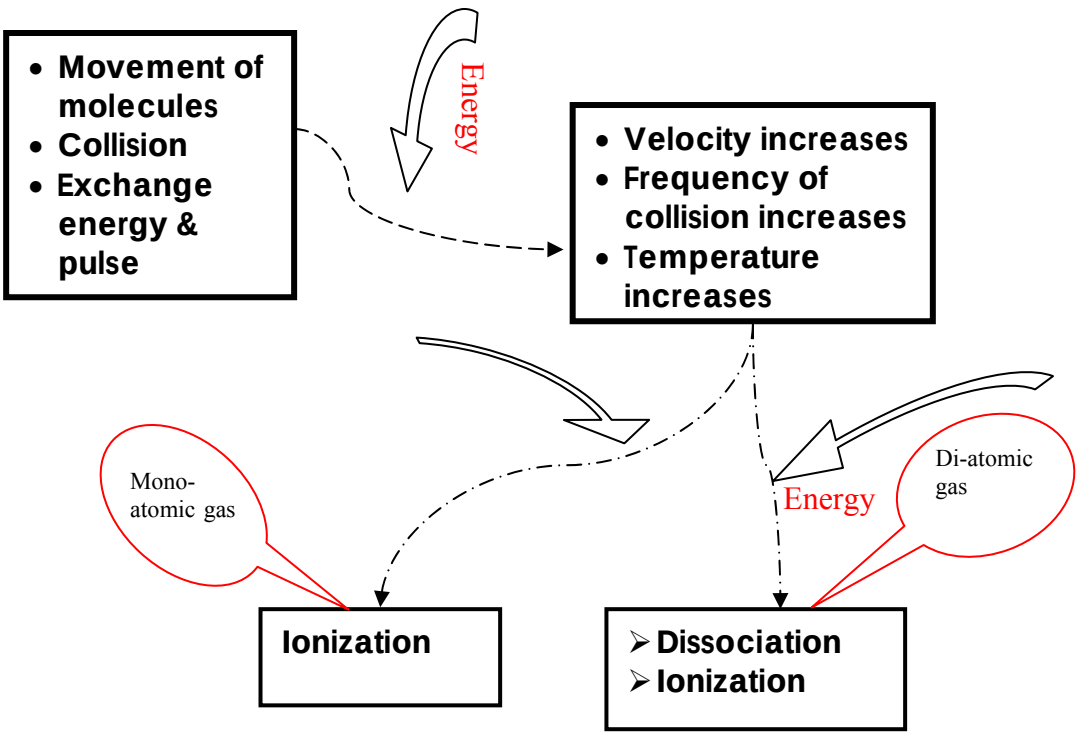

Fig.2.4 Theory of Gas Mechanics

On the other hand, the mono-atomic plasma gases, i.e. argon or helium, approach a much higher temperature in the normal enthalpy range. Good heating ability is expected from them for such high temperature [31]. In addition, hydrogen followed by helium has a very high specific heat, and therefore is capable of acquiring very high enthalpy. When argon is doped with helium the spray cone becomes quite narrow which is especially useful for spraying on small targets. The low cost and high internal energy of nitrogen makes it the most commonly used gas. If a completely inert atmosphere is required, argon is usually preferred. Reactive gases like hydrogen, oxygen, chlorine, methane and ammonia/nitrogen can be used to impart reducing, oxidizing, chloriding, carburizing, or nitriding effects, respectively, to the plasma.

Carrier gas: Particle injection into the plasma stream is not a trivial problem. In fact, it can be very difficult due to the high viscosity of the plasma. Precursor powders are usually entrained in a carrier gas for injection into the plasma. The carrier gas can be inert or reactive. Normally the primary gas itself is used as a carrier gas. The flow rate of the career gas is an important factor. A very low flow rate cannot convey the power effectively to the plasma jet, and if the flow rate is very high then the powders might escape the hottest region of the jet. There is an optimum flow rate for each powder at which the fraction of unmelted powder is minimum and hence the deposition efficiency is maximum [19].

Mass flow rate of powder: Ideal mass flow rate for each powder has to be determined. Spraying with a lower mass flow rate keeping all other conditions constant results in under utilization and slow coating buildup. On the other hand, a very high mass flow rate may give rise to an incomplete melting, resulting a high amount of porosity in the coating. The unmelted powders may bounce off from the substrate surface as well keeping the deposition efficiency low [19,32].

Torch to base distance: It is the distance between the tip of the gun and the substrate surface. A long distance may result in freezing of the melted particles before they reach the target, whereas a short standoff distance may not provide sufficient time for the particles in flight to melt [19,26]. The relationship between the coating properties and spray parameters in spraying alpha alumina has been studied in details [33]. It is found that the porosity increases and the thickness of the coating (hence deposition efficiency) decreases with an increase in standoff distance. The usual alpha-phase to gamma-phase transformation during plasma spraying of alumina has also been restricted by increasing this distance. A larger fraction of the unmelted particles go in the coating owing to an increase in torch to base distance.

Spraying angle: This parameter is varied to accommodate the shape of the substrate. In coating alumina on mild steel substrate, the coating porosity is found to increase as the spraying angle is increased from 30^0 to 60^0. Beyond 60^0 the porosity level remains unaffected by a further increase in spraying angle [34].The spraying angle also affects the adhesive strength of the coating [35,36].The influence of spraying angle on the cohesive strength of chromia, zirconia-8 wt% yttria, and molybdenum has been investigated, and it has been found that the spraying angle does not have much influence on the cohesive strength of the coatings [37].

Substrate cooling: During a continuous spraying, the substrate might get heated up and may develop thermal-stress related distortion accompanied by a coating peel-off. This is especially true in situations where thick deposits are to be applied. To harness the substrate temperature, it is kept cool by an auxiliary air supply system. In additions, the cooling air jet removes the unmelted particles from the coated surface and helps to reduce the porosity [26].

Powder related variables: These variables are powder shape, size and size distribution, processing history, phase composition etc. They constitute a set of extremely important parameters. For example, in a given situation if the

powder size is too small it might get vaporized. On the other hand a very large particle may not melt substantially and therefore will not deposit. The shape of the powder is also quite important. A spherical powder will not have the same characteristics as the angular ones, and hence both could not be sprayed' using the same set of parameters [17,38,39].

Preheating of the substrate: The nascent shot blasted surface of the substrate absorbs water and oxygen immediately after shot blasting. Before spraying, the substrate should be preheated to remove moisture from the surface and also for a sputter cleaning effect of the surface by the ions of the plasma [26].

Angle of powder injection: Powders can be injected into the plasma jet perpendicularly, coaxially, or obliquely. The residence time of the powders in the plasma jet will vary with the angle of injection for a given carrier gas flow rate. The residence time in turn will influence the degree of melting of a given powder. For example, to melt high melting point materials a long residence time and hence oblique injection may prove to be useful. The angle of injection is found to influence the cohesive and adhesive strength of the coatings as well [2,27].

2.5 INDUSTRIAL APPLICATIONS OF PLASMA SPRAYING

Plasma spraying is extensively used in hi-tech industries like aerospace, nuclear energy as well as conventional industries like textiles, chemicals, plastics and paper mainly as wear resistant coatings in crucial components. There has been a steady growth in the number of applications of thermally sprayed coatings. Availability of hardware and adaptability of the technique are the most important factors for this growth. Plasma spraying has been successfully applied to a wide range of industrial technologies. Automotive industry, aerospace industry, nuclear industry, textile industry, paper industry

and iron and steel industry are some of the sectors that have successfully exploited thermal plasma spray technology [5, 15].

Textile Industry: Plasma spraying was for the first time employed in textile industry in Czechoslovakia. Plasma spraying has replaced the classical technologies of chrome plating, anodization and chemical surface hardening. Advantages of this technique are a lot, all of which add to the quality and quantity of textile production.

- ☞ Critical machinery parts**:** Different thread guiding & distribution rollers, ridge thread brakes, distribution plates, driving & driven rollers,gallets, tension rollers, thread brake caps, lead-in bars etc.

- ☞ Coatings and advantages**:** High wear resistance coatings are required on textile machinery parts which are in contact with synthetic fibers. For this purpose especially Al_2O_3 + 3% TiO_2, Al_2O_3 + 13% TiO_2, Cr_2O_3, WC + Co are applied. These coatings with hardness ranging from 1800 to 2600 HRV are extraordinarily dense, have high wear resistance and provide excellent bonding with the substrate. Plasma spraying has following advantages in textile industries:

  - Replacement of worn out parts is minimized and hence reduces the idle times
  - Physical and mechanical properties of fibers are improved
  - Revolution speed of these lighter parts can be increased

  - Shelf life of the textile machinery parts with plasma sprayed coating last 5 to 20 times longer than parts coated by chrome plating or another classical technique

- Economic savings are realized considerably by substituting heavy steel or cast iron parts with aluminum or durable ones with wear-resistant coatings

Paper and printing industry: The machinery in the paper and printing industry is usually quite large and is subjected to considerable wear from the sliding and friction contact with the paper products.

- ☞ Critical machinery parts**:** Paper drying rolls, sieves, filters, roll pins etc.in paper machines, printing rolls, tension rolls and other parts of printing machines.
- ☞ Coatings and advantages**:** Spraying of oxide layers is an available economical solution which can be employed right in place in the production shop. Here again oxide layers composed of Al_2O_3 with 3 to 13 % additions of TiO_2, Cr_2O_3 or MnO_2 are applied. Cast iron rolls are typically first sprayed with NiCr 80/20, 50μm thick and then over it 0.2mm thick Al_2O_3 + 13% TiO_2 layer is coated. The special advantages are mentioned below:
  - Ensures corrosion resistance of rolls i.e. the base metal
  - Resistance of oxide layers against printing inks extends the life of machine parts
  - Production cost is reduced considerably
  - Coating resulted to the so-called “orange peel” phenomena, surface finishing obtainable that prevents paper foil, dyes etc.from sticking and allows their proper stretching

Automotive Industry and the production of Combustion engines: Plasma sprayed coatings used, in automotive industries of many industrially advanced countries, endure higher working pressure and temperature to improve wear resistance, good friction properties, resistance against burn-off

and corrosion due to hot combustion products and resistance against thermal loading. Some of the several applications developed for the automotive industry at the Slovak Academy of Sciences (SAV) in Bratislava are spraying torsion bars with aluminium coatings against corrosion. The plasma spraying technology is introduced in the production of gear-shift forks for gear boxes in fiat car factory and on the critical parts of big Diesel engines. The coating materials and their advantages are given below, Table 2.3.

Glass Industry: Molten glass quickly wears the surface of metal which comes in contact with it. In order to protect the metal tools, plasma sprayed coatings are made onto it. The machine parts, typical coatings used and their advantages are tabulated below, Table 2.4.

Electrochemical Industry: In the electromechanical and computer industries the electrically conductive Cu, Al, W and the semi-conductive and insulating ceramic layers are widely used. Some contacts of electrodes, e.g. the spark gaps of nuclear research equipment, are produced of massive tungsten. Such electrodes can be replaced by modern electrodes with a sprayed tungsten coating about 0.5mm thick. This electrode ensures short- time passages of 300,000A current with a life of several hundred switching. Some more applications are given below, Table 2.5.

Hydraulic machines and mechanisms: The range of possible applications in this field is very extensive, mainly in water power plants, in production and work of pumps, where many parts are subjected to combined effects of wear, corrosion, erosion and cavitations. Specific applications in this field are mentioned below, Table 2.6.

Critical machinery parts	Typical coatings applied	Advantages
Steel piston rings	Friction surface sprayed with Mo or other alloys type Mo+NiCrBSi, Mo+Chromium Carbide+NiCr, Al_2O_3+TiO_2	Engine speed increases. The variation of speed of the engine depends upon the type pf coating material to be sprayed. Shelf life of piston ring increases. Coating (especially Mo) provides good plasticity, resistance against seizing & is easily hardened by hammering at engine run. The porosity of Mo layer ensures excellent sliding property and self-lubrication.
Gear-shift forks for gear boxes	Bronze forks replaced with steel, coated with a layer of bronze 0.4mm over a bond coat NiAl.	Wear resistance increases
Synchron rings in gear boxes & on crank-shaft pins	Mo alloy coating is applied on the frictional surfaces	Improves friction wear resistance
Ship engine valves	Al_2O_3+TiO_2+Y_2O_3 on valve shanks	Improve wear resistance & thermal insulation
	NiCrAl on valve heads	Improve resistance against high temperature corrosion
	ZrO_2+Y_2O_3 on valve discs	Improve thermal insulation & resistance against high temperature corrosion
Diesel engine pistons	A thermally insulating working layer, ZrO_2+CaO, ZrO_2+MgO or ZrO_2+Y_2O_3 is deposited on an interlayer (bond coating), NiCr, NiCrAl or NiCrAlY over the faces of piston, cylinder head etc.	Protect the substrate against high temperature corrosion, sulphidization & burn-off
Piston crown & cylinder head in adiabatic diesel engine	Thermal barrier coatings, e.g. ZrO_2 + 20 wt. % Y_2O_3 of 1000μm as working layer & CoCrAlY of 500μm as interlayer is applied.	Increase engine efficiency, protect the metal parts from the degradation processes
Water pumps	Al_2O_3+TiO_2 or Cr_2O_3	Protect against wear & corrosion
Brake drum	Mixture of ceramic material	Reduce wear & thermal loading

Table 2.3 Application of Plasma Spray Coating in Automotive industry

Machine tools	Typical coatings applied	Advantages
Cast iron pressing mandrels used for production of goblets, bowls and other utility glass products	Ni-Al coating sprayed 0.15 to 0.3 mm thick	Protect the base metal from the thermal, abrasive and corrosive effects of molten glass, hence increasing the shelf life of machine tools.
	Thermally insulating and wear resistant ceramic coatings, e.g. $ZrSiO_4$, ZrO_2, Al_2O_3	Prevent sticking of molten glass
Plungers of glass melting, dip rings & pans and on the lining of platinum furnaces for glass fiber production,	Heat resistance coatings, $ZrSiO_4$, $ZrO_2+SiO_2+Y_2O_3$	Protect the parts of equipments and Reduces the loss due to diffusion of $PtRh_7$ alloy into the lining material in glass fiber production.
Glassmaking water cooled mandrels for production of packing glass	Wear resistance coatings, WC-Co, $Al_2O_3+TiO_2$, NiCrBSi alloys	Prolonged the life of parts

Table 2.4 Application of Plasma Spray Coating in Glass Industry

Rolling mills and foundry: In Rolling mills and pressing shops the wear resistant coatings are used to renovate the heavy parts of heavy duty machines whose replacement would be very costly. Several applications in this field are presented herewith:

- Rolling strand journals being repaired by giving a coating layer of stainless steel. Blooming roll mill journal renovated with a NiCrBSi layer.
- Gears of rolling mill gear box being renovated by a wear resistance coating.
- To repair a rolling mill slide and the plungers of a forging press a hard wear resistance is applied.
- Heat resistant plasma coating is widely used for foundry and metallurgical equipment where molten metal or very high temperatures

are encountered. This equipment includes the sliding plugs of steel ladles with alumina or zirconia coatings.

- Conveyer rollers in plate production with zirconia based refractory coatings,
- Oxygen tubes, cast iron moulds in continuous casting of metals, with $Al_2O_3+TiO_2$,$ZrSiO_4+ZrO_2+MgO$

Critical parts	Typical coatings	Advantages
Forming frame for the machine production of printed circuit boards made of steel	$Al_2O_3+TiO_2$	In the production process the frame is alternatively dipped into colophony and molten tin. The coating increases the life of the frame. The sprayed friction surfaces and cutting blades of the frame are wear resistant, repel the colophony and tin and improve the quality of printed circuits.
Aluminium Power Grips in the HT and SHT power distribution systems	Cu coating is made on the working surface.	Copper plasma sprayed coating increases the electric conductivity and hence reduces power loss. Due to heating by electric current and due to the effect of electrolytic phenomena at the Al-Cu joint, resistance and heat increases in the contact point which results power losses.

Table 2.5 Application of Plasma Spray Coating in Electrochemical Industry

Critical parts	Typical coatings	Advantages
Turbine blades	WC, Al_2O_3	Resistance against cavitations.
Pump parts	Seal bushings of stainless steel sprayed with $ZrSiO_4$. This working layer is sprayed on a NiAl interlayer.	Wear resistance with extraordinary corrosion resistance in pumping H_2SO_4 in chemical plants.
Piston rod of Hydraulic cylinders	Coating of Cr_2O_3 or NiCrBSi is made. Steel rods coated with bronze layer replace all bronze type pistons.	Reduces frictional wear and also contribute in saving of non-ferrous metals.
Bronze valve and bearing plates in the production of hydrostatic transducers	Steel plates with sprayed coatings of Mo or special alloys type NiCrBSi + CuSn + MoS_2, can replace bronze plates.	As an alternatives to bronze

Table 2.6 Application of Plasma Spray Coating in Hydraulic Equipments

High Temperature wears resistance coatings on Slide Gate Plates: In steel plants severe erosion of refractory teeming plates (slide gate plates) and generation of macro-micro cracks during teeming of steel is observed, rendering the plates unstable for reuse. Plasma sprayed ceramic coatings on refractory plates is made to minimize the damage and hence increase the life of slide gate plate.Al_2O_3, $MgZrO_3$, ZrO_2, TiO_2, Y_2O_3 and calcia stabilized. Zirconia can be coated.

Chemical Plants: The base metal of machine parts is subjected to different kind of wear in chemical plants. In such cases plasma sprayed coatings are applied to protect the base metal. They can be used for various blades, shafts, bearing surfaces, tubes, burners, parts of cooling equipments etc.Few specific applications are tabulated below, Table 2.7.

Critical parts	Typical coatings	Advantages
Blades of a chemical mixer	NiCrBSi	Increases wear resistance of surfaces.
Roll for the production of plastic foils	Al_2O_3	Increases wear resistance of surfaces and keep the foil from adhering to the surface.
Fan blades		Increases resistance against abrasion and aggressive vapors
Polymer Cutter Nozzle worn by rotary friction movement during the production of granulated polymer	Cutter nozzle sprayed with WC+ 12% Co deposited on the annulus	WC having the property of hard, tough and wear resistance prolongs the life of equipment.
Induction Flow meter	$ZrSiO_4$ on the internal surfaces	Provide resistance to wear, hot and corrosion of aggressive fluids like NH_4NO_3,NH_4OH and the meter functions properly forming a dielectric layer

Table 2.7 Application of Plasma Spray Coating in Chemical Industries

Aircraft Jet engines: The working parts of Aircraft jet engines are subjected to serve mechanical, chemical and thermal stresses. A jet engine has a number of construction nodes where plasma coating is employed with much success in order to protect them. There are for example, face of the blower box, compressor box and disc, guide bearing, fuel nozzles, blades, combustition chambers.

Critical parts	Typical coatings	Advantages
Different running and stationary blades of jet engines	MCrAlY, NiCrAlY, FeCrAlY, CoNiCrAlY	To protect from the adverse environment of high pressure and high temperature.
Combustition chambers and guide blades	ZrO_2+MgO,ZrO_2+Y_2O_3 as working layer and NiCr as self bonding layer	Heat resistance

2.6 WEAR AND CORROSION RESISTANCE COATINGS

The materials covered in the formation of these coatings are most frequently based on the followings [2].

- Metals and alloys (W, Mo, Ti, Ta, NiCoCrAlY etc.)
- Hard oxides (Al_2O_3, TiO_2, Cr_2O_3, ZrO_2 etc.)
- Transition metal carbides (WC, TiC, SiC, ZrC, Cr_3C_2 etc.)
- Diamond

The choice of a material depends on the application.However; the ceramic coatings are very hard and hence on an average offer more abrasion resistance than their metallic counterpart.

Metallic Coatings: Metallic coatings can be easily applied by flame spraying or welding techniques making the process very economical. Moreover plasma sprayable metallic consumables are also available in abundant quantity. Metallic wear resistant materials are classified into three categories:

(i) cobalt based alloys

(ii) nickel based alloys

(iii) iron based alloys

The common alloying elements in a cobalt based alloy are Cr, Mo, W and Si.The microstructure is constituted by dispersed carbides of M_7C_3 types in a cobalt rich FCC matrix. The carbides provide the necessary abrasion resistance and corrosion resistance. Hardness at elevated temperatures is retained by the matrix [40,41]. Sometimes a closed packed intermetallic compound is formed in the matrix, which is known as the Laves phase. Although this phase is relatively soft but offers significant wear resistance [42]. The principal alloying elements in Ni-based alloys are Si, B, C, and Cr .The abrasion resistance can be attributed to the formation of extremely hard chromium borides. Besides carbides, Laves phase is also present in the matrix [40].

Iron based alloys are classified into pearlitic steels, austenitic steels, martensitic steels, and high alloy irons. The principal alloying elements used are Mo, Ni, Cr, and C. The softer materials, e.g., ferritic, are for rebuilding purpose. The harder materials, e.g., martensitic, on the other hand provide wear resistance. Such alloys do not posses much corrosion, oxidation or creep resistance [40,43,44]. Nickel aluminide is another example of coating material for wear purpose. The prealloyed Ni-Al power, when sprayed, reacts exothermically to form nickel aluminide. This reaction improves the coating substrate adhesion. In addition to wear application, it is also used as bond coat for ceramic materials [45]. NiCoCrAIY is an example of plasma sprayable super alloy. It shows an excellent high temperature corrosion resistance and hence finds application in gas turbine blades .The compositional flexibility of such coatings permits tailoring of such coating's composition for both property improvement and coating substrate compatibility. In addition, it serves as a bond coat for zirconia based thermal barrier coatings [2, 46].

Oxide Coatings: Metallic coatings and metal containing carbide coatings sometime are not suitable in high temperature environments in both wear and corrosion applications. Often they fail owing to oxidation or decarburization. In such case the material of choice can be an oxide ceramic coating, e.g., Al_2O_3, Cr_2O_3, TiO_2, ZrO_2, or their combinations. However, a high wear resistance, and chemical and thermal stability of these materials are counterbalanced by the disadvantages of low values of thermal expansion coefficient, thermal conductivity, mechanical strength, fracture toughness, and somewhat weaker adhesion to substrate material. The thickness of these coatings is also limited by the residual stress that grows with thickness. Therefore, to obtain a good quality coating it is essential to exercise proper choice of bond coat, spray parameters, and reinforcing additives [2].

Chromia (Cr_2O_3) Coatings: These coatings are applied when corrosion resistance is required in addition to abrasion resistance. It adheres well to the

substrate and shows an exceptionally high hardness 2300 $HV_{0.5\,kg}$ [2]. Chromia coatings are also useful in ship and other diesel engines, water pumps, and printing rolls [2]. A Cr_2O_3 – 40 wt% TiO_2 coating provides a very high coefficient of friction (0.8), and hence can be used as a break liner [2]. The wear mode of chromia coatings has been investigated under various conditions. Depending on experimental conditions, the wear mode can be abrasive [47], plastic deformation [48,49,50], micro fracture [51], or a conglomerate of all of these [52].This material has also been tested under lubricated conditions, using inorganic salt solutions(NaCl, $NaNO_3$, Na_3PO_4) as lubricants and also at a high temperature. The wear rate of self mated chromia is found to increase considerably at 4508C, and plastic deformation and surface fatigue are the predominant wear mechanisms [53]. Under lubricated condition, the coatings exhibit tribochemical wear [54]. It has also been tested for erosion resistance [55].

Zirconia (ZrO_2) Coatings: Zirconia is widely used as a thermal barrier coating. However, it is endowed with the essential qualities of a wear resistant material, i.e., hardness, chemical inertness, etc., and shows reasonably good wears behaviour. In the case of a hot pressed zirconia mated with high chromium containing iron (martensitic, austenitic, or pearlitic), it has been found that in course of rubbing the iron transfers on to the ceramic surface and the austenitic material adheres well to the ceramic as compared to their martensitic or pearlitic counterparts [56].The thick transfer film improves the heat transfer from the contact area keeping the contact temperature reasonably low; thus the transformation of ZrO_2 is prevented. On the other hand with the pearlitic or martensitic iron the material transfer is limited. The contact temperature is high enough to bring about a phase transformation and related volume change in ZrO_2 causing a stress induced spilling. In a similar experiment the wear behaviour of sintered, partially stabilized zirconia (PSZ) with 8 wt% yttria against PSZ and steels has been tested at 200^0C. When metals are used as the mating surface, a transferred layer soon forms on the

ceramic surface (coated or sintered) [57]. In ceramic-ceramic system the contact wear is of abrasive and micro fracture in nature. However, similar worn particles remain entrapped between the contact surfaces and induce a polishing wear too. In the load range of 10 to 40 N, no transformation of ZrO_2 occurs [57, 58]. However, similar tests conducted at 800^0C show a phase transformation from monoclinic ZrO_2 to tetragonal ZrO_2 [59]. The wear debris of ZrO_2 sometimes get compacted in repeated loading and gets attached to the worn surface forming a protective layer [60]. During rubbing, pre-existing or newly formed cracks may grow rapidly and eventually interconnect with each other, leading to a spallation of the coating [61]. The worn particles get entrapped between the mating surfaces and abrade the coating. The wear performance of ZrO_2-12 mol% CeO_2 and ZrO_2-12 mol% CeO_2-10 mol% Al_2O_3 coatings against a bearing steel under various loads has been studied [62]. Introduction of alumina as a dopant has been found to improve the wear performance of the ceramic significantly. Here plastic deformation is the main wear mode. The wear performance zirconia at 400^0C and 600^0C has been reported in the literature [63]. At these temperatures the adhesive mode of wear plays the major role.

Titania (TiO_2) Coating: Titania coating is known for its high hardness, density, and adhesion strength [47,48].It has been used to combat abrasive, erosive, and fretting wear either in essentially pure form or in association with other compounds [64,65].The mechanism of wear of TiO_2 at 450^0C under both lubricated and dry contact conditions has been studied [48,49]. It has been found to undergo a plastic smearing under lubricated contact, where as it fails owing to the surface fatigue in dry condition.TiO_2-stainless steel couples in various speed load conditions have also been investigated in details [66]. At a relatively low load, the failure is owing to the surface fatigue and adhesive wear, whereas at a high load the failure is attributed to the abrasion and delamination associated with a back and forth movement [67]. At low speed the transferred layer of steel oxidizes to form Fe_2O_3 and the wear progresses by

the adhesion and the surface fatigue. At a high speed, Fe_3O_4 forms instead of Fe_2O_3 [68].The TiO_2 top layer also softens and melts owing to a steep rise in temperature, which helps in reducing the temperature subsequently [69].The performance of the plasma sprayed pure TiO_2 has been compared with those of Al_2O_3-40 wt% TiO_2 and pure Al_2O_3 under both dry and lubricated contact conditions [70]. TiO_2 shows the best results.TiO_2 owing to its relatively high porosity can provide good anchorage to the transferred film and al so can hold the lubricants effectively [71].

Alumina (Al_2O_3) Coatings: Alumina is obtained from a mineral called bauxite, which exists in nature as a number of hydrated phases, e.g., boehmite (γ-Al_2O_3, H $_2$O) , hydragillate (γ-Al_2O_3 , H $_2$O), diaspore (α-Al_2O_3,$3H_2O$). It also exists in several other metastable forms like, β, δ, υ, η, κ and ξ [72]. The α-Al_2O_3 is known to be a stable phase, and it is available in nature in the form of corundum. In addition, α-Al_2O_3 can be extracted from the raw materials by fusing them:

Boehmite$\longrightarrow 450^0C \rightarrow \gamma\text{-}Al_2O_3 \rightarrow 750^0C \rightarrow \delta\text{-}Al_2O_3 \rightarrow 1000^0C \rightarrow \upsilon\text{-}Al_2O_3 \rightarrow 1200^0C \rightarrow \alpha\text{-}Al_2O_3$

Bayererite$\longrightarrow 230^0C \rightarrow \eta\text{-}Al_2O_3 \rightarrow 850^0C \rightarrow \upsilon\text{-}Al_2O_3 \rightarrow 1200^0C \rightarrow \alpha\text{-}Al_2O_3$

The phase transformation during freezing of the plasma sprayed alumina droplets has been studied in details [73,74]. From the molten particles, γ-Al_2O_3 tends to nucleate, since liquid to γ transformation involves a low interfacial energy. The phase finally formed upon cooling, depends on the particle diameter. For particle diameter less than 10 μm, the metastable form is retained (γ, δ, β or υ).Plasma spraying of alumina particles having a mean diameter of 9 μm results in the development of the gamma phase in the coating after cooling [75]. The α form is found in the large diameter particles. In fact larger is the diameter; greater is the fraction of α-Al_2O_3 in the cooled solid. This form is desirable for its superior wear properties. Other than the cooling rate, one way to achieve the phase finally formed is to vary the temperature, of the substrate. If the substrate temperature is kept at 900 ^{0}C, the δ phase forms. The α-Al_2O_3

can be formed by raising the temperature of the substrate to 1100 ^{0}C resulting a slow cooling. During freezing the latent heat of solidification is absorbed in the still molten pool. If this heat generation is balanced by the heat transfer to the substrate, columnar crystals grow. On the other hand, if the aforesaid heat transfer is faster than the heat injection rate from the growing solidification front, equiaxed crystals are supposed to form. In reality columnar crystals are generally found.

There are several advantages of alumina as a structural material, e.g., availability, hardness, high melting point, resistance to wear and tear, etc. It bonds well with the metallic substrates when applied as a coating on them. Some of the applications of alumina are in bearings,valves.pump seals,plungers,engine components, rocket nozzles, shields for guided missiles, vacuum tube envelops, integrated circuits,etc.Plasma sprayed alumina coated railroad components are presently being used in Japan [76].

Properties of alumina can be further complemented by the particulate (TiO_2, TiC) or whisker (SiC) reinforcement [77].TiC reinforcement limits the grain growth, improves strength and hardness, and also retards crack propagation through the alumina matrix [78]. The sliding wear behaviour of both monolithic and SiC whisker reinforced alumina has been studied [79].The whisker reinforced composite has been found to have good wear resistance. The monolithic alumina has a brittle response to sliding wear, whereas the worn surface of the composite reveals signs of plastic deformation along with fracture. The whiskers also undergo pullout or fracture.

Cobalt clad Al_2O_3 and WC or TiC can be sintered or hot pressed to form strong composites. These cermets, when rubbed against a diamond pin, exhibit good wear properties. Presence of cobalt in the grain boundary reduces the fraction coefficient. The wear mechanism is of micro cutting, brittle fracture, or pronounced plastic deformation in nature [80]. Al_2O_3- 40 wt% ZrO_2 coating is also useful for tribological applications in dry and lubricated conditions at

room temperature [81]. Its tribological properties at 320 ^{0}C with respect to plasma sprayed Cr_2O_3, in presence of lubricants, have been studied with an objective to study its efficiency as I.C.engine cylinder liner material [82,83]. The coefficient of friction is found to be as low as 0.04. The main wear mechanisms are smearing and flaking off of the ceramic coating. TiO_2 is a commonly used additive in plasma sprayable alumina power [15,84] . TiO_2 has a relatively low melting point and it effectively binds the alumina grains. However, a success of an Al_2O_3 – TiO_2 coating depends upon a judicious selection of the arc current which can melt the powders effectively. This results in a good coating adhesion along with high wear resistance [28]. The wear performance of Al_2O_3 and Al_2O_3-50 wt% TiO_2 has been reported in the literature [70]. In dry sand abrasion testing, alumina outperformed others presumably owing to its high hardness [85]. In dry sliding at low velocity range, the tribocouple (ceramic and hardened stainless steel) exhibits stick-slip [86]. At relatively high speed range, the coefficient of friction drops owing to the thermal softening of the interface [69]. The wear of alumina is found to increase appreciably beyond a critical speed and a critical load. Alumina has been found to fail by plastic deformation, sheer, and grain pullout. In dry and lubricated sliding as well, the mixed ceramic has been found to perform better than pure alumina. A coating of Al_2O_3-50 wt% TiO_2 is quite porous and hence is quite capable of holding the transferred metallic layer which protects the surface [71]. Wear performance of such coatings can further be improved by a sealing of the pores by polymeric substances [87].A low thermal diffusivity of the alumina coatings results in a high localized thermal stress on the surface. The mode of wear of alumina is mainly abrasive. The pore size and pore size distribution also play a vital role in determining the wear properties. The Al_2O_3 -TiO_2 coating has a high thermal diffusivity and hence it is less prone to wear.

Carbide Coatings: Melting temperature of carbides is extremely high. It is characterized by a strong interaction of metal to carbon. The composite materials of carbides with a binder metal of low melting point and high

ductility is known as cemented carbides. The principal use of these materials is to produce cutting tools but plasma-sprayed coatings of cemented carbides enjoy wide applications as surface layers to protect an extraordinarily wide range of machinery and tools from wear, erosion and corrosion. Amongst carbides, WC is very popular for wear and corrosion applications [88].During spraying WC with Co the cobalt layer undergoes melting and upon solidification forms a metallic matrix in which the hard WC particles remain embedded. Spraying of WC-Co involves a close control of the process parameters such that only the cobalt phase melts without degrading the WC particles. Such degradation may occur in two ways. Oxidation of WC leading to the formation of $CoWO_4$ and WC_2 [89] is the one way .The other way is dissolution of WC in the cobalt matrix leading to the formation of brittle phases like CoW_3C which embrittles the coating [90].An increase in the spraying distance and associated increase of time in flight lead to a loss of carbon and a pickup of oxygen. As a result the hardness of the coating decreases [91].An increase in plasma gas flow rate reduces the dwell time and hence can control the oxidation to some extent. However, it increases the possibility of cobalt dissolution in the matrix [92]. The other option to improve the quality of such coating is to conduct the spraying procedure in vacuum [90].

Often carbides like TiC, TaC and NbC are provided along with WC in the cermets to improve upon the oxidation resistance, hardness, and hot strength. Similarly the binder phase is also modified by adding chromium and nickel with cobalt [2]. The wear mechanism of plasma sprayed WC-Co coatings depends on a number of factors, e.g., mechanical properties, cobalt content, experimental conditions, mating surfaces, etc. The wear mode can be abrasive, [47,93,94] adhesive or surface fatigue [48,95]. The coefficient of friction of WC-Co increases with increasing cobalt content [95]. A WC-Co coating when tested at a temperature of 4508C exhibits signs of melting [49].The wear resistance of these coatings also depends on porosity [47]. Pores can also act as source from where the cracks may grow. Thermal diffusivity of

the coatings is another important factor. In narrow contact regions, an excessive heat generation may occur owing to rubbing. If the thermal diffusivity of the coating is low the heat cannot escape from a narrow region easily resulting a rise in temperature and thus failure occurs owing to thermal stress [47,49]. The wear mechanism of WC-Co nanocomposite coating on mild steel substrates has been studied in details [96]. The wear rate of such coatings is found to be much greater than that of commercial WC-Co composite coating, presumably owing to an enhanced decomposition of nanoparticles during spraying. Wear has been found to occur by subsurface cracking along the preferred crack paths provided by the binder phase or failure at the inter-splat boundary.

Coatings of TiC or TiC+TaC with a nickel cladding are alternative solutions for wear and corrosion problems. High temperature stability, low coefficient of thermal expansion, high hardness and low specific gravity of these coatings may outperform other materials, especially in steam environment [2]. Instead of nickel, nickel-chromium alloy can serve as the matrix material [97,98]. The mode of wear can be adhesive, abrasive, surface fatigue, or micro fracture depending on operating conditions [48,98].

A coating of Cr_3C_2 (with Ni-Cr alloy cladding) is known for its excellent sliding wear resistance and superior oxidation and erosion resistance, through its hardness is lower than that of WC [2]. After spraying in air, Cr_3C_2 loses carbon and transforms to Cr_7C_3. Such transformation generally improves hardness and erosion resistance of the coating [99]. The sliding wear behavior of the Cr_3C_2-Ni-Cr composite has been studied by several authors against various metals and ceramics [47,48,100]. It is felt that at lower loads the wear is owing to the detachment of splats from the surface. Melting, plastic deformation, and shear failure come into play, as the load increases. The corrosion resistance of cemented carbide coatings is determined by both the corrosion resistance of the carbide(s) and the binder metals. The latter are generally soluble in acids so that their corrosion performance limits the

application of such coatings in operations where highly acidic solutions or gases occur. In such cases the design engineer often resorts to oxide ceramic coatings such as alumina. In addition to mixed carbides and carbide solid solutions, ternary complex carbides have been developed [101]. These hexagonal carbides T_2MC (T= group 3b-6b) elements of the periodic table; M = group 2b, 3a-6a elements) are called H-Phases. Their crystal structure has been determined for Cr_2AlC [102] and Ti_2AlC [103]. The latter was used as hard phase in a pseudo-alloy matrix together with a hard Ni-Cr-10B-Si alloy [104] to flame and plasma spray wear-resistant coatings onto steel [101]. Such tribological coatings show improved wear resistance.WC/Co coating materials are widely applied in industry as wear-resistance coatings because of their high hardness and excellent abrasion resistance. Owing to the complex interactions of the spray powder with the plasma jet, the environment and the substrate material, the coating process requires careful control of the powder characteristics and the plasma parameters [105,106].

Diamond Coatings: Thin diamond films for industrial applications are commonly produced by CVD, plasma assisted CVD, ion beam deposition, and laser ablation technique [107,108]. Such coatings are used in electronic devices and ultra wear resistant overlays. The limitation of the aforesaid methods is their slow deposition rates .The DIA-JET process involving a DC Ar/H_2 plasma with methane gas supplied at the plasma jet is capable of depending diamond films at a high rate [109]. However, the process is extremely sensitive to the process parameters. Deposition of diamond film is also possible using a oxy-acetylene torch [110]. One significant limitation of a diamond coating is that it cannot be rubbed against ferrous materials, owing to a phase transformation leading to the formation of other carbon allotropes [111]. Diamond films are tested for the sliding wear against abrasive papers, where wear progresses by micro fracturing of protruding diamond grits. The process continues till the surface becomes flat and thereafter wears progresses by an

interfacial spilling. Therefore, the life of the coating is limited by its thickness [112].

2.7 THERMAL BARRIER COATING

The loss of heat through any metal components exposed to a hot atmosphere can be reduced by providing a proper ceramic coating. These coatings are called thermal barrier coatings (TBC). Internal combustion engine components such as pistons, valves and intake & exhaust ports have been successfully coated with TBC. The quest for increasing fuel economy and decreasing levels of hydrocarbons in exhaust gases necessitates an increase in combustion temperatures. Thick TBCs and other ceramic wear coatings have been developed. The thick (0.75mm) Zirconia- based TBC (called TTBC) is applied to the recess in the combustion face, to the intake and exhaust ports, and to the piston combustion bowl. The intermediate piston rings are coated with alumina-titania wear ceramic, and the cylinder with a proprietary tribological coating. Fuel economy is improved from 16 to 37% and the engine is survived a 400h durability test with very low lubricating oil consumption.

Thick thermal barrier coatings (TTBCs) satisfy requirements of thermal efficiency but pose problems with residual stresses that are maximized in such thick coatings. Therefore, optimization of the ceramic material has been performed in two areas: Chemical modifications and microstructural modifications. As a result of chemical modifications, the life time of a TBC has been maximized by varying the yttria content in zirconia. The microstructural modifications relate to porosity control. Porosity and micro-crack distribution impart to the material a tolerance to thermal and residual stresses. Thus the lifetime of a TBC is sensitive to density variations that can be controlled by proper adjustment of the plasma spray parameters. Thermal barrier coatings fulfill a vital function by increasing turbine blade cooling efficiency and in

conjunction with MCrAlY (M=Ni,Co,Fe) bond coats; prevent hot corrosion of the super alloy by molten salts and corrosive gases.

TBC yields following advantages:

- Increase in efficiency due to high temperature operation.
- Energy saved by thermal insulation is transferred to the exhaust gas resulting in rise in exhaust gas temperature which can be used for turbo charging of IC engine.
- Improved economics due to reduction or elimination of the cooling system as well as increased life of the components.

Plasma sprayed coatings of various ceramics such as calcia (CaO) stabilized zirconia (ZrO_2) (CaSz), alumina (Al_2O_3) and other refractory materials have been developed and studied for various high temperature applications [102-106]. Although these materials have a very good thermal stability and other desirable features, there is an increasing demand on coatings with improved thermal characteristics. In system operating under a high thermal flux and large thermal gradient, apart from thermal stability, the coating should have good resistance to damage by thermal shock. Metal reinforced ceramic coatings and metal ceramic composite coatings have been developed to meet these requirements [104,113]. In these coatings the metal acts as a thermal stress relief center and helps to increase the thermal shock resistance. Ceramic coatings with enhanced thermal shock resistance have also been developed by using partially stabilized ZrO_2 (PSZ) powders [105].

Thermal barrier coatings, currently being used, can be classified as three layers, two layer and graded systems as shown in figure 2.5. The three layer system consists of a bond coat of suitable alloy over the substrate followed by a cermet coating and a top ceramic coating. In the two layer system the intermediate cermet is dispensed with. The graded system, as its name indicates has a graded metal-ceramic coating over the bond coat. In order to balance the

thermal expansion coefficients, a system of graded layers, starting with a metal backing layer up to ceramic working layer are often used . The ceramic material often used is ZrO_2 stabilized with Yttria (Y_2O_3), calcia (CaO) or MgO. Plasma sprayed composite coatings of Calcia stabilized Zirconia (CSZ) and alumina have been developed by premixing different weight % of CSZ and alumina powders [114].

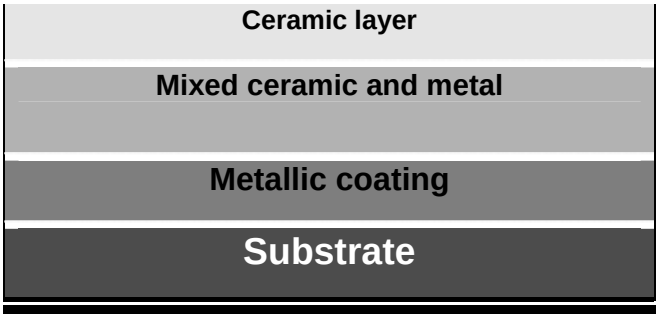

Fig.2.5 Schematic Diagram of Graded Coating System

The effect of annealing and powder composition on the properties of the coating such as phase composition, thermal shock resistance etc. has been studied [115].The coatings are found to have excellent thermal shock resistance and are potentially useful in many high temperature applications. Applications like piston faces, cylinder heads and high-speed Diesel engine liners, the interlayer (bond coat) of NiCr, NiCrAl or NiCrAlY and the working layers of ZrO_2+CaO, ZrO_2+MgO or ZrO_2+Y_2O_3 can be considered.

2.8 BIO CERAMIC COATING

Surgical implants to repair or argument parts of the skeleton (bone, teeth, joints) can be made from a number of materials among which ceramic play an important role**.** Due to their similarity with the mineral phase of bone,

bioactive ceramic like hydroxyl apatite (HA) $Ca_{10}(PO_4)_8(OH)_2$ bond to bone in a natural way. However due to their poor mechanical properties especially in tension, it is not possible to use them directly for load bearing implants. Surface modification of metallic implants (Ti-6Al-4V) by HA is most promising approach of combining strength, ductility, ease of fabrication and biocompatibility. In this aspect, thermal plasmas have gained a distinct position in biomaterials research due to their ability to produce the coatings of the desired quality required for the surgical purchase.

Plasma sprayed hydroxy apatite coatings for dental implant applications have been developed. Thermal plasmas generated in D.C plasma torch have been used for this purpose. Due to the high temperature of the plasma the stability of HA plays an important role. Hydroxy apatite coatings when prepared under ambient conditions, shows presence of β-tricalcium phosphate [β $Ca_3(PO_4)_2$] and tetra calcium phosphate by the thermal dissociation of HA, rendering it unsuitable for biomedical applications [116]. The decomposition of HA to biodegradable compounds has been eliminated by a reactive plasma spray technique [117,118].

2.9 BOND COAT

Bond coat is a thin layer of thermal sprayed bonding material that is first applied to a substrate to be subsequently coated. The objective is to achieve a higher strength, more reliable attachment of the coating to the substrate. The foremost reason for using a bond coat is the desire to improve the adhesive bond strength of a coating system. Table 2.8 indicates that when spraying onto a steel substrate, arc sprayed 95/5 nickel aluminium nearly doubles the bond strength of arc sprayed 18/8 stainless steel onto a similar substrate [119, 120]. A bond coat is also very useful when a substrate can not be properly roughened to apply the desired coating material directly. This might be due to an extremely hard substrate where blasting can not produce adequate roughness, a

thin-sectioned substrate where blasting would result in distortion, the need to apply an extremely thick coating or, cases where blasting equipments is simply not available.

Coating material	Surface preparation	Pull tensile
18/8 Stainless	Grit Blasted	47.8 MPa
18/8 Stainless	Cleaned only	0
95/5 Ni-Al	Grit Blasted	72.8 MPa
95/5 Ni-Al	Cleaned only	62.9 MPa

Table 2.8 Arc Spray Bond Strength

Materials like ceramic cannot be sprayed directly onto metals, owing to large difference between their thermal expansion coefficients(α) and temperature gradients between coating and the substrate [121]. Ceramics have a much lower value of α, and hence undergo much less shrinkage as compared to the metallic base to form a surface in compression. If the compressive stress exceeds a certain limit, the coating gets peeled off. To alleviate this problem a suitable material, usually metallic of intermediate α value, is plasma sprayed on to the substrate followed by the plasma spraying of ceramics. Bond coat may render itself useful for metallic top coats as well. Molybdenum is a classic example of bond coat for metallic top coats. Molybdenum adheres very well to the steel substrate and develops a somewhat rough top surface ideal for the top coat spraying. The choice of bond coats depends upon the application. For example, in wear application an alumina and Ni-Al top and bond coats combination can be used [122]. In thermal barrier application, CoCrAlY or Ni-Al bond coat and ziconia top coat are popular [123]. Ceramic coatings when subjected to hertzian loading deforms elastically and the metallic substrate deforms plastically. During unloading elastic recovery of the coating takes place, whereas for the metallic substrate a permanent set has already taken place. Owing to this elastoplastic mismatch the coating tends to spall off at the interface. A bond coat can reduce this mismatch as well [124]. The Ni-5wt%

Al bond coat is preferred over the high carbon iron bond coat when a superior thermal fatigue resistance property is desired.

Commercial thermal barrier coating (TBC) systems typically consist of a metallic bond coat applied to the substrate on top of which is a ceramic coating, applied either by plasma spraying (PS) or electron beam-physical vapor deposition (EB-PVD) [125-130]. The underlying bond coat must be resistant to both thermo-mechanical fatigue, oxidation and to bear the mismatch of thermal expansion of the substrate and the coated ceramic layer. Although not of sole importance, oxidation of the bond coat is a primary failure mechanism of commercial TBCs and a potential weak link for improving coating lifetimes [127-130]. It is also investigated that, the addition of Pt to a nickel aluminide was clearly beneficial to scale adhesion but it was not as effective as Hf and Zr improving scale adhesion [131]. This difference is presumably because secondary RE effects of reducing the scale growth rate and changing the α-Al_2O_3 microstructure which does not occur with the Pt additions [132,133].

Premature failure of thermal barrier coatings (TBCs), which are used to reduce the temperatures of air-cooled super alloy hardware in gas turbine engine hot-sections, is a significant concern for the gas turbine industry [136]. A typical TBC system consists of an oxidation-resistant metallic bond coat and a thermally-insulating Y_2O_3-stabilized ZrO_2 (YSZ) top coat. Although the mechanisms that drive failure of these complex coatings are not well understood, it is generally agreed that durability of state-of-the-art electron beam-physical vapor deposition (EB-PVD) TBC's is strongly influenced by the adherence of the thermally-grown alumina scale that forms at the bond coat-YSZ interface [134-136]. If the oxide scale delaminates, then the overlying ceramic top coat also detaches from the substrate and eventually spalls when a sufficiently large area debond.

In recent years, Platinum-modified aluminide diffusion coatings are being used as bond coatings for EB-PVD TBCs [136-138]. Addition of Pt significantly improves alumina scale adherence to bond coat alloys [139,140], but the mechanism underlying this beneficial effect is not understood. Although TBC's with platinum aluminide bond coatings typically exhibit excellent durability, they are also prone to premature failures. However, Pt modified bond coat are costly, so restricted to be used for general applications.

2.10 NICKEL ALUMINIDE

The Nickel aluminide, Ni_3Al, has drawn enormous attention because of its technological and scientific interest. Technologically Ni_3Al is the most important strengthening constituent, generally referred to as γ-phase of commercial Ni- base super alloys used extensively as high temperature structural materials for jet engine and aerospace applications. It is responsible for the strength and creep resistance of the super alloys at elevated temperatures. Ni_3Al containing about 25 wt % Al has the ability to form protective aluminum oxide scales, resulting in excellent oxidation resistance.

.

Industrial interest in Ni_3Al based alloys is high at the present time. This interest arises because the alloys possess a unique combination of properties including high strength and good oxidation and corrosion resistance at elevated temperatures and relatively low density compared with many Nickel-base, high temperatures super alloys. A brief summary of these applications is outlined below [141].

Properties	Applications
• Improved fatigue life and potential for low cost • Good high temperature oxidation resistance, excellent strength at high strain rates. • Resistance to carburizing and oxidizing atmospheres. • High temperature strength, good oxidation & corrosion resistance. • Excellent vibration, cavitations resistance in water • Low & high temperature strength & cutting properties. • Superior strength & creep resistance.	• Turbo Charger rotors in diesel engine trucks. • Die materials for isothermal forging. Mold material for glass processing • Fixture material for heat treatment of auto parts in high temperature furnaces. • Rollers for steel slab heating furnaces. • Hydro turbine rotors • Cutting tools. • Turbine blades vanes for jet engines.

The addition of Boron to Ni_3Al (up to 0.45 wt %) on the microstructure & the mechanical properties of Ni-Al-Mo system γ-base DS cast alloy, has been studied. The mechanical properties have been evaluated by tensile tests at room temperature and 870 ^{0}C and stress rupture tests at 1100 ^{0}C. The results show that the addition of B affects micro structure and mechanical properties significantly. The optimum B content in the alloy is 0.03-0.05 wt %.

In order to improve the performance of the turbine blades and the vanes of advanced aero engines operating in the temperature range of 1050-1150 ^{0}C, a high performance Ni-Al-Mo-B γ′-base DS casting alloy has been developed.

Boron has been found to be most effective in improving the tensile ductility of Ni_3Al tested in air at room temperature (RT). Boron-free Ni_3Al (24% Al) showed a ductility of only 8% in dry oxygen while boron doped Ni_3Al exhibited > 40%. This comparison suggests that boron enhances the intrinsic grain-boundary properties of Ni_3Al.

Ni-Al alloys offer significant payoffs as structural materials in high pressure turbine applications due to a unique range of physical and mechanical properties. These properties include:

- Low density (5.95 g /c.c.). The density of Ni-Al provides one of the major benefits of Ni-Al. The decreased density results in lower self-induced stresses in the rotating turbine air foils and the turbine disks may be down-sized to reflect the lower operating stresses imposed by the reduced mass of the blades.

- High thermal conductivity. The coefficient of thermal expansion (CTE) is important for structural applications since thermal stresses depend directly on the magnitude of the CTE. The CTE of NiAl varies from 14 x 10^{-6} C^{-1} to 15 x 10^{-6} C^{-1} in the temperature range of 800^0C to 1100^0C for stoichiometric NiAl. The high thermal conductivity also provides improved cooling efficiency.

- Excellent oxidation resistance.

- Simple ordered body centered cubic crystal structure.

- Lower ductile to brittle transition temperature relative to other intermetallics.

- High melting temperature 1638^0C.

- Several features in the binary Ni-Al phase diagram are worth mentioning. Ni-Al melts congruently at ~ 1638^0C and has a wide single phase field which extends from 45 to 60 % Nickel. This feature is different from the majority of other intermetallic compounds or has a very narrow phase field.

2.11 IRON ALUMINIDE

The Fe_3Al based intermetallic alloys offer unique benefits of excellent oxidation and sulfidation resistance at a potential cost lower than many stainless steels. Such benefits of Fe_3Al- based alloys have shown since the 1930's. However, development of these materials has been limited by, at least two major issues:

- Poor room-temperature (RT) ductility and
- Low high- temperature strength.

Recent understanding of environmental effects on RT ductility of these alloys has led to progress toward taking commercial advantage of good properties of Fe_3Al-based materials. The cause of low ductility appears to be related to hydrogen formed from the reaction of aluminum in the alloy with moisture in the air.

$$2Al + 3H_2O \rightarrow Al_2O_3 + 6H$$

The environmental effect has been reduced in these intermetallic alloys by two methods. The first deals with producing a more hydrogen-resistant microstructure through thermo-mechanical processing and the second has dealt with compositional modification.

The alloys shows reduced environmental effect have been melted and processed by many different methods. These materials have been tested for their aqueous corrosion response in various media and their resistance to stress corrosion cracking. Oxidation and sulfidation data have been generated over a range of compositions. Several commercial applications have been identified for the newly developed iron aluminides.The potential applications are noted below. [141]

Applications	Component systems
Heating elements	Toasters, stoves, Ovens, Cigarette lighters & dryers
Regenerator Disks	Automotive gas-turbine engines
Wrapping wire	Insulation wrapping for investment casting molds
Hot-gas filters	Coal gasification systems
Tooling	Dies for super plastic forming of titanium based alloys
Shields	Coal-fired power plants to protect the super heater and reheated tubes.
Molten metals	Sensor sheathing material for molten aluminum, zirconium and cadmium
Others	Components needing high temperature sulfidation and oxidation resistance.

Fe_3Al based alloys are hot workable with typical hot-working temperature ranging from 900 to 1100 ^{0}C. The Fe-16 % Al alloys can also be cold finished with intermediate anneals at 800 ^{0}C. However, the Fe_3Al based alloys are not cold workable.

Fe-Al is currently of commercial interest because of its excellent oxidation resistance, retention of good strength to intermediate temperatures and its low density. The mechanical behaviour of Fe-Al depends strongly on both temperature and Fe **:**Al ratio.

2.12 APPLICATIONS OF ALUMINA COATINGS

The powders used for thermal spraying applications have grown enormously in varieties during recent years. The list of powders now includes a vast number of metal, metal alloy and ceramic powders. In addition to the above, there is a growing demand for oxide ceramics such as TiO_2, Al_2O_3, Cr_2O_3, ZrO_2 and are mainly used on an industrial scale for thermally sprayed coatings [142], as listed in Table 2.9.

Of all the oxide ceramics, aluminium oxide (Al_2O_3 traditionally referred to as alumina) is the most established engineering ceramics. As a naturally occurring oxide component, alumina is abundant, comprising about 15 wt. % of the earth's crust. Useful properties such as chemical inertness, hardness, electrical resistivity and high temperature strength (listed in table 2.10) have

Ceramic materials	Application areas
Al_2O_3, Cr_2O_3,TiO_2,Cr_2O_3-TiO_2 Al_2O_3-TiO_2, Carbides	Wear/erosion resistant coating on textile machinery, jet engine and automobile parts, pump components etc
ZrO_2-Y_2O_3, Magnesium Zirconate	Thermal barrier coatings on gas turbine engine parts, diesel engines, aircraft parts.
Al_2O_3,Al_2O_3-TiO_2	Electrical insulation coatings on high voltage components, computer systems etc.
Al_2O_3, Hydroxy apatite	Bioceramics (coating on implants)

Table 2.9 Some application areas of few ceramics as coating material

Properties	Alumina (99.9%)
Composition	Al_2O_3(corundum)
Density,g/c.c.	3.90
Melting point,^{0}C	2015
Thermal conductivity, J/kg.K	35.60
Hardness, HV, Kgf/mm^2	1500
Flexural strength,MPa	380
Tensile strength, MPa	262
Poisson's ratio	0.26
Young's modulus, GPa	370
Co-efficient of thermal expansion,μm/m.^{0}C	7.10
Heat capacity, J/kg.K	880

Table 2.10 Physical properties of Al_2O_3 [143]

made Al_2O_3 the material of choice for diverse applications ranging from biological implants to abrasives, insulators and refractory [143].

Alumina ceramics have outstanding resistance to heat, wear and chemicals and which has lead to their multiplicity of applications and their use in almost every industry. Wear resistance, hardness and mechanical strength are exploited in ball-mill grinding pebbles in chute and pipe-liner wear tiles, in textile guides and in cutting tools. The use alumina in circulating pump bearings for central-heating system, in automobile cooling systems and in washing machines has eliminated the tedious biennial part exchange that was familiar ten years ago. Agricultural spray nozzles, gumming rollers for cigarette manufacture and rain resistance rocket radomes illustrate the variety of applications dependent on the wear resistance of alumina. Ball valves, plug gauges, shower faucet valves, hip joint prosthetic devices, tooth and ear implants, wire drawing pulleys, armor plating and coin-polishing assemblies provide additional examples [144,145].

Al_2O_3 coatings are being sprayed onto the front plate inside the hard-disk drive of a computer to provide both electric insulation and wear resistance surface [146]. They are also used as radio-frequency-transmitting valve envelopes, wave guide windows, diode and transistor housings, resistor and potentiometer substrates and even wrist watch fascias. Nuclear applications range from spacer pellets within the fuel-elements cans to constructional engineering components for chambers for particle accelerators. An important optical application is an envelope material with a transmittance of 94% for sodium vapor discharge lamps for street lighting. Established applications since 1960’s include welding nozzles, mechanical-pump sets, thermocouple tubes, laboratory ware, element supports, sealed lead-through terminals and fuse core bodies.

2.13 PLASMA SPHEROIDIZATION

Powders of metals, alloys and ceramics can be melted in a plasma jet. Melting of particles results in the formation of a spherical drop under the action of the surface tension forces and this shape is usually retained after solidification, thus providing the name to the process. This treatment may be used simply to give a spherical particle shape for particular application, such as Fe_3O_4 for photocopying, plasma spray quality powders for thermal spray applications and UO_2 for dispensed nuclear fuels. Spheroidization is particularly useful to prepare spray quality powders of special materials for thermal spray applications [147].

Spheroidization of a powder blend of Ni-15%Al has been carried out in a thermal plasma reactor [148]. The as-collected powder showed poor crystallinity as indicated by broad X-ray diffraction pattern [149]. Annealing at 800K in an atmosphere of flowing argon resulted in the formation of well-crystalline Ni_3Al. Besides possessing spherical morphology, the powder has excellent flow characteristics, making it ideally suited for thermal spray application.

Spheroidized particles may also be prepared by atomization of rods or wires fed into a plasma. The diameter of the particles produced depends on the diameter of the torch nozzle, the gas flow rate, plasma density and temperature and surface tension of the material in the liquid state [150]. Alumina particles of 40 μm diameter have been produced by feeding alumina rod in hydrogen plasma. The heat transfer can be improved if the arc is transferred to the wire but this is not possible with non-conducting materials. An example of large scale industrial application is the spheroidization of magnetite for photocopying applications, where magnetite particles, 125 μm diameter, are produced in 600 kW AC air plasma heater with a power consumption of 2 kWh/kg [151].

Powder plasma treatment rounds up the particulates and refined them from contaminations. For example, by spheroidization of the aluminium oxide powder the content of other oxides (Na, Fe, and Mg) is diminished. The refining effect of plasma powder processing, simultaneously spheroidizing particulates, helps to create new porous materials for various purposes (filters, cathodes, electrodes) to operate at very high temperatures. Spherical particulates of aluminium oxide are used to produce new types of cathodes, powerful vacuum tubes. Spherical refractory powders, obtained in plasma provided a means for developing new refractory products.

When manufacturing powder materials in plasma jets, the dispersity and shape of powder particles, their purity and surface physico-chemical properties are controlled by the jet parameters (power, temperature, flow rate, gas partial pressure) and the tempering intensity. As the reactions proceed within the plasma jet and its wake, the processed materials have no contact with the reactor walls, so the reaction products are not contaminated by the lining material.Therefore,a jet of plasma makes it possible to obtain high purity powders (ultra dispersed, spheroidized, composite etc.) based on metals, alloys, oxides, nitrides, carbides, hydrides and complex compounds.

Spherical particulates of pre-determined size are produced by plasma heating: from wire or rod melted by plasma arc or by supplying powders to the plasma jet. The process has been realized in both versions on installations rated up to 100kW [152,153].

Particles of tungsten, molybdenum, nickel and other metals and high temperature oxides from 0.1mm up to 3mm with an output up to 15kg/hr are produced by wire or rod melting. By powder surface melting particulates are obtained of high temperature metals and their alloys, titanium and chromium carbides,tungsten,aluminium and zirconium oxides measuring from 1μm up to 1mm with an output of the spherical fraction of over 90%.This process is realized in electric arc plasmatrons with a sectioned anode and in argon plasma jets with admixtures of hydrogen or hydrocarbon gases (when spheroidizing

carbides).The decarburization of carbides is slowed down by adding hydrocarbons to the plasma forming or transporting gas and by adding some soot to the starting carbide powder [154].

References

1. D.S.Rickerby and A.Matthews, Advanced Surface Coatings: A Handbook of surface engineering, Chapman and Hall, New York, pp.1-13, **1991.**
2. R.B.Hieman, Plasma Spray Coating-Principles and Applications, VCH Publishers Inc., NY, USA, **1996.**
3. K.G.Budinski, Surface Engg.For Wear Resistance,N.J.,USA,**1988**
4. K.N.Stratford, Coatings and Surface treatments for Corrosion and Wear resistance, Inst. Of Corrosion Sc.and Tech., Birmingham, UK, **1984**.
5. L. Pauloski, The Science and Engineering of Thermal Spray Coatings, John Wiley & Sons Ltd, Chichester,UK,**1989.**
6. R.Edwards, Cutting Tools, The Institute of materials, UK, **1993.**
7. K.T.Scott and R.Kingswell, Thermal Spraying in "Advanced Surface Coatings: a Hand book of surface Engg." by D.S.Rickerby and A.Matthews, (ed.) Chapman and Hall, New York, Ch.9, pp.213-243, **1991.**
8. R.W.Smith and R.Novak, Powder Metallurgy International, 23(**1991**)147.
9. S.Grainger and J.Blunt, Engg.Coatings-Design and Appli, Abington Publi., Englond, **1998.**
10. P.Fauchais, E.Bourdin, J.F.Coudert and R.McPherson, in Topics in Chemistry, Vol.107, eds. S.Veprek and M.Venugopalan (Springer-Verlag, Berlin/Heidelberg), pp59, **1983.**
11. J.Fineman, Plasma Technology in Metallurgical Industry, Iron and Steel Society, Warrendale, PA, **1987**.

12. Y.Eliezer and S. Eliezer, The Fourth State of Matter: An Introduction to the Physics of Plasma, Adam Hilger, Bristol, UK, **1989.**
13. J.V.R.Herberlein, Pure applied Chem., 64(**1992**)629.
14. D.A.Gerdeman and N.L.Hecht, Arc Plasma Techno. in Material Science, Springer-Verlag,Wien,**1972.**
15. D. Matejka and B. Benko, Plasma Spraying of Metallic and Ceramic Materials, John Wiley & Sons Ltd, Chichester,UK,**1989.**
16. P.V.Ananthapadmanabhan,N.Venkatramani,Thermal Plasma Processing in Non-equilibrium processing of materials, by C.Suryanarayana,(ed.) PERGAMON MATERIALS SERIES,V2,ch.6,pp124-125,**1999.**
17. L. Pauloski, The Science and Engineering of Thermal Spray Coatings, John Wiley, New York, **1995.**
18. R.L.Little, Welding and Welding Tech., TMH Publi., New Delhi, **1979**.
19. A.R.Nash, N.E.Weare and D.L.Walker, J.Metals, pp473, **1961.**
20. H.Gruner, Thin Solid Film, V118, pp409, 1984**.**
21. H.Eaton and R.C.Novak, Surface and Coating Tech., V27, pp257, **1986**.
22. H.Eaton and R.C.Novak, proc.Int.Conf. on Metallurgical Coatings, an Diego, USA.
23. J.Wrigren, Surf. Coat Tech.V45, pp263, **1991**.
24. V.V.Sobolev, J.M.Guilemany, J.Nutting and J.R.Miquel, Int. Mat. Rev., V42 (3), pp117, **1997**.
25. M.G.Nicholas and K.T.Scott, Surfacing Journal, V12, pp5, **1981**.
26. W.Funk and F.Goebe, Thin Solid Film, V128, pp45, **1985.**
27. Metco Plasma Spraying Manual, Metco, USA, **1993.**
28. K.Ramchandran and P.A.Selvarajan, Thin Solid Film, V315, pp149, **1998.**
29. N.Venkatramani, Bull. Material Sci. (India), 18(**1995**)741.
30. D.A.Gerdeman and N.L.Hecht, Arc Plasma Techno. in Material Science, Springer-Verlag,Wien,**1972.**
31. H.S.Ingham and A.J.Fabel, Welding Journal, pp101, **1975.**
32. R.C.Novak, J.Gas Turbines and Power, v110, pp110, **1988**.

33. S.Oki, S.Gonda and M.Yanokawa, Proc. 15th Int. Thermal Spray Conference, 25-29th may, France, pp593, **1998.**
34. A.F.Puzryakov, S.A.Levitin and V.A.Garanov, Poroshkovaya Metallurgya, V8 (272), pp55, **1985**.
35. J.Hennaut, J.Othmezouri and J.Charlier, Thin Solid Film, V192, pp97, 174, **1990.**
36. S.Sampath, R.A.Neiser, H.Herman, J.P.Kirkland and W.T.Elan, J.Mater.Res., V8 (1), pp78, **1993**.
37. J.Hennaut, J.Othmezouri and J.Charlier, Mat.Sci.and Tech., V11, pp174, **1995.**
38. B.Elvers, S.Hawkins and G.Schultz (Eds), Ulhmann's Encyclopedia of Industrial Chemistry, V1/16, VCH, pp433, **1990**.
39. E.J.Kubel, Adv.Mat.Proc., V12, pp24, **1990**.
40. Metals Handbook, ASM, Metals Park, Ohio, USA.
41. S.Atamert and J.Stekly, Microstructure, Surf.Engg. V9 (3), pp231, **1993**.
42. M.O.Price, T.A.Wolfla and R.C.Tucker, Thin Solid Films, V45, pp309, **1977.**
43. M.A.Moore, Wear, V29, pp59, **1994.**
44. P.L.Hurricks, Wear, V22, pp291, **1972.**
45. N.Y.Lee, D.P.Stinton, C.C.Brandt, F.Erdogan, Y.D.Lee and Z.Mutasion, J.Am.Cer.Soc, V79 (12), pp3003, **1996.**
46. M.G.Habsur and R.V.Miner, Mat.Sc.Engg. V83, pp239, **1986**.
47. D, Chuanxian, H.Bingtang and L.Huiling, Thin Solid Films, V118, pp485, **1984.**
48. Y.Wang, J.Yuansheng and W.Shizhu, Wear, V128, pp265, **1988.**
49. A.Tronche and P.Fauchais, Mat.Sc.Engg. V102, pp1, **1988.**
50. J.M.Cuetos, E.Fernandez, R.Vijande, A.Rucon and M.C.Perez, Wear, V169, pp173, **1993.**
51. W.Jainjun and X.Qunji, Wear, V162-164, pp229, **1993.**
52. J.F.Lin and T.R.Li, Wear, V160, pp201, **1990.**
53. H.S.Ahn and O.K.Kwon, Wear, V225-229, pp814, **1999.**

54. W.J.ainjun, X.Qunji and W.Huiling, Wear, V152, pp161, **1992.**
55. S.Lathabai, M.Ottmuller and I.Fernandez, Wear, V22, pp93, **1998.**
56. L.Zhou, Y.M.Gao, J.E.Zhou and Q.D.Zhou, Wear, V176, pp39, **1994.**
57. H.S.Ahn and O.K.Kwon, Wear, V162-164, pp636, **1993.**
58. T.F.J.Quinn and W.O.Winer,Wear,V102,pp67,**1985**
59. J.Y.Kim, D.S.Lim and H.S.Ahn, J.Kor, Cer.Soc. V30, pp1059, **1993.**
60. H.S.Ahn, J.Y.Kim and D.S.Lim, Wear, V203-204, pp77, **1997.**
61. Y.Fu, A.W.Batchelor, H.Xing and Y.Gu, Wear, V210, pp157, **1997**.
62. Y.Sun, B.Li, D.Yang, T.Wang, Y.Sasaki and K.Ishii, Wear, V215, pp232, **1998.**
63. Y.S.Song, J.C.Han, M.H.Park, B.H.Ro, K.H.Lee, E.S.Byun, S.Sasaki, Proc. 15th International Thermal Spray Conference, 25th –29th May, France, pp225, **1998.**
64. M.I.Mendelson, Wear, V50, pp71, **1978.**
65. Metco Technical Bulletin on TiO_2, Metco Inc., NY, USA, **1971.**
66. W.W.Dai, C.X.Ding, J.F.Li, Y.F.Zhang and P.Y.Zhang, Wear, V196, pp238, **1996.**
67. N.P.Suh, Wear, V25, pp111, **1973**.
68. H.So, Wear, V184, pp161, **1995.**
69. T.S.Eyre, Wear, V34, pp383, **1975.**
70. Halling, Principles of Tribology, The McMillan Press Ltd., NY, USA, **1975**.
71. Y.Guilmad, J.Denape and J.A.Patil, Trib.Int.V26, pp29, **1993**.
72. M.G.Gee, Wear, V153, pp201, **1992.**
73. R.Mcpherson, J.Mat.Sci., V8, pp859, **1973.**
74. R.Mcpherson, J.Mat.Sc. V15, pp3141, **1980**.
75. A.R.D.A.Lopez and K.T.Faber, J.Am.Cer.Soc. V82 (8), pp2204, **1999.**
76. H.Ono, T.Teramoto and T.Shinoda, Mat. Mfg. Processes, V8 (4&5), pp451, **1993.**
77. S.Musikant, What Every Engineer Should Know About Ceramics, Marcell Dekker Inc., NY, USA, **1991.**

78. R.P.Wahi and B.Iischner, J.Mat.Sc. V15, pp875, **1980**.
79. T.Yamamota, M.Olsson and S.Hogmark, Wear, V174, pp21, **1994.**
80. S.Y.Guo, J.Li, D.S.Mao, M.H.Xu and Z.Y.Mao, Wear, V203-204, pp319, **1997.**
81. T.Yamamota, M.Olsson and S.Hogmark, Wear, V174, pp21, **1994.**
82. Y.Y.Yang, Y.S.Jin and T.Yan, Wear, V210, pp136, **1997.**
83. H.Wu, Y.Jin, A.R.Nicoll and G.Barbezat, Wear, V176, pp49, **1994**.
84. D.Lamy and T.N.Sopkow,Proc.3rd National Thermal Spray Conference, Long Beach,CA,USA,20-25th May,pp491,**1990.**
85. M.A.Moore and F.A.King, Wear, V60, pp123, **1980.**
86. G.Cheo, W.D.Kulhmann and D.M.David, Wear, V173, pp1, **1994**.
87. B.Wielage, V.Hofmann, A.Steinhauser and G.Zimmerman, Wear, V14 (2), pp136, **1998**
88. M.Codenas, R.Vijande, H.J.Montes and J.M.Sierra, Wear, V212, pp244, **1997.**
89. D.Nolan, P.Mercer and M.Samadi, Surf.Engg. V11 (2), pp124, **1998.**
90. Y.Naerheim, C.Coddet and P.Droit, Surf.Engg. V11 (1), pp66, **1995**.
91. K.Hojmrle and M.Dorfman, Mod.Dev.Powder Met., V15 (15), pp609, **1985.**
92. O.Knotek, E.Lugscheder and H.Reiman, J.Vac.Sc.Tech. V12 (4), pp75, **1975.**
93. M.Roy, C.V.S.Rao, D.S.Rao and G.Sundarrajan, Surf.Engg. V15 (2), pp129.
94. J.M.Guilemay and J.M.De Paco, Surf.Engg. V11 (2), pp129, **1998.**
95. Y.Wang, Wear, V161, pp69, **1993.**
96. D.A.Stuart, P.H.Shipway and D.G.McCartney, Wear, V225-229, pp789, **1999**.
97. S.Economou, M.DeBonte, J.P.Celis, J.R.oos, R.W.Smith, E.Lugscheider and A.Valencic, Wear, V185, pp93, **1995**.
98. U.Menne, A.Molar, M.Bonner, C.Varpoort, K.Ebert and R.Bauman, Proc.Thermal Spraying, V93, pp280, **1993.**

99. M.Mohanty, R.W.Smith, M.De Bonte, J.P.Celis and E.Lugscherder, Wear, V198, pp251, **1996.**

100. J.F.Li, C.X.Ding, J.Q.Huang and P.Y.Zhang, pp177, **1997**.

101. P.V.Ananthapadmanabhan, T.K.Thiyagarajan, K.P.Sreekumar, R.U.Satpute, N.Venkatramani and K.Ramachandran, Surf. and Coating Techn. 168, 231, **2003**.

102. S. Stecura, Am.Ceram. Soc. Bull., 56(**1977**) 1082.

103. K.P Sreekumar, J. Karthikeyan, N.Venkatramani and V.K Rohatgi, Proc. Symp. Workshop on beams and plasmas: Applications in materials technology, Bombay, **1990**, P.436.

104. J. Karthikeyan, K.P Sreekumar, N. Venkatramni and V.K Rohatgi high temp., high press., 20(**1989**)653.

105. R.J Bratton and S.K Lau, in A.H Heuer and L.W Hobbs (ed), Advances in ceramics, Vol III, Science and technology of zirconia, American ceramic society, Columbus OH, **1981**, P.226.

106. J.W. Vogan, L.Hsu and A.R Stetson, Thin solid films, 84(**1981**)75.

107. K.E.Spear, J.Am.Cer.Soc. V72, pp171, **1989**.

108. M.Marakawa, Mat.Sc.Forum, V247, pp1, **1997**.

109. K.Oyoda, S.Komatsu, S.Matsumoto, Y.Moriyoshi, J.Mat.Sc. V26, pp3081, **1991**.

110. W.Zhu, B.H.Tan and H.S.Tan, Thin Solid Films, V236, pp106, **1993**.

111. P.Hollman, A.Athelisteten, T.Bjorke and S.Hogmark, Wear, V179, pp11, **1994.**

112. A.Alahelisten, Abrasion of Hot Flame Deposited Diamond Coatings, Wear, V185, pp213, **1995**.

113. D.A.Gerdeman and N.L.Hecht, Arc Plasma Technology in Material Science, Springer, Newyork, **1972.**

114. P.V.Ananthapadmanabhan, K.P.Sreekumar, K.V.Murleedharan, N.Venkatramni, Plasma Sprayed Composite Coatings for High Temperature Applications, Surface and Coating Techn. 49(**1991**)62-66.

115. P.V.Ananthapadmanabhan, et.al., Destabilization of calcia stabilized zirconia, J.Mat.Sc.pp24-44, **1989**.
116. L.L.Hench, J.Amer.Ceram.Soc. 14, 1487(**1991**).
117. D.S.Patil, K.P.Sreekumar et.al.Bull.Mat.Sci (India), 19,115, (**1996**).
118. P.K.Chu, J.Y.Chen, L.P.Wang & N.Hung, Mat.Sci. & Engg.R.36, pp143-206, **2002**.
119. Bond strength and hardness of Arc Spray Coating, TAFA Application Bulletin, 1.9.1.1.3, Feb.**1987**, TAFA, Inc., concord, N.H.
120. ASTM C633-79, Standard Test Method for Adhesion of Cohesive Strength of Flame-Sprayed Coatings, ASTM, Philadelphia, PA, **1980.**
121. Marynowski, et.al., Electrochem.Tech. 3, **1965**,109.
122. B.Wielage, V.Hofmann, A.Steinhauser and G.Zimmerman, Wear, Vol.14 (2) pp136, **1998.**
123. N.Y.Lee, D.P.Stinton, C.C.Brandt, F.Erdogon, Y.D.Lee and Z.Mutasim, J.Am.Cer.Soc. Vol.79 (12) pp3003, **1996.**
124. A.Pajares, Lwei, B.R.Lawn and C.C.Berndt, J.Am.Cer.Soc. 79(7), pp1907, **1996.**
125. A.Miller, J.Am.Cer.Soc, 67(**1984**), pp517-521.
126. A.Bennett, Mat.Sci.Techn, 2(**1986**), pp257-261.
127. T.A.Cruse, S.E.Stewart and M.Ortiz.J.Eng.Gas Turbine Power 110 (**1988**), pp. 610-616.
128. R.A.Miller, J.Eng.Gas Turbine power 111 (**1989**), pp.301-305.
129. J.T.DeMasi-Marcin, K.D.Sheffler and S.Bose, J.Eng.Gas Turbine Power 112 (**1990**), pp.522-527.
130. M.Meier, D.M.Nissley, K.D.Sheffler and T.A.Cruse.J.Eng.Gas Turbine Power 114 (**1992**), pp.258-263.
131. B.A.Pint et.al, Materials Science Engg. A, vol.245, no.2, pp201-211, **1998.**
132. B.A.Pint, A.J.Garratt-Reed and L.W.Hobbs, Mater.High Temp. 13 (**1995**), pp.3-16.
133. B.A.Pint, Oxid.Metals, 45 (**1996**), pp.1-37.

134. Rigney, R.Viguie, D.J.Wortman and D.W.Skelly.J.Thermal Spray Techno. 66 (**1997**), p.167.
135. Meier, D.K.Gupta and K.D.Sheffler.JOM 43 (**1991**), pp.50.
136. Y.Lee, Y.Zhang, I.G.Wright, B.A.Pint and P.K.Liaw.Metall.Trans.A. 29A (**1998**), p.833.
137. Gell, E.Jordan, K.Vaidyanathan, K.McCarron, B.Barber, Y.Sohn, and V.Tolpygo, Surf.Coat.Technol. 120-121, 53 (**1999**).
138. llen Haynes, Scripta Materialia, vol.44, No7,**2001**,pp1147-1152.
139. Felten and F.S.Pettit. Oxid. Met. 10 (**1976**), p. 189.
140. Zhang, W.Y.Lee, J.A.Haynes, I.G.Wright, B.A.Pint, K.M.Cooley and P.K. Liaw. Metall.Trans.A.30A (**1999**) pp.2679.
141. Structural Intermetallics, Edited by R. Daroliaetal, The minerals metals and materials society, **1993.**
142. D.Ganguli and M.Chatterjee, Ceramic Powder preparation: A Handbook, Kluwer Academic publishers, London, **1992.**
143. ASM Hand book, Vol.–18, Friction, Lubrication and wear technology, ASM International, The material information Society, **1992**, P.813.
144. L.D Hart, Alumina Chemicals science technology handbook, the American ceramic society, Inc., **1990.**
145. E. Lugscheider, H. Eschnauer, U. Miller and Th. Weber, powder metallurgy international, 23 (**1991**)33.
146. N.N.Rykalin, Plasma engineering in metallurgy and inorganic materials technology, Pure and Applied Chem.Vol.48.pp179-194(**1976**).
147. P.V.Ananthapadmanabhan,N.Venkatramani,Thermal Plasma Processing in Non-equilibrium processing of materials, by C.Suryanarayana,(ed.) PERGAMON MATERIALS SERIES,V2,ch.6,pp135-136,**1999.**
148. P.V.Ananthapadmanabhan, K.P.Sreekumar, el.at. in EPD Congress (**1997**), ed. B.Mishra (TMS, Warrandale PA), pp209.
149. P.V.Ananthapadmanabhan, K.P.Sreekumar, N.Venkatramani, (**1995**) in Thermal spray-Current status and Future Trends, V2, ed., A.Ohmori (High Temperature Soc.of Japan, Tokyo) pp1127.

150. N.N.Rykalin, Pure Appl.Chem., 48(**1976**)179.

151. M.G.Fey, C.B.Wolf and J.F.Harvey, Proceedings of the International Round Table: Transport Phenomena in Thermal Plasmas, Odeillo, France, **1975**.

152. A.B.Gugnyak, E.B.Koroleva, I.D.Kulagin, V.I.Mikhalev, V.A.Petrunichev and L.M.Sorokin, Ph.Ch.Obr.Mat.4 (**1967**).

153. N.N.Rykalin, V.A.Petrunichev, I.D.Kulagin, L.M.Sorokin, E.B.Koroleva & A.B.Gugnayak, Manual-Plasma processes in metallurgy and in process engineering of non-organic materials, pp.220, Nauka, Minsk (**1973**).

154. Yu.L.Krasulin, High temperature construction material on ceramic base.Ph.Ch.Obr.Mat.5 (**1974**).

*****

Chapter 3

Experimental Set up and Methodology

- Spray Torch System
- Electro-thermal Efficiency
- Preparation of Substrates and Coating Materials
- Plasma spraying
- Plasma Spheroidization
- Powder Characterization
- Characterization of Coatings
- References

Chapter III

EXPERIMENTAL SET UP & METHODOLOGY

This chapter deals with the details of the experimental procedures followed in this study. The coating procedure itself requires some basic preparation, i.e. sand blasting and cleaning etc. After plasma spraying, the coated materials have been subjected to various characterizations. The details of the processes are outlined here.

3.1 SPRAY TORCH SYSTEM

The complete experimental setup together with brief specifications of equipments and methodology are presented in this chapter. The plasma spray system developed at the Laser & Plasma Technology Division, Bhabha Atomic Research Centre, Mumbai, has been used for plasma spray experiments. The experimental set up is shown in Figure 3.2. The spray system consists of (1) DC plasma spray torch (2) Power supply (3) control console, (4) gas feeding system (5) water cooling arrangement and (6) powder feeder.

3.1.1 DC Plasma Torch

The plasma torch used in the experiment is a non-transferred DC arc type (Fig.3.1). Plasma torches used for plasma spray deposition operate in the non-transferred mode at high currents and gas flow rates. The arc energy is extracted by the plasma gas, which issues out of the torch nozzle with high velocity (600-800 m/s) and high temperature (typically 10,000-20,000K). Metallic or ceramic powder introduced in the plasma jet melts and the molten

droplets strike the substrate surface with high velocity forming adherent coating. The design of a dc plasma spray torch in its present form was

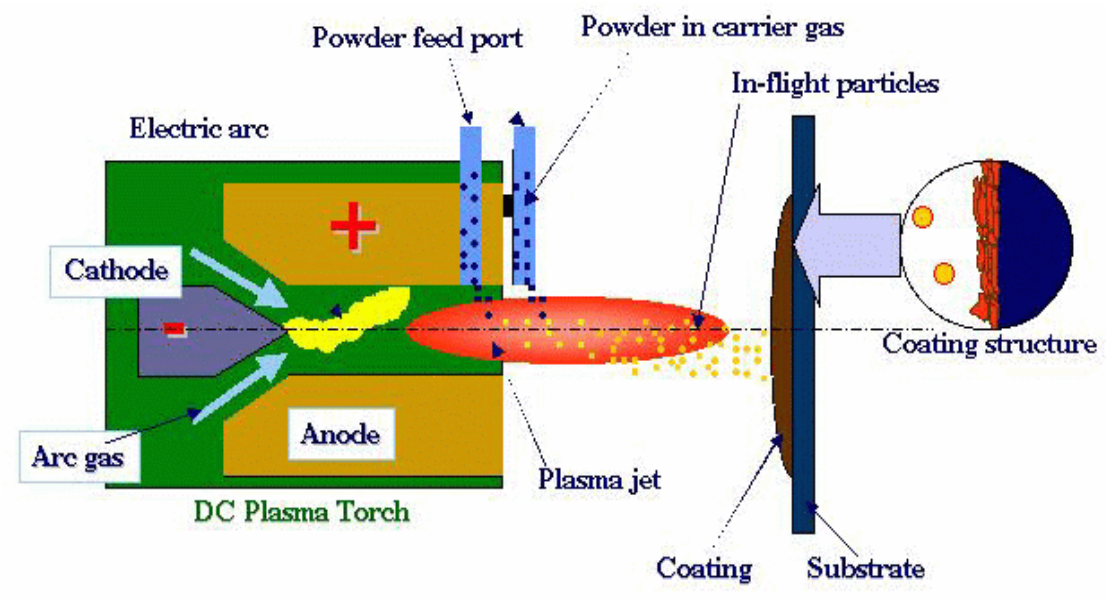

Fig. 3.1 DC Plasma Torch and Accessories

introduced in 1957 by Gage [1]. The cathode consists of a tungsten rod with a conical tip. About 2% thorium oxide is added to tungsten to improve the thermionic emission characteristics of tungsten. The nozzle is made of copper and is designed in the form of a nozzle. An insulating block of nylon separates the electrodes. The plasma gas, usually argon, is injected into the inter-electrode region through a side port in the insulator. The electrodes are intensely water-cooled. The nozzle has a port near its edge for feeding carrier gas and powders. When an electric arc is struck between the cathode and anode, the plasma gas extracts the energy from the arc and issues out of the nozzle as a high temperature, high velocity jet. A thermal pinch effect is produced by the combined action of the cold wall of the nozzle and the cold gas sheath around a very high temperature, conducting core of the arc column.

Any powder introduced into the plasma jet melts and the molten particles, traveling at high velocity (about 100 m/s) are projected onto the substrate surface, where they solidify forming an adherent coating. The dimensions are: nozzle diameter: 6 mm, gap between the cathode and anode fixed at 12 mm and cathode length: 50 mm.

3.1.2. Power supply

The torch is energized by a power supply with an open circuit voltage of 80 V. The maximum current drawn could be 800 A DC. It is cooled by forced air. The power supply has a full control HF unit consisting of a HF (1 MHz) transformer, tuned circuit, spark gap and 5 stage timer circuits for initiating pilot arc. The power supply is connected to control console through cables.

3.1.3. Control console

The control console displays the arc current, arc voltage, flow rate of primary gas and secondary gas, test/run mode switches. It has also water flow and gas flow indication lamp. Appropriate flow meters were used to monitor the plasma forming gas flow rates. It also consists of the relays and solenoid valves and other interlocking arrangements essential for safe running of the equipment. For example, the arc can only be started if the cooling water supply is on and water pressure & flow rate is adequate.

3.1.4. Gas feeding system

The gas feeding system consists of gas cylinders, pressure gauges and gas tubes. The cylinders each have $7m^3$ capacities. The pressure was maintained at 75 kg/cm^2. There is a gas feeding arrangement for primary gas, secondary gas and carrier gas. Appropriate gas flow rates can be selected depending on the operating power and nature of the material to be coated.

3.1.5. Water cooling system

Water cooling system consists of 2 HP electric mono-block pump set, reservoir, cooling tower and pipelines. Water-cooling is made for power cables,

power supply unit, cathode and anode separately. There are water flow meters and thermometers for measurement of water flow rate and inlet and outlet temperature respectively.

3.1.6. Powder feeding system

A turn-table type powder feeder, designed and developed at the L&PT Division, BARC was used for injecting the powders into the plasma jet. Powder flow rate could be varied by motor speed. The carrier gas flow rate was chosen such that the powder particles enter the plasma core. At lower flow rate, the particles may not be able to enter the core of the plasma leading to poor coating quality. On the other hand, if the carrier gas flow is very large, the powder particles will cross the central plasma zone without proper melting leading to poor quality of coating. The carrier gas flow rate needs to be optimized for each particular powder.

3.2 ELECTRO THERMAL EFFICIENCY

Electro thermal efficiency is an important parameter that decides the plasma power to be chosen while spraying different powders. It is the fraction of the input electrical power that is extracted by the plasma gas and available for plasma processing [2,3]. Electro thermal efficiency is defined as follows:

$$Efficiency(\eta) = \frac{Inputpower - Q_{loss}}{Inputpower} x100 \qquad (1)$$

The expression for calculating Q_{loss} is given below:

$$Q_{loss} = 4.18 x C_p x V (t_2 - t_1)$$

(4.18) is the conversion factor for converting cal/s into watts

Cp- is the specific heat capacity of water (1 cal.cm^2)

V –is the amount of cooling water supplied (cm^3/s)

t_1 and t_2 are the inlet and outlet water temperatures

Q_{loss} has to be the summation of losses from cathode and anode.

Q_{loss} is the power lost at the electrodes and is experimentally determined by calorimeter. The plasma torch is operated at different power and different plasma gas flow rates. The inlet and outlet temperatures of cooling water are determined by resistance thermometers. Water flow rate is measured by water flow meters and the torch efficiency is calculated by the expression (1). Typical results of torch operating parameters are presented in Table 3.1 and 3.2.

3.3 PREPARATION OF SUBSTRATES AND COATING MATERIALS

The metal plates, namely mild steel (MS), stainless steel (SS), Copper (Cu), Aluminium (Al) have been chosen as different substrate material. These substrates were roughened by blasting quartz sands of 16-20 mesh. The blasting was carried out at an air pressure of about 5 kg/cm^2. The standoff distance in the blasting was kept between 120-150mm.These substrate samples were cleaned thoroughly with acetone in an ultrasonic cleaner. The average roughness of all the substrates ranged 4.9-5.8 μm Plasma spraying was done immediately after the cleaning. Dimensions of the substrates used for coating deposition were 40x25x3 cubic millimeter and square specimen of 1"x1".The first set of substrates were used for SEM, XRD and microhardness. From mechanical point of view, adhesion can be estimated by the force corresponding to interfacial fracture and is macroscopic in nature. Coating adhesion tests have been carried out by many investigators with various coatings. It has been stated that the fracture mode is adhesive if it takes place at the coating-substrate interface and that the measured adhesion value is the value of practical adhesion, which later is strictly an interface property, depending exclusively on the surface characteristics of the adhering phase and the substrate surface condition [4, 5]. The 1"square specimens were used for adhesion test measurement.

Powders of nickel, aluminium, iron and aluminium oxide (alumina) of commercial grades were procured and have been used in the studies. Each of these powders was sieved to proper particle size range with the help of a roto-tap sieve shaker machine by using Laboratory test sieves (ISO R565).The particle size range the powders considered in the study, segregated in the sieving operation are given in the table-3.3

Type of powders	Ranges
Aluminium	-106μm to +53μm
Iron	-73 μm to +45 μm
Nickel	-74 μm to +53 μm
Alumina	-53 μm to +44 μm

Table 3.3 Particle size range used for coating

The raw powders were characterized for their chemical purity by standard wet chemical analysis. It was observed that all the materials were not less than 99% purity. The major impurity in alumina was found to be 0.002% SiO_2 and 0.02% Fe_2O_3.All the metal powders were found to contain about 0.8% of metal oxides of their respective metals.

Powders of nickel /iron and aluminum taken in suitable ratio (Ni/Fe-85% **:** Al-5%) by weight are mechanically milled by FRITSCH-Planetary ball mill for 3 hours to get a homogeneous mixture. The planetary ball mill has 4 numbers of zirconia balls (20g) and 20 numbers of zirconia balls (2g) for milling. These powder blends were used as feed stock powders for all experiments.

3.4 PLASMA SPRAYING

Plasma spraying was carried out using the 40 kW atmospheric plasma spray system described above. A mixture of argon and nitrogen was used as the

plasmagen gas. Input power to the plasma torch was varied from 10 kW to 20 kW by controlling the arc current. In the range of operating conditions used,

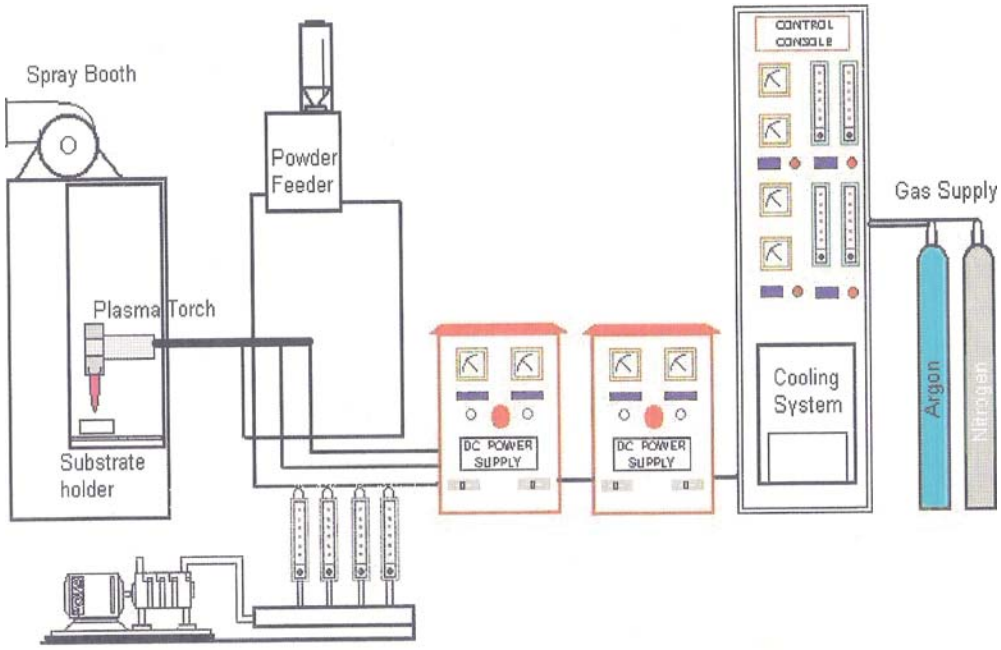

Fig 3.2 General arrangement of the plasma spraying equipment

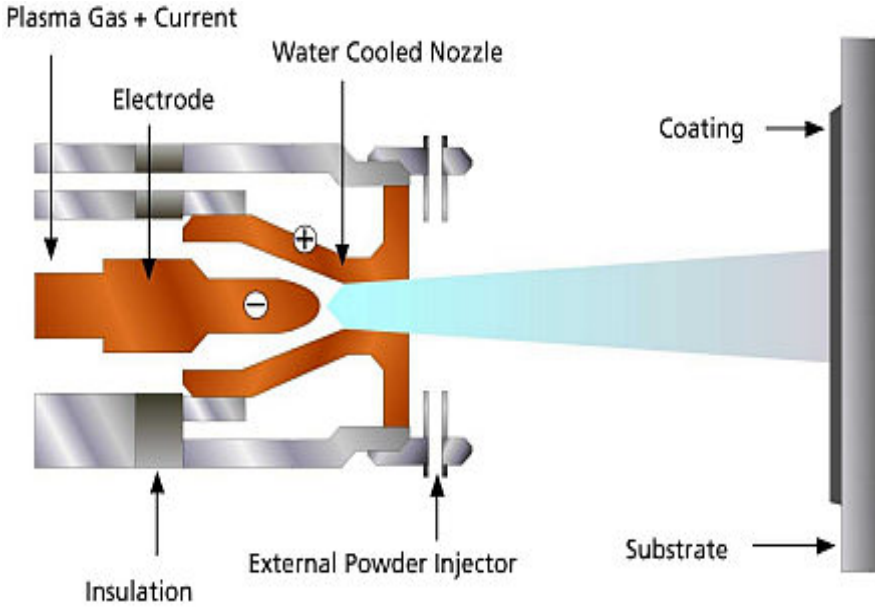

Fig 3.3 Schematic diagram of the plasma spraying operation

the torch efficiency, determined by standard calorimetric method, is found to be 60%. Metallic coupons, namely mild steel, stainless steel, copper and aluminium was used as substrates. The sample substrates were arranged inside the plasma spray booth and suitably placed in order to achieve uniform coating thickness for all the samples and to minimize the powder wastage. Prior to applying coating on the sample pieces, two trial runs were carried out to optimize the powder flow rate and other conditions to obtain desired coating thickness. Experimental parameters for the single layer deposition (Ni-Al & Fe-Al) and the top layer deposition (Al_2O_3) are given in Table 3.1 and Table 3.2 respectively.

Parameters	Range	
	Ni-Al	Fe-Al
Torch input power	10-16 kW	10-16 kW
Plasma gas (Ar) flow rate	20 LPM	20 LPM
Secondary gas(N_2) flow rate	3 LPM	3 LPM
Powder feed rate	50 g/min	50 g/min
Powder carrier gas(Ar) flow rate	12 LPM	12 LPM
Torch to base distance	100- 400 mm	100- 400 mm

Table 3.1 Operating Parameters for plasma spraying Ni-Al & Fe-Al powders

Parameters	Range
Torch input power	10-20 kW
Plasma gas (Ar) flow rate	20 LPM
Secondary gas(N_2) flow rate	3 LPM
Powder feed rate	50 g/min
Powder carrier gas(Ar) flow rate	12 LPM
Torch to base distance	100 mm

Table 3.2 Operating Parameters for plasma spraying Alumina powders

3.5 PLASMA SPHEROIDISATION

In order to study the 'in-flight' formation of iron aluminide and nickel aluminide a set of plasma spheroidization experiments were carried out under identical conditions as the spray experiments. Nickel, iron and aluminium powders were weighed in the appropriate ratio and thoroughly mixed. The mixed powder was used for spheroidization experiments. The plasma reaction chamber and collection chamber were cleaned and arranged in order. The plasma torch was seated vertically at the top of the reaction chamber in such a way that the nozzle end is housed inside the reaction chamber, the nozzle axis coinciding with the chamber axis. Cooling arrangements for reaction chamber and collection chamber were checked. The exhaust was also connected to one end of the collection chamber.

The plasma jet was generated. The powder was injected into the plasma jet by using argon as carrier gas. Powder flow rate and carrier gas flow rate were fixed at a suitable level. Particles gain thermal energy from the plasma jet through heat transfer and melt. The molten particles react to form the product, which is quenched and collected as spherical particles in the collector vessel (i.e. a flat bottomed stain less steel vessel). In order to see the effect of plasma torch power on the in-flight reaction, spheroidization experiments were carried out at different input power levels.

3.6 POWDER CHARACTERIZATION

3.6.1 Particle Size Analysis

The particle sizes of the raw materials used for bond coat (iron-aluminium powder and nickel-aluminium powder) are characterized using Laser particle size analyzer of Malvern Instruments make.

3.7 CHARACTERIZATION OF COATINGS

3.7.1 Coating Thickness Measurement

Specimens were polished along the coating interface prior to the thickness measurement. The thickness of the coatings was measured using a vernier calipers and an optical microscope fitted with a screw gauge arrangement. The data point values expressed in microns, are the average of three readings.

3.7.2 Scanning Electron Microscopic (SEM) Analysis

Plasma sprayed coated specimens and plasma processed powders were studied by scanning electron microscope (JEOL T330) mostly using the secondary electron imaging. The surface as well as the interface morphology of all coatings was seen in the microscope. SEM analysis was also carried out on plasma processed powder samples to ascertain spheroidisation phenomena during the in-flight. The coating cross-sections were polished in three stages using SiC abrasive papers of reducing grit sizes and then with diamond pastes on a wheel. For ease handling in the polishing operation as well as during analysis, 20 mm x 5 mm rectangular size samples were sliced from the original coated specimens and were mounted using thermosetting molding powders. These samples were also utilized for the micro hardness measurement.

3.7.3 Microhardness testing

Vickers microhardness was determined on all the coated samples of aluminides and alumina by using a LEITZ microhardness tester equipped with a monitor and a microprocessor based controller, under a load of 0.493N and a loading time of 20seconds.Ten readings were taken on each sample and the average value is reported as the data point.

3.7.4 X-Ray Diffraction Studies

X-ray diffraction technique was used to identify the different phases present in the coatings [6]. XRD analysis was done using Ni-filtered Cu-Kα radiation in a Philips X-ray diffractometer. The characteristic d-spacing of all possible values were taken from JCPDS cards and were compared with d-values obtained from XRD patterns to identify the various X-ray peaks obtained.

3.7.5 Porosity Measurement

The porosity of the coatings was measured using a microscope (Neomate) equipped with a CCD camera (JVC, TK 870E).This system is used to obtain a digital image of the object [7].The digitized image of the polished surface (coated samples) is transmitted to a computer fitted with VOIS image analysis software. The total area captured by the objective of the microscope or a fraction thereof can be accurately measured by the software. Hence the total area and the area covered by the pores are separately measured and the porosity of the surface under examination is determined.

3.7.6 Tensile Adhesion Test (TAT) [8]

The tensile adhesion strength of the bond coats (Ni-Al &Fe-Al) and the top alumina coat was measured separately using a special type of specimen holder (Fig.3.4). Cylindrical mild steel dummy samples (length 25mm,top and bottom diameter 9.5mm)were prepared. The surfaces of all the dummies were roughened by punching. The rough surface of each dummy was then fixed on top of a coating sample with the help of a polymeric adhesive (epoxy 900-C) and pulled with tension after being mounted on the jig (Fig.3.5). The coating pull out test was carried out using the set up Instron 1195 at a crosshead speed

of 1mm/min.The moment the coating got torn off from the specimen, the reading (of the load), which corresponds to the bond strength of coating, was

Fig 3.4 Jig used for the test

Fig.3.5 Specimen under tension

Fig.3.6 Adhesion test set up Instron 1195

recorded. A typical set up of the test is shown in figure 3.6. The test is performed as per ASTM C-633.

3.7.7 Determination of Coating Deposition Efficiency

Deposition efficiency is defined as the ratio of the weight of the coating deposited on the substrate to the weight of the expended feedstock. Weighing method is accepted widely to determine this.

Each specimen was weighed accurately before and after the coating deposition. The difference of these weights (Gc) measured the deposition of coating material on the substrate. The weight of the expended feed stock (Gp) was determined from the powder feed rate and time period of deposition. The deposition efficiency (η) was then calculated using the following equation [9].

$$\eta = (Gc / Gp \text{ X } 100)\ \%$$

Weighing of the samples was done using a precision electronic balance with ± 0.1mg accuracy.

References

1. M.I. Boulos, IEEE Trans. Plasma Sci., 19(6) (**1991**) 1078.
2. W.L. Weise, Plasma Diagnostics Techniques, eds. R.H. Huddlestone, S.L. Leonard, Academic Press, New York, **1965.**
3. K.S. Drellishak, Ph.D Thesis, Northwestern Univ. Evanston, IL, **1963**.
4. G.B. Willamson and R.C. Smallman, Philos. May. 1 (**1956**) 34.
5. V. Mikli, H. Kaerdi, P. Kulu and M. Besterct, Proc. Estonian Acad.Sci. Eng., 7(1), **2001**, p. 22.

6. B.D. Cullity, Elements of X-Ray Diffraction, Addition-Wasley, Reading, MA, **1972**, p.102.

7. L. Wojnar, Image Analysis Applications In Materials Engineering, CRC Press, Boca Raton, **1999.**

8. C.K.Lin and C.C.Berndt, J. of Thermal Spray Technology, 3(**1994**), 75.

9. H.Chen,S.W.Lee,Hao Du,Chuan X Ding and Chul Ho Dho ; Materials Letter Vol.58, Issues 7-8,March **2004** pp.1241-1245,Influence of feed stock & spraying parameters on the dep.eff.and microhardness of plasma sprayed zirconia coatings.

*****

Chapter 4

Results and Discussion

- Coating Deposition Efficiency
- Evaluation of Coating-Substrate Adhesion Strength
- Particle Size Analysis
- Microhardness
- X-Ray Phase Analysis
- Morphology

RESULTS AND DISCUSSION

All the test results pertaining to deposition, characterization and performance evaluation of coatings and the processed powders are presented and discussed in this chapter.

4.1. COATING DEPOSITION EFFICIENCY

Thickness of the coatings was measured using vernier calipers and using an optical microscope fitted with a screw gauge arrangement. The average thickness was about 240μm for Fe-Al and about 225μm for Ni-Al on copper substrates. Aluminium oxide deposited on copper was about 205μm thick.

The plasma sprayed coating thickness of Fe-Al, Ni-Al and alumina powders obtained at different power levels on aluminium(Al), copper(Cu), mild steel (MS) and stainless steel(SS) metal substrates are presented in Fig. 4.1 to fig. 4.4. Each data point on the curves is the average of three measurements.

Deposition efficiency is an important factor that determines the techno-economics of the process. This was determined by simple gravimetric method as described in chapter-III and it is calculated using the relation as mentioned below [1].

$$\eta = (Gc / Gp) \times 100\ \%$$

Where η is the deposition efficiency

Gc is the weight of coating deposited on the substrate and

Gp is the weight of the expended feedstock

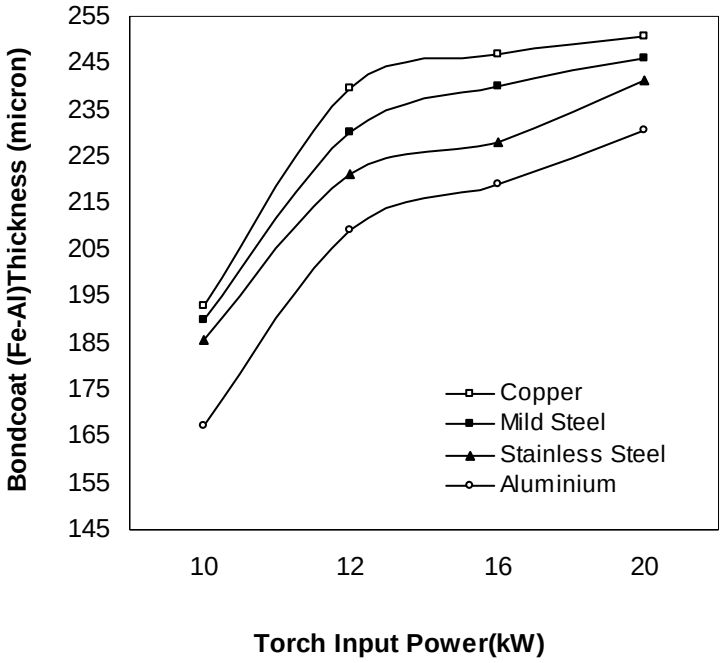

Fig.4.1 Variation of Bond coat (Fe-Al) Thickness with Torch Input Power.

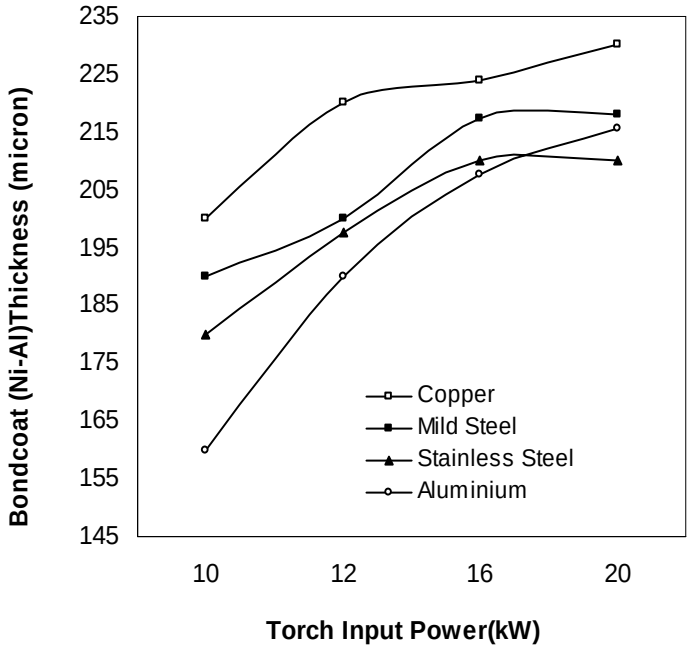

Fig.4.2 Variation of Bond coat (Ni-Al) Thickness with Torch Input Power.

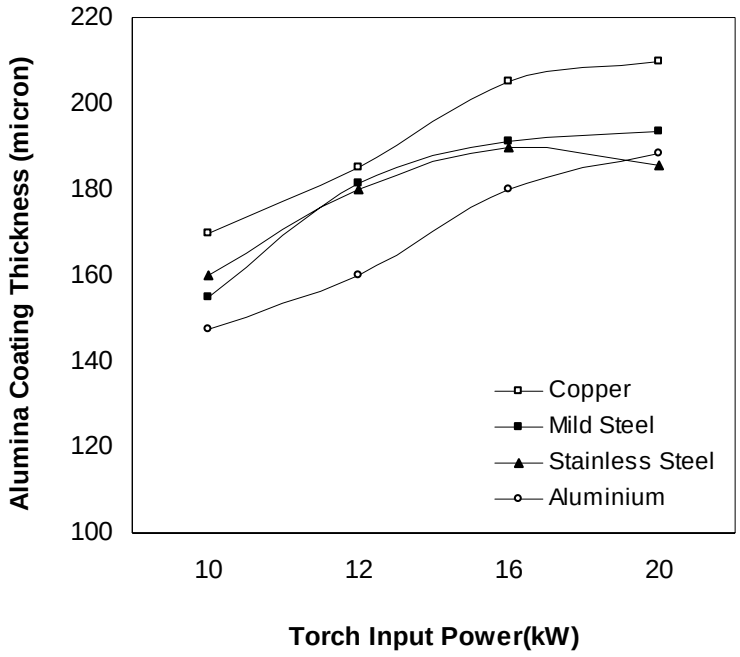

Fig.4.3 Alumina Coating Thickness (made over Fe-Al bondcoat) Vs Power.

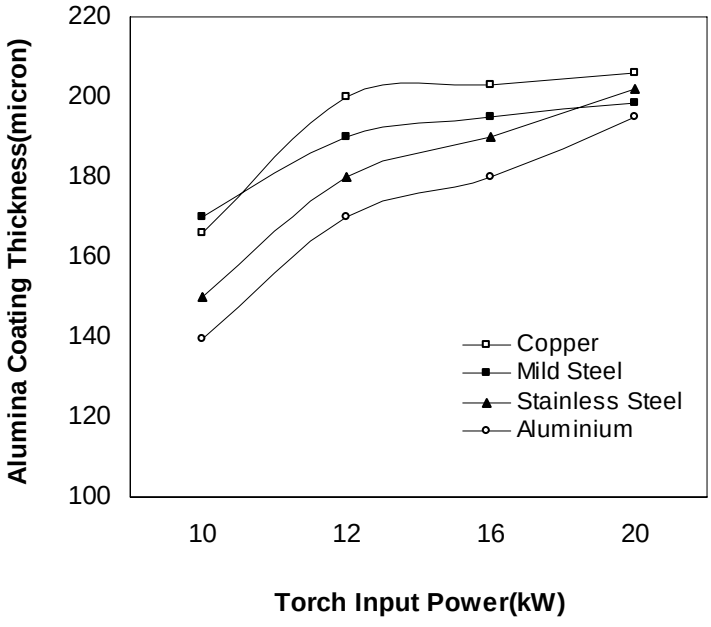

Fig.4.4 Alumina Coating Thickness (made over Ni-Al bondcoat) Vs Power.

Deposition efficiency depends on many factors that include the input power to the plasma torch, material properties, such as melting point, grain size and heat capacity of the powder being sprayed, stand off distance(torch to base distance) etc. For a given stand off distance and given material with specific particle size, torch power appears to be an important factor for the deposition efficiency. The deposition efficiency is a measure of the fraction of the powder that has melted, but that has not vaporized or decomposed into gaseous products. Fig. 4.5 to fig .4.7 shows the variation of deposition efficiency of Fe-Al, Ni-Al and alumina with operating power level. It is interesting to note that the deposition efficiency, in all cases, has increased in a step up fashion with the increase in torch input power. For example, deposition efficiency ranges from 32% to 60% in case of Fe-Al, 34% to 54% in the case of Ni-Al and 28% to 46% for alumina coatings.

Plasma spray deposition efficiency of a given materials depends on its melting point, thermal heat capacity and particle size of the powder. At lower input power to the plasma torch, the plasma jet temperature is not high enough to melt the entire powder particles that enter the plasma jet. As the power is increased, the average plasma temperature increases melting a larger fraction of the powder. The spray efficiency, therefore, increases with plasma power. However, beyond a certain power level of plasma, the temperature of the plasma gas is very high, leading to vaporization/dissociation of the powder particles. This causes the deposition efficiency to decrease at higher power levels. This tendency is observed in all materials. However, the plasma power above which the efficiency decrease depends on the chemical nature of the powder and its particle size. In the present investigation the deposition efficiency increased from 20% to 50% on aluminum substrates, from 32% to 60% on copper, from 28% to 54% on mild steel and from 24% to 48% on stainless steel substrates (with input power to plasma torch increasing from 10 kW to 20 kW) in case of Fe-Al bond coating.

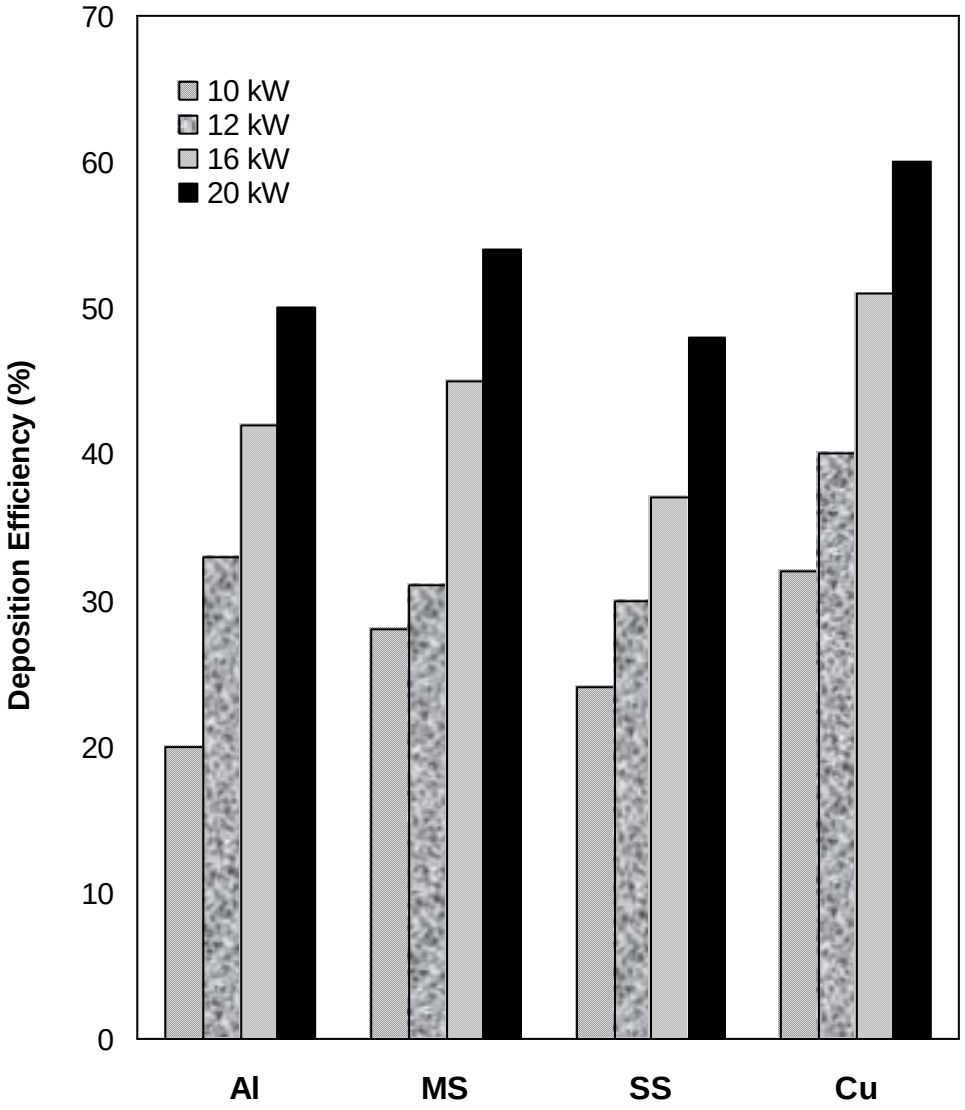

Fig.4.5 Deposition Efficiency of Fe-Al Bondcoat on metal substrates.

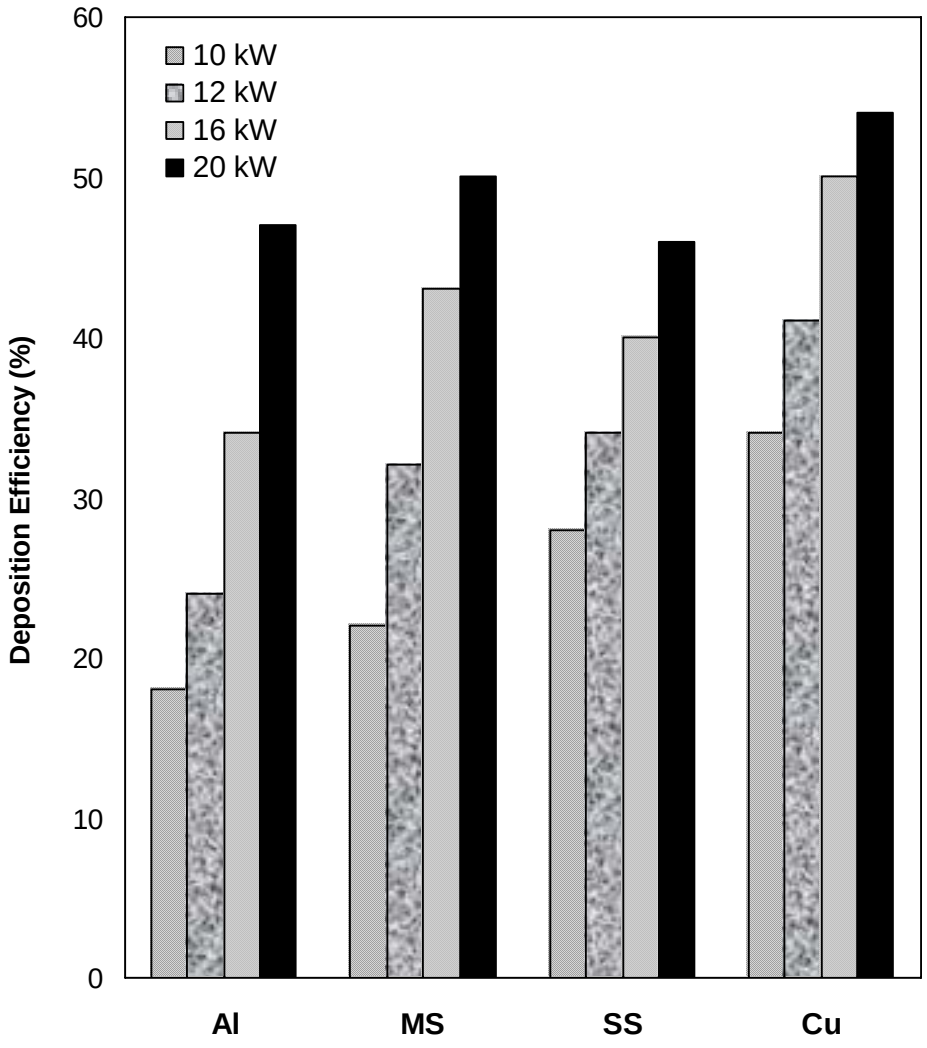

Fig.4.6. Deposition Efficiency of Ni-Al Bondcoat on metal substrates.

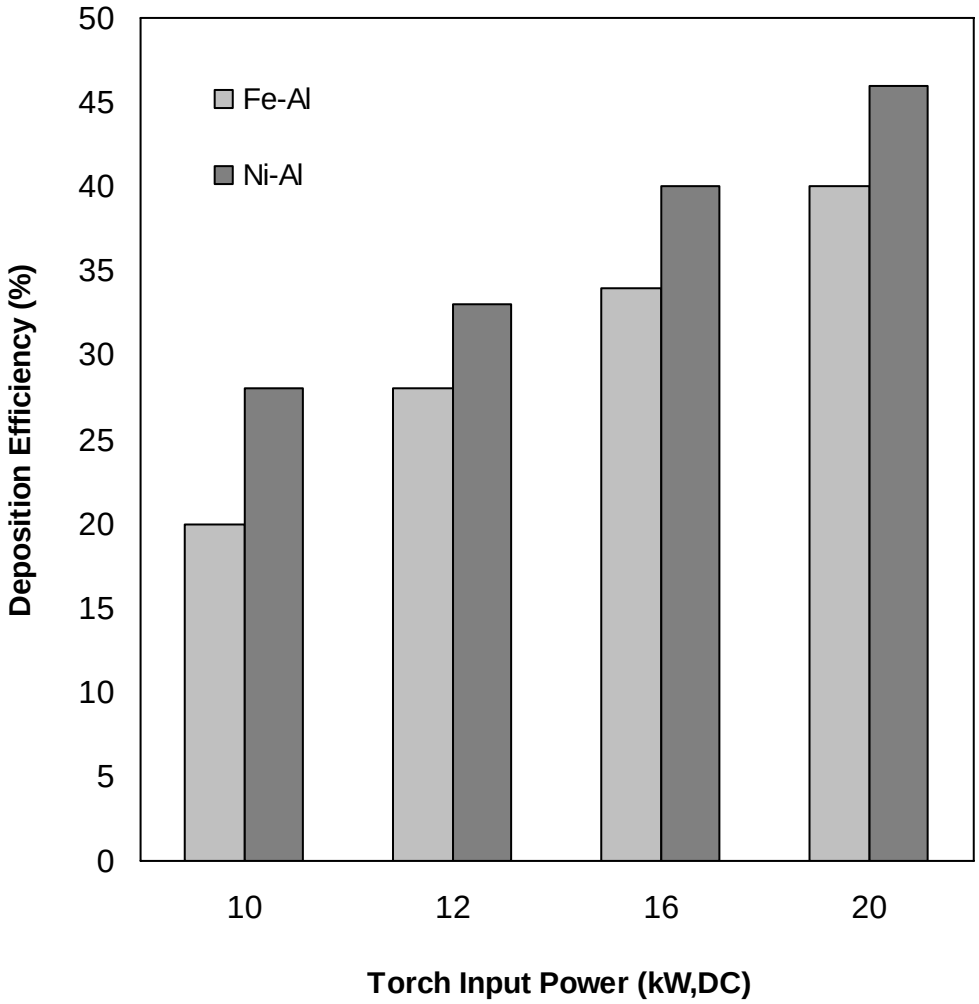

Fig.4.7 Deposition Efficiency of Alumina Coating Over Bondcoats.

Similarly, for Ni-Al bond coating the value increased from 18% to 47% on aluminium substrates, from 34% to 54% on copper, from 22% to 50% on mild steel and 28% to 46% on stainless steel substrates. Where as, when alumina deposition was made on the bond coatings, the efficiency of deposition found to vary from 20% to 40% on Fe-Al bond coat and 28% to 46% on Ni-Al bond coat.

4.2 EVALUATION OF COATING-SUBSTRATE ADHESION STRENGTH

From microscopic point of view, adhesion is due to the physico-chemical surface forces (vander-walls, co-valent, ionic etc.) which can be established at the coating substrate interface [2]. In this work, evaluation of coating interface bond strengths was done using coating pull out method, conforming to ASTM C-633 standard. Adhesion measurements were carried out on 3 samples and the average value is reported. It was found that in all the samples fracture occurred at the coating-substrate interface. The results of coating adhesion measurements for the bond coatings (.Fe-Al & Ni-Al) and the top alumina coating are tabulated in Table 4.1 and Table 4.2 respectively.

From mechanical point of view, adhesion can be estimated by the force corresponding to interfacial fracture and is macroscopic in nature. Coating adhesion tests have been carried out by many investigators with various coatings. It should be noted that the fracture mode is adhesive if it takes place at the coating-substrate interface and that the measured adhesion value is the value of practical adhesion, which later is strictly an interface property, depend exclusively on the surface characteristics of the adhering phase and the substrate surface condition [3, 4]. The variation of interface bond strength of Fe-Al and Ni-Al coatings on selected substrates with respect to different power

Power (kW)	TBD (mm)	Adhesion strength of bond coatings (in MPa)		
		Fe+Al over MS	Ni+Al over MS	Ni+Al over Cu
10	100	15.0	10.5	22.5
10	200	11.0	8.0	16.0
10	400	7.4	6.2	8.9
16	100	23.5	18.46	27.0
16	200	18.54	11.87	18.52
16	400	13.75	7.5	10.34

Table 4.1 Adhesion strength of bond coatings.

Description of sample	Type of substrate	TBD (mm)	Adhesion strength of alumina coating (in MPa)			
			10kW	12kW	16kW	20kW
Alumina coated over Fe +Al	MS	100	15.71	21.87	27.0	22.47
	SS	100	17.16	24.8	30.0	26.7
	Cu	100	19.18	30.4	32.50	31.0
	Al	100	12.86	18.42	23.00	21.0
Alumina coated over Ni +Al	MS	100	10.5	14.0	22.0	13.0
	SS	100	16.0	20.6	25.0	17.0
	Cu	100	18.0	23.0	27.0	20.0
	Al	100	13.0	17.00	20.00	15.00

Table 4.2 Adhesion strength of Alumina coating.

level as well as at various torch to base (i.e. substrate) distances are shown in Fig.4.8 and Fig.4.9. Maximum adhesion strength of ~15 MPa and of ~23.5 MPa was found in the case of Fe-Al bond coatings (fig. 4.8), deposited at a torch to base distance (TBD) of 100mm both at 10kW and at 16 kW input power levels respectively. It is observed that, with increase in torch input power level; there is an increase in the coating adhesion strength. But increase

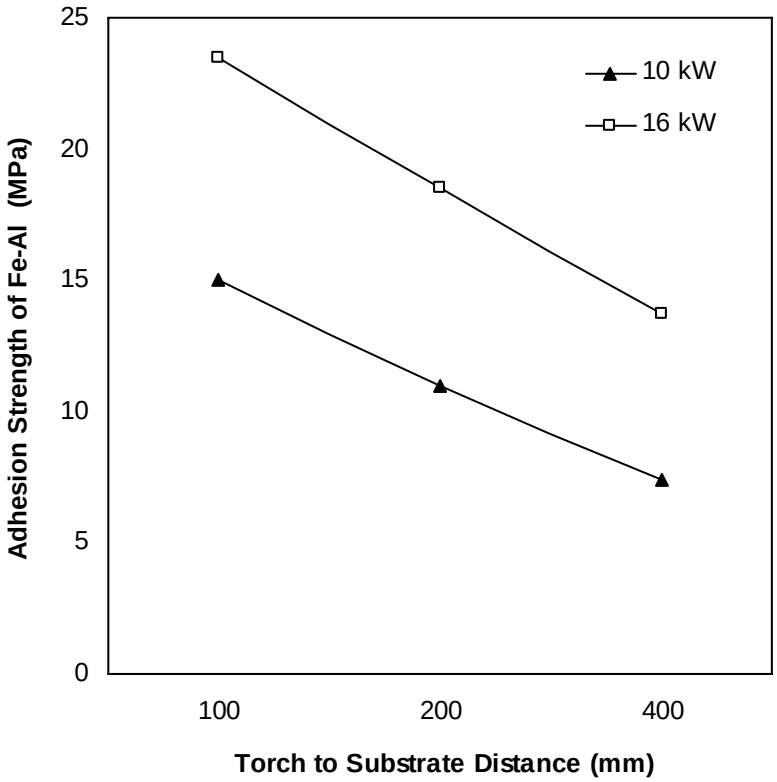

Fig.4.8 Adhesion Strength of Fe-Al BondCoat on MS.

in the spraying distance (TBD), the adhesion strength decreases. The coating adhesion strength of Ni-Al deposited on MS & Cu substrates is shown in fig.4.9. It is seen from the figure that adhesion has increased with increase in power level for both the substrates. However, with increase in the spraying distance the adhesion strength shows a decreasing trend. It is also observed that there is a marked difference in the coating adhesion strength depending upon the substrate material. Adhesion strength is more in case of copper substrate than that of mild steel.

The variation of interface bond strength of top alumina coating over the Fe-Al as well as the Ni-Al coated substrates with respect to the operating

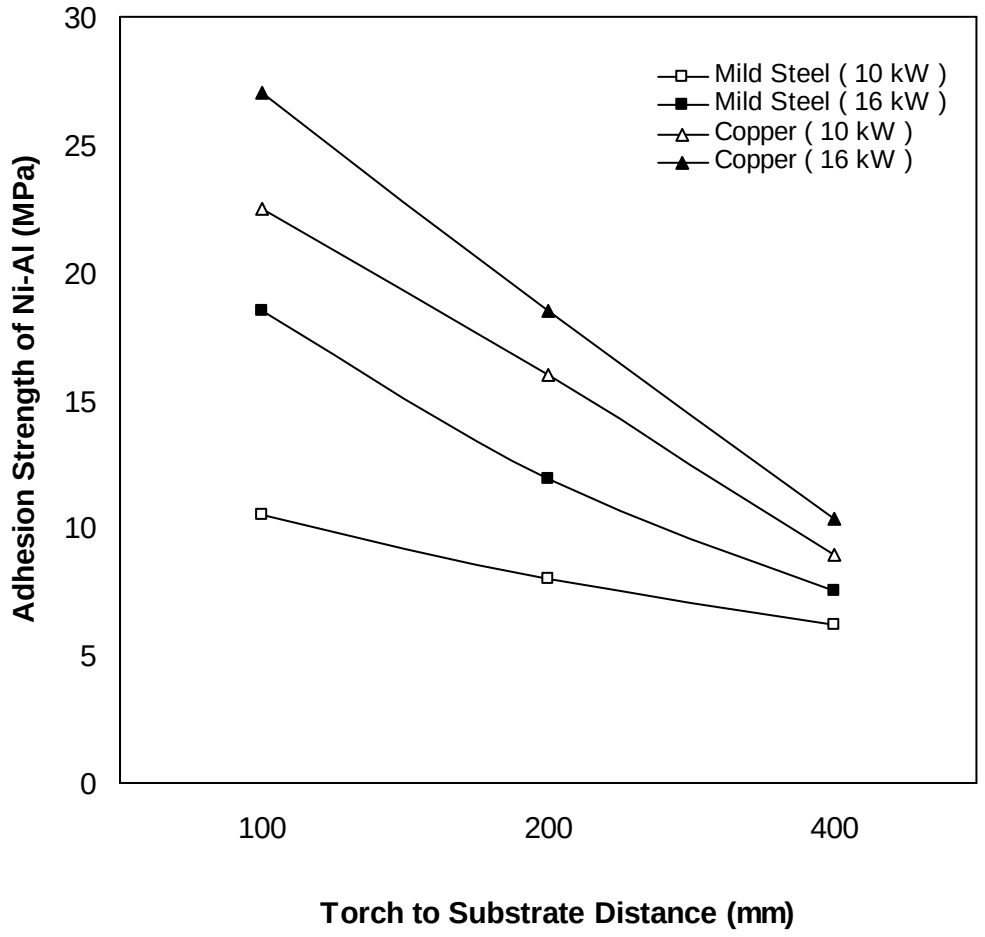

Fig.4.9 Adhesion Strength of Ni-Al Bondcoat on MS & Cu.

power of plasma torch is presented in fig.4.10 and fig.4.11. Maximum adhesion strength of 32.5 MPa was found in the case of alumina coating deposited over Fe-Al bond coat at 16kW power and maximum of 27 MPa was found over Ni-Al bond coat at 16kW power on copper substrates.

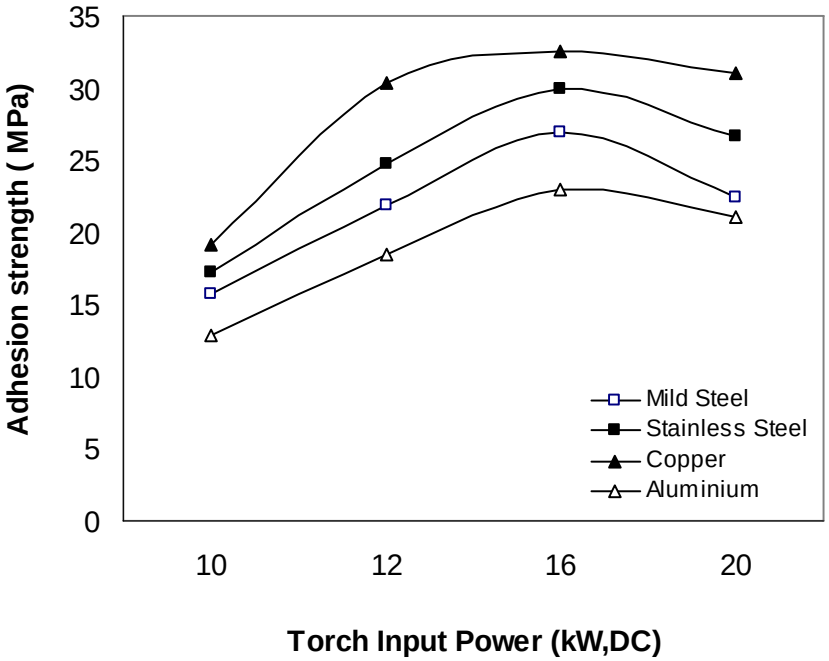

Fig.4.10 Adhesion Strength of Alumina Coating on Fe-Al Bondcoat.

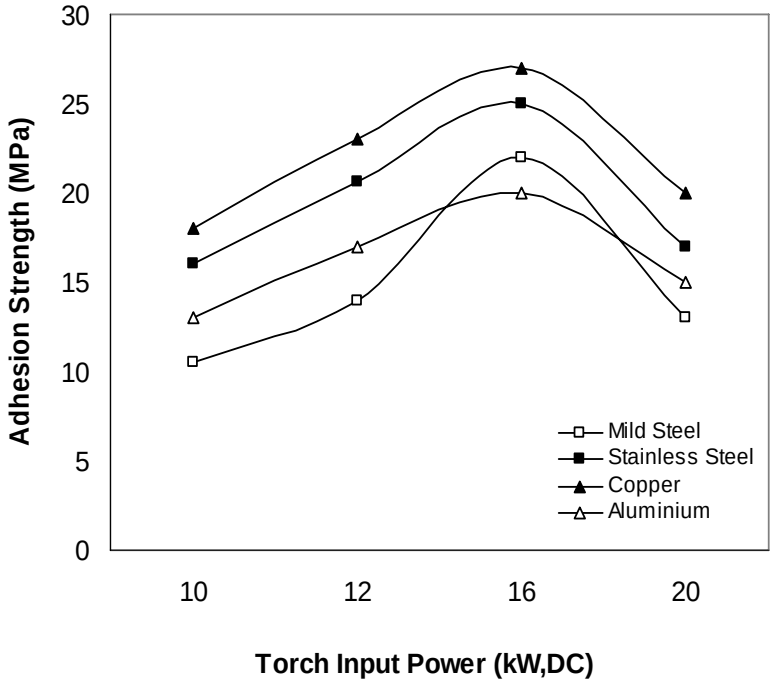

Fig.4.11 Adhesion Strength of Alumina Coating on Ni-Al Bondcoat.

4.3 PARTICLE SIZE ANALYSIS

The particle sizes of the iron-aluminium powder (after mixing in ball mill) and the nickel-aluminium powder (after mixing in ball mill) are characterized using Laser particle size analyzer of Malvern Instruments make. The particle size of iron-aluminium powder mix and the iron-aluminium powders processed at different power levels are shown in fig.4.12.

Figure.4.12 (a) shows the particle size distribution of Fe-Al powder mix before plasma spraying. It can be seen that majority of particles are in the range of 40 to 100 micron. The mean particle diameter is found to be 61.78 micron. The powder processed at 10 kW and collected at a standoff distance (TBD) of 100 mm; fig.4.12 (b) shows that the mean particle diameter has reduced to 53.9 micron with surface area of 21.2 micron. Maximum particles are in the range of 50 micron. When the particles are collected at a standoff distance of 400 mm the mean particle diameter has increased to 57 micron and also surface area increased to 27 micron, fig.4.12(c).The Fe-Al powders processed at 16kW power level and collected at a distance of 100 mm, the mean particle diameter has reduced to 36 micron with surface area to 6 micron, fig.4.12 (d). When the same powder is collected at a distance of 400mm, the surface area has increased to 16.94 micron but the particle diameter found of similar size i.e. of 40micron, fig.4.12 (e).

Similarly the particle size of nickel-aluminium powder mix and nickel-aluminium powder processed at different power levels were analyzed and are shown in fig.4.13.

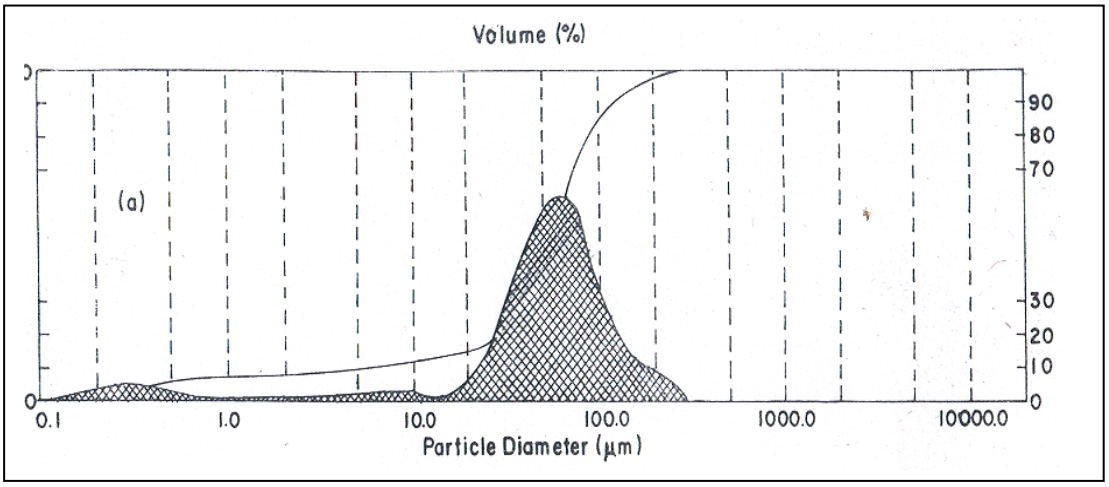

Dist. Type : Volume	Conc.=0.0239%Vol.	Density=1.000g/cm^3	Spec. S.A.=1.7913m^2/g
Mean Diameters:	D(v,0.1)=4.72µm	D(v,0.5)=54.07µm	D(v,0.9)=117.06µm
D[4,3]=61.78µm	D[3,2]=3.35µm	Span=2.078E+00	Uniformity=6.113E-01

Result Statistics

Fig.4.12 (a) Particle size distribution of Fe-Al powder mix before plasma spraying.

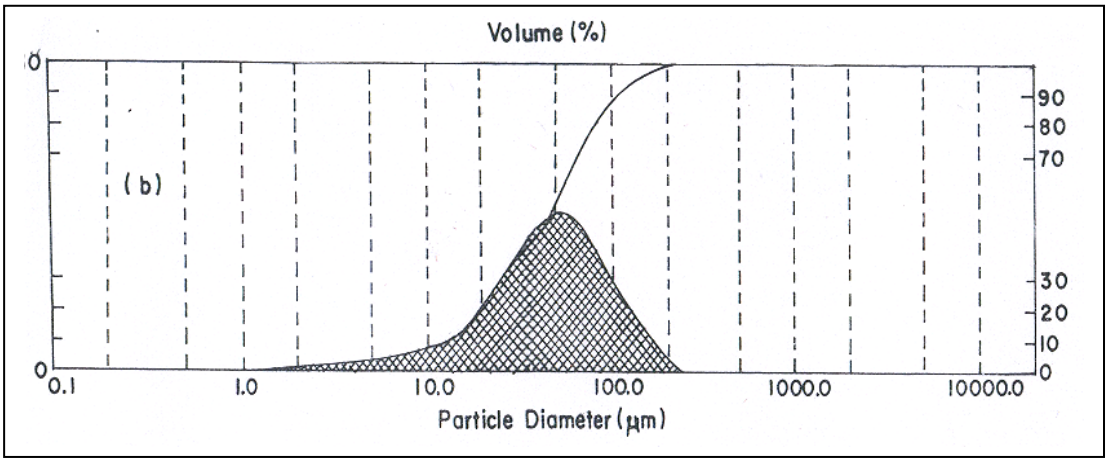

Dist. Type : Volume	Conc.=0.0460%Vol.	Density=1.000g/cm^3	Spec. S.A.=0.2830m^2/g
Mean Diameters:	D(v,0.1)=12.01µm	D(v,0.5)=45.35µm	D(v,0.9)=107.53µm
D[4,3]=53.92µm	D[3,2]=21.20µm	Span=2.106E+00	Uniformity=6.406E-01

Result Statistics

Fig.4.12 (b) Particle size distribution of Fe-Al processed powders at 10kW and 100mm TBD.

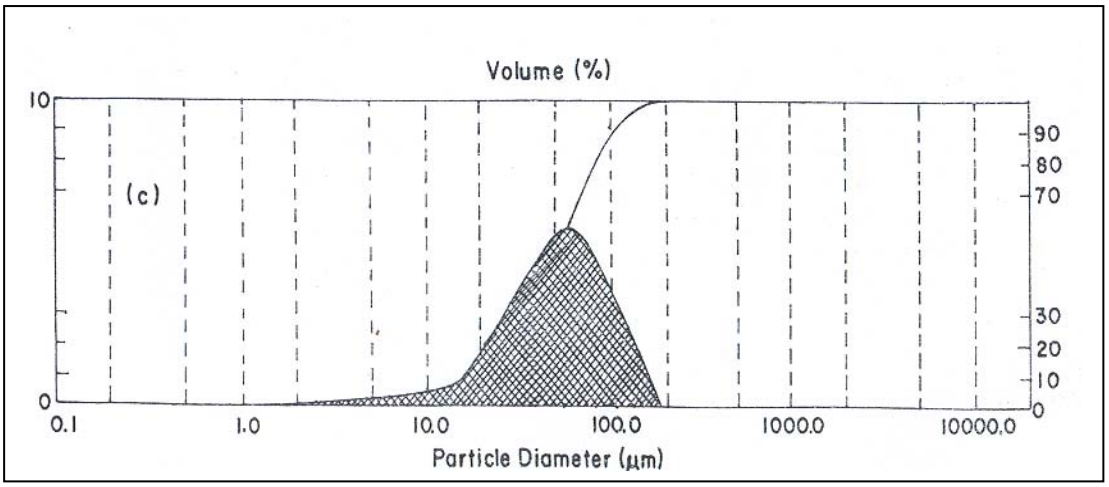

Dist. Type : Volume	Conc.=0.0591%Vol.	Density=1.000g/cm^3	Spec. S.A.=0.2226m^2/g
Mean Diameters:	D(v,0.1)=17.75µm	D(v,0.5)=51.11µm	D(v,0.9)=105.81µm
D[4,3]=57.03µm	D[3,2]=26.95µm	Span=1.723E+00	Uniformity=5.268E-01

Result Statistics

Fig.4.12 (c) Particle size distribution of Fe-Al processed powders at 10kW and 400mm TBD.

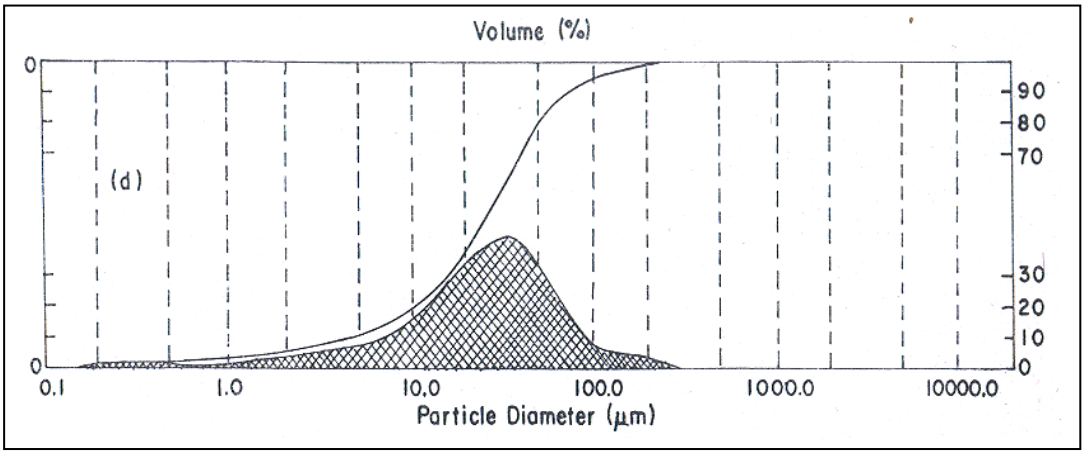

Dist. Type : Volume	Conc.=0.0235%Vol.	Density=1.000g/cm^3	Spec. S.A.=1.1551m^2/g
Mean Diameters:	D(v,0.1)=4.17µm	D(v,0.5)=26.20µm	D(v,0.9)=72.95µm
D[4,3]=35.89µm	D[3,2]=5.19µm	Span=2.625E+00	Uniformity=8.925E-01

Result Statistics

Fig.4.12 (d) Particle size distribution of Fe-Al processed powders at 16kW and 100mm TBD.

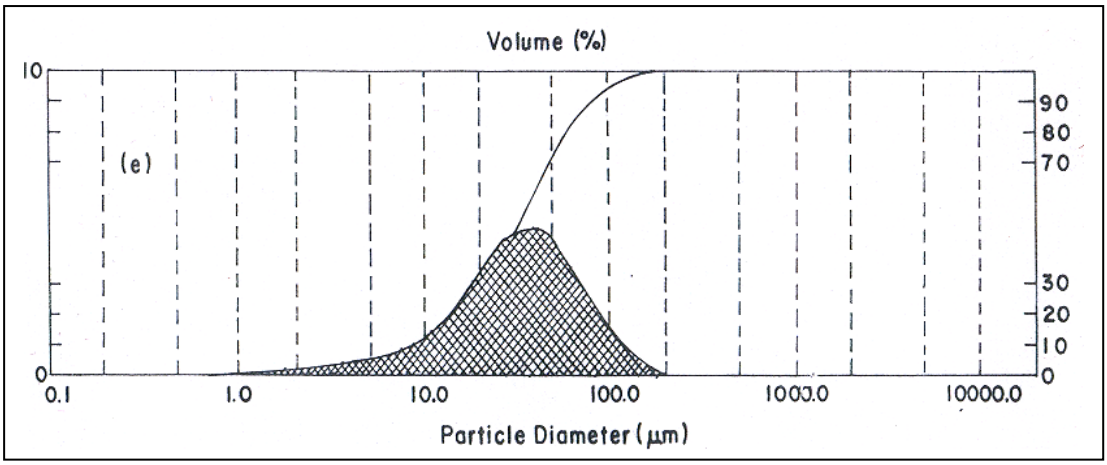

Dist. Type : Volume	Conc.=0.0391%Vol.	Density=1.000g/cm^3	Spec. S.A.=0.3542m^2/g
Mean Diameters:	D(v,0.1)=9.06µm	D(v,0.5)=32.70µm	D(v,0.9)=80.24µm
D[4,3]=39.94µm	D[3,2]=16.94µm	Span=2.177E+00	Uniformity=6.731E-01

Result Statistics

Fig.4.12 (e) Particle size distribution of Fe-Al processed powders at 16kW and 400mm TBD.

Figure 4.13(a) shows the particle size distribution of Ni-Al powder mix before plasma spraying. The mean particle diameter is found to be 203.28 micron and surface area is 53.9 micron. The powder is processed at 10 kW and collected at a distance of 100 mm; fig.4.13 (b) shows that the mean particle diameter has reduced to 87.85 micron with surface area of 20 micron. When the particles are collected at a distance of 400 mm the mean particle diameter has increased to 160micron and surface area found to 16.2 micron, fig.4.13(c). The Ni-Al powders processed at 16kW power level and collected at a distance of 100 mm, the mean particle diameter has reduced to 66.2 micron with surface area to 31.3 micron, fig.4.13 (d). When the same powder is collected at a distance of 400mm, the surface area has increased to 21micron but the particle diameter found is of similar size i.e. of 77 micron, fig.4.13 (e).

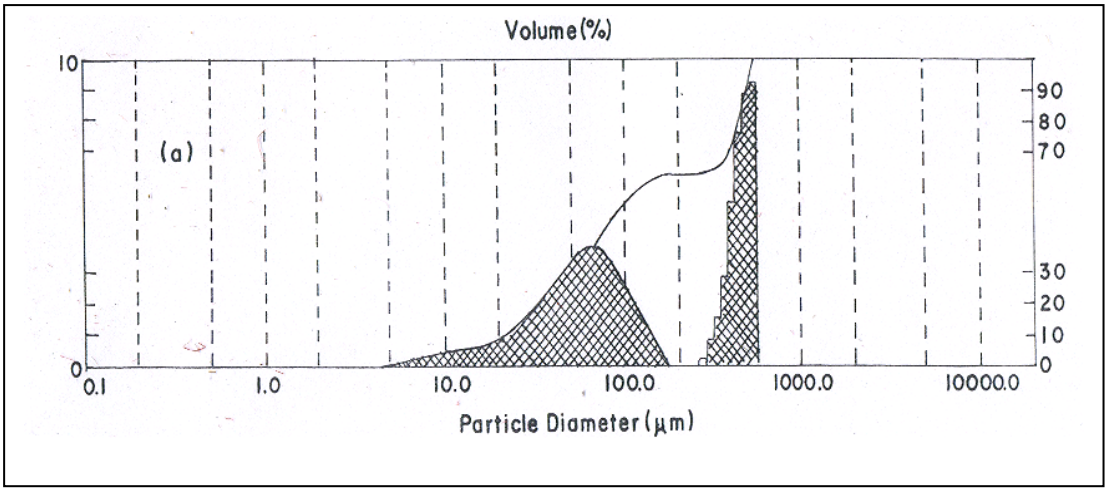

Dist. Type : Volume	Conc.=0.1559%Vol.	Density=1.000g/cm^3	Spec. S.A.=0.1113m^2/g
Mean Diameters:	D(v,0.1)=25.32µm	D(v,0.5)=84.79µm	D(v,0.9)=502.94µm
D[4,3]=203.28µm	D[3,2]=53.89µm	Span=5.633E+00	Uniformity=1.859E+00

Result Statistics

Fig.4.13 (a) Particle size distribution of Ni-Al powder mix before plasma spraying.

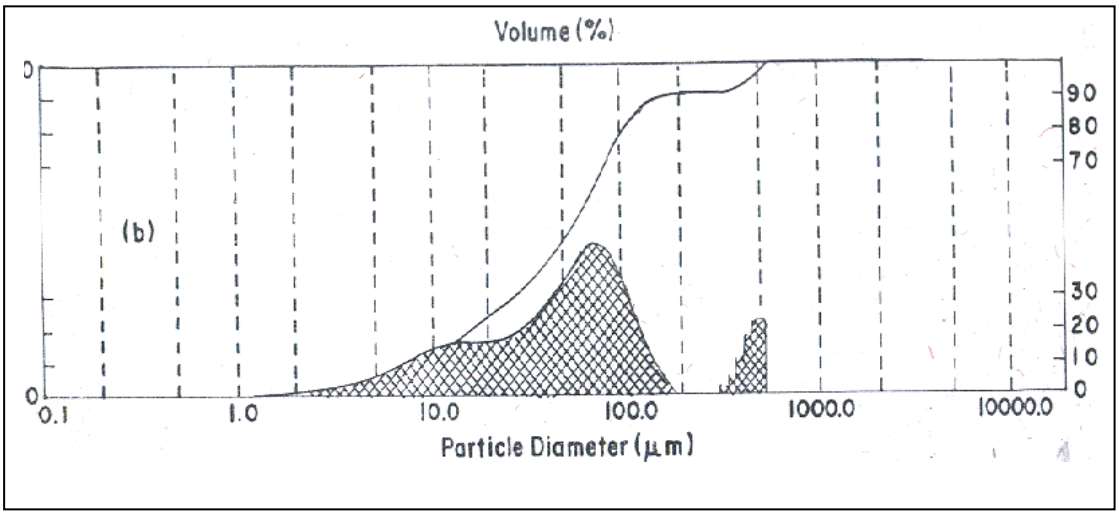

Dist. Type : Volume	Conc.=0.0506%Vol.	Density=1.000g/cm^3	Spec. S.A.=0.2950m^2/g
Mean Diameters:	D(v,0.1)=8.55µm	D(v,0.5)=53.02µm	D(v,0.9)=150.46µm
D[4,3]=87.85µm	D[3,2]=20.34µm	Span=2.676E+00	Uniformity=1.213E+00

Result Statistics

Fig.4.13 (b) Particle size distribution of Ni-Al processed powders at 10kW and 100mm TBD.

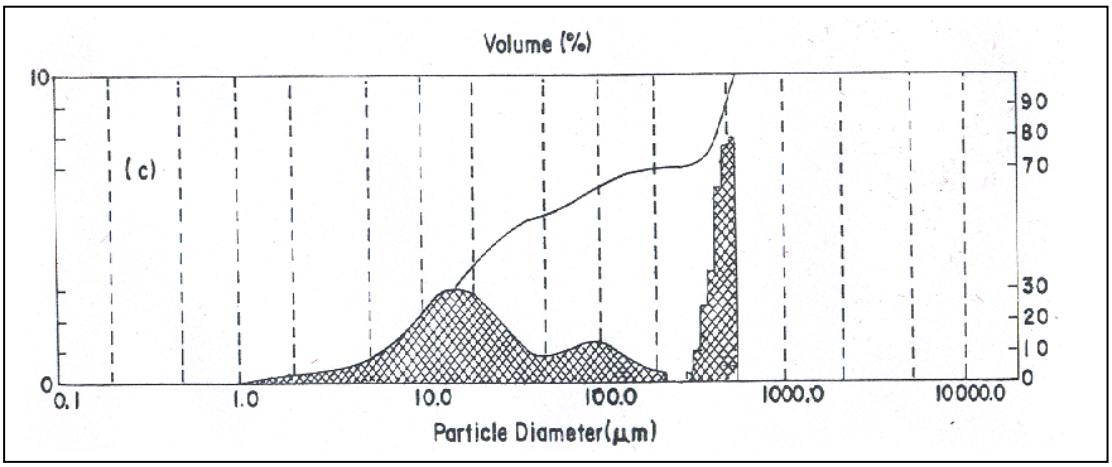

Dist. Type : Volume	Conc.=0.0438%Vol.	Density=1.000g/cm^3	Spec. S.A.=0.3714m^2/g
Mean Diameters:	D(v,0.1)=7.12µm	D(v,0.5)=32.30µm	D(v,0.9)=494.52µm
D[4,3]=160.10µm	D[3,2]=16.15µm	Span=1.509E+01	Uniformity=4.519E+00

Result Statistics

Fig.4.13 (c) Particle size distribution of Ni-Al processed powders at 10kW and 400mm TBD.

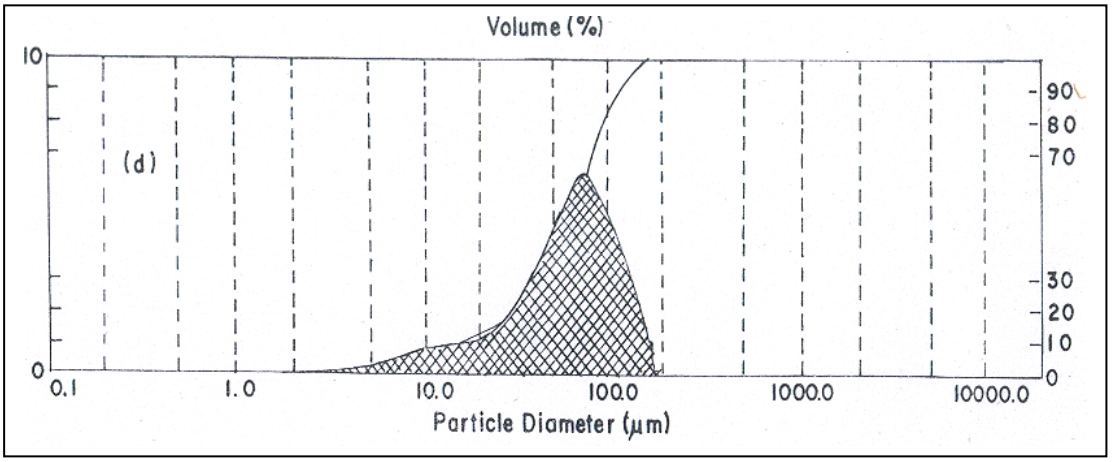

Dist. Type : Volume	Conc.=0.0702%Vol.	Density=1.000g/cm^3	Spec. S.A.=0.1919m^2/g
Mean Diameters:	D(v,0.1)=15.30µm	D(v,0.5)=62.15µm	D(v,0.9)=120.99µm
D[4,3]=66.17µm	D[3,2]=31.27µm	Span=1.700E+00	Uniformity=5.070E-01

Result Statistics

Fig.4.13 (d) Particle size distribution of Ni-Al processed powders at 16kW and 100mm TBD.

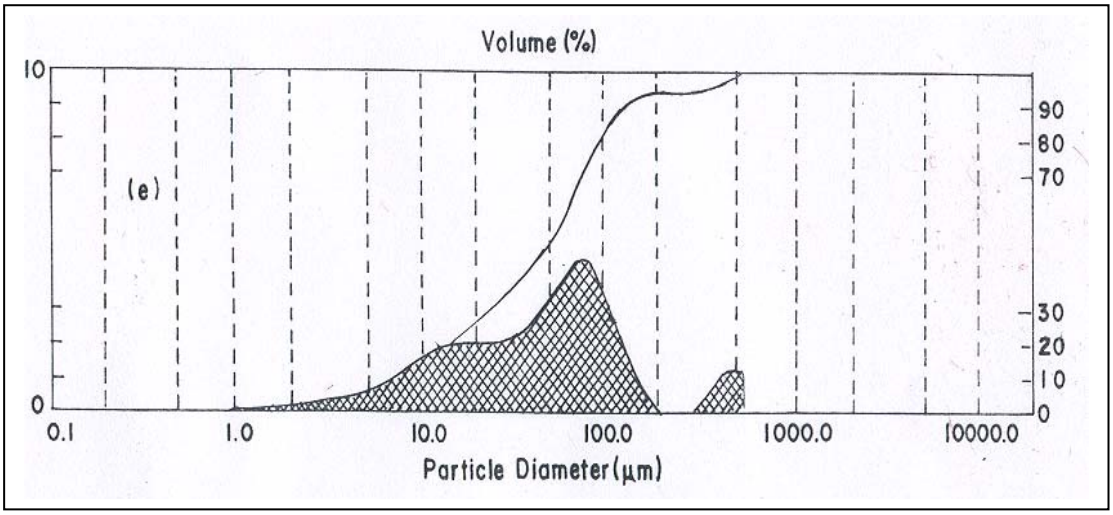

Dist. Type : Volume	Conc.=0.0482%Vol.	Density=1.000g/cm^3	Spec. S.A.=0.2914m^2/g
Mean Diameters:	D(v,0.1)=8.90µm	D(v,0.5)=50.51µm	D(v,0.9)=136.23µm
D[4,3]=77.04µm	D[3,2]=20.59µm	Span=2.521E+00	Uniformity=1.091E+00

Result Statistics

Fig.4.13 (e) Particle size distribution of Ni-Al processed powders at 16kW and 400mm TBD.

The above observations shows that with increase in power level, the particle size is reduced; the reason may be that, some of the particles are broken/fragmented into smaller sizes. But when the particles are collected at longer stand off distance from the torch (i.e.TBD), there is increase in surface area, which may be due to coagulation of smaller particles during in-flight traverse.

4.4 MICROHARDNESS

Microhardness measurement was done on the optically distinguishable phases with Leitz Microhardness Tester using 50 Pa (0.493 N) on polished cross section of the coatings. The results are summarized in Table 4.1. In case of Fe+Al bond coat four different range of hardness values were observed ranging from 120 HV to 300 HV. In the case of Ni-Al bond coat four different

range of hardness values were also observed ranging from 210 HV to 350HV. In the case of alumina coating two different range of hardness were noted. The variation of hardness values may be due to the formation of different phases i.e. aluminides during coating deposition and existence of two different phases of alumina i.e. α- and γ-alumina.

Coating material	Sl.No.	Range of hardness values (HV)
Iron-Aluminium powder mix	1	120 ± 10
	2	150 ± 10
	3	200 ± 10
	4	280 ± 15
Nickel-Aluminium powder mix	1	210 ± 10
	2	250 ± 10
	3	295 ± 15
	4	340 ± 10
Alumina powder	1	1050 -1130
	2	500 -560

Table 4.3 Micro hardness of Alumina, Fe-Al & Ni-Al Plasma spray coatings

4.5 X-RAY PHASE ANALYSIS

Microhardness test of these plasma sprayed coating materials shows different hardness values on different optically distinct phases/regions. Therefore, to ascertain the phases present and phase changes/transformation taking place during plasma spraying, the X-ray diffractograms are taken on the raw materials (Fe-Al &Ni-Al ball milled powders) and on some selected spheroidized powders using a Philips X-Ray Diffractometer. The XRD results are shown in fig.4.14 & 4.15.

The formation of different aluminide phases is observed in the plasma processed raw materials. From the diffractograms it is seen that the major constituents formed during plasma spraying in the Ni-Al bond coat are the nickel aluminides such as AlNi, Al_3Ni, $AlNi_3$, Al_3Ni_2. In the case of Fe-Al, the presence of iron aluminides such as Fe_2Al_5, $FeAl_3$, and Fe_4Al_{13} are evident from the figure. Presence of Al, Ni and Fe are also observed. This may be due to the fact that, phase transformation/formation of aluminide phases has taken place during in-flight traverses of the feed powders through the plasma flame and has very short dwelling time. So, (a) all the powder particles have not faced the required high temperature i.e. not sprayed through the axis of the plasma jet and (b) limited phase transformation prevailed as per the phase diagram. But, in the case of alumina coating deposition, two different range of hardness can be due to the presence of γ-alumina and α-alumina. The presence/formation of different alumina phases i.e. α-alumina and γ-alumina during plasma sprayed alumina coating has been observed and described in the literature [5].

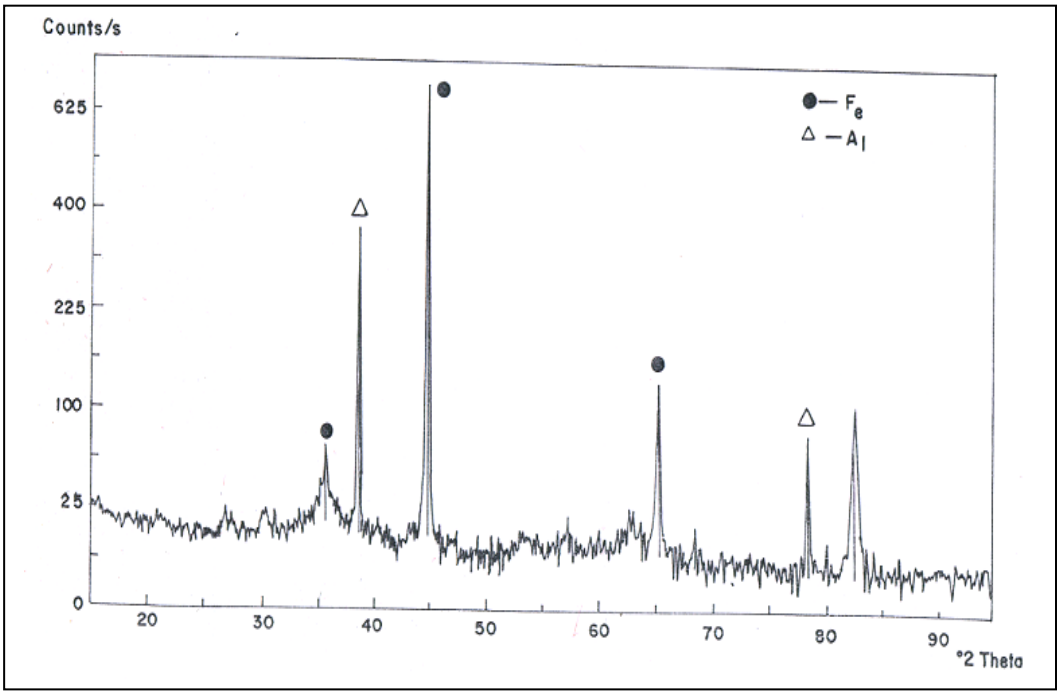

Fig.4.14 (a) XRD of Fe-Al Powder-after Ball milling, before Plasma spraying.

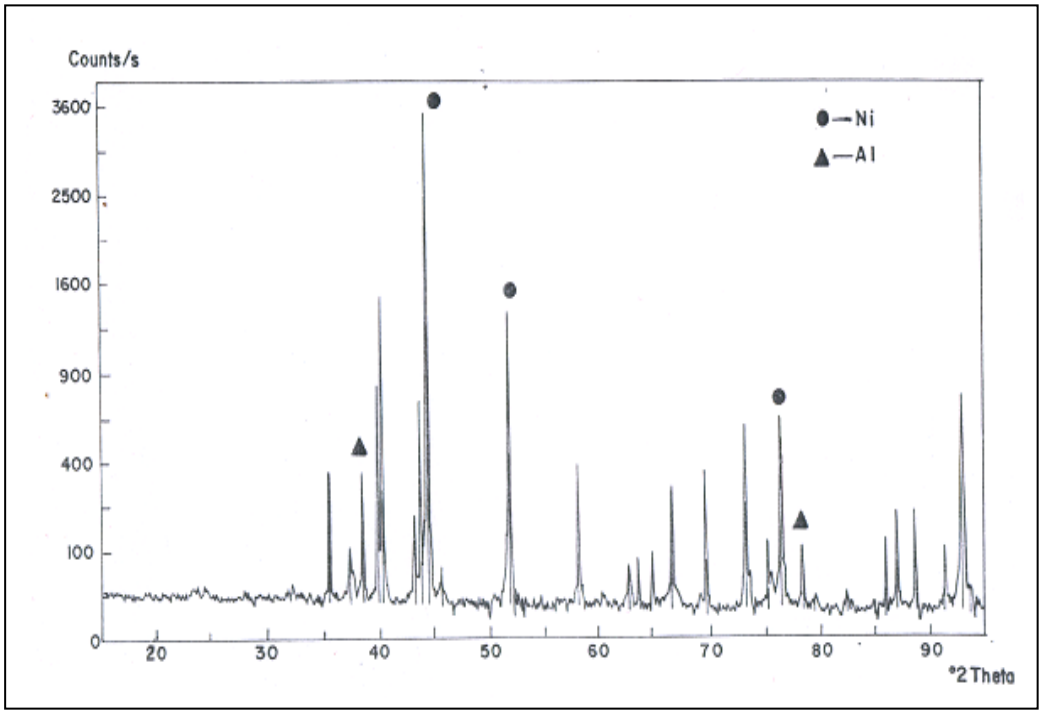

Fig.4.14 (b) XRD of Ni-Al Powder-after Ball milling, before Plasma spraying.

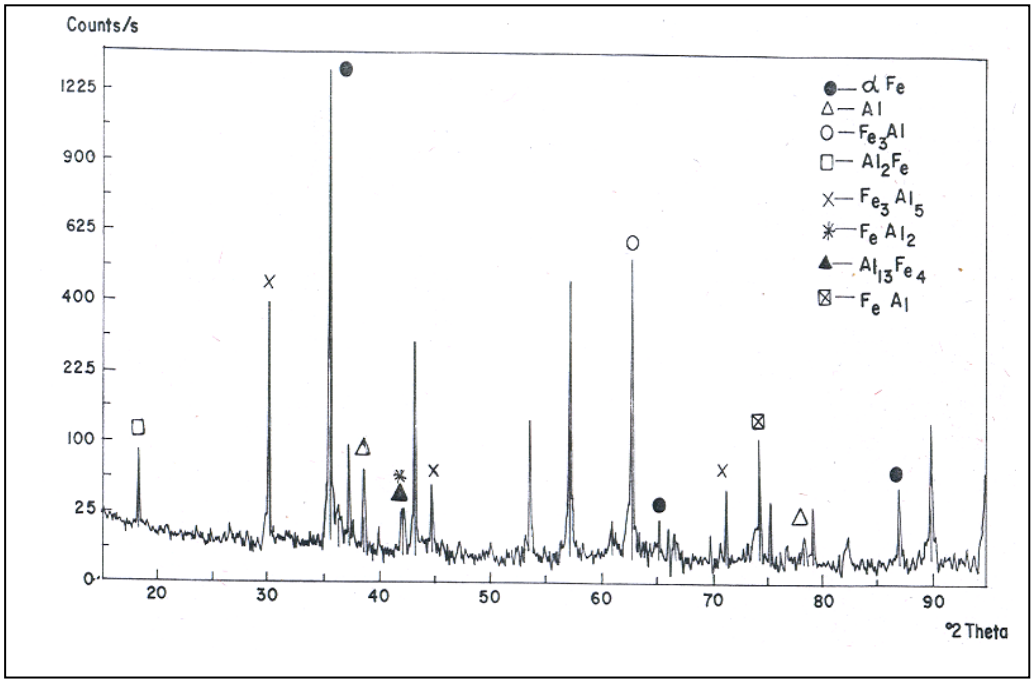

Fig.4.15 (a) XRD of Plasma Spherodised Fe-Al Powder at 16 kW power level.

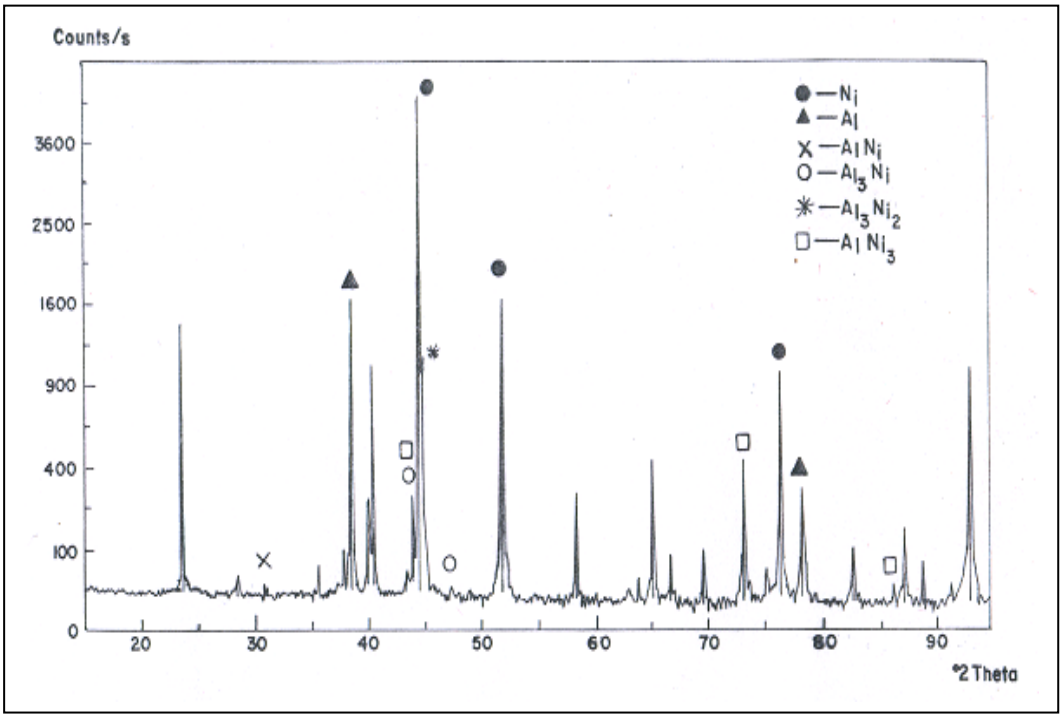

Fig.4.15 (b) XRD of Plasma Spherodised Ni-Al Powder at 16 kW power level.

4.6 MORPHOLOGY

4.6.1 Surface morphology of plasma processed powders for bond coat

The structural investigation of the aluminides (Fe-Al and Ni-Al powders) is carried out with Scanning Electron Microscope (SEM). Figure 4.16(a) shows the scanning electron micrograph of Fe-Al ball milled powders. The particles are found very much irregular in shape. Some particles are elongated type and some are multifaceted. The particle size analysis shown in Figure 4.12(a), envisages that the mean particle size is 61.78 μm. The morphology of Fe-Al plasma sprayed powder processed at 10 kW power and collected at 100mm standoff distance (TBD) is shown in Figure 4.16(b). Most of the particles are spherical in shape. Some particles, of larger diameter have been cracked, may be due to thermal pinch effect/fragmentation. At some places coagulation of particles is also observed in the figure; along with some

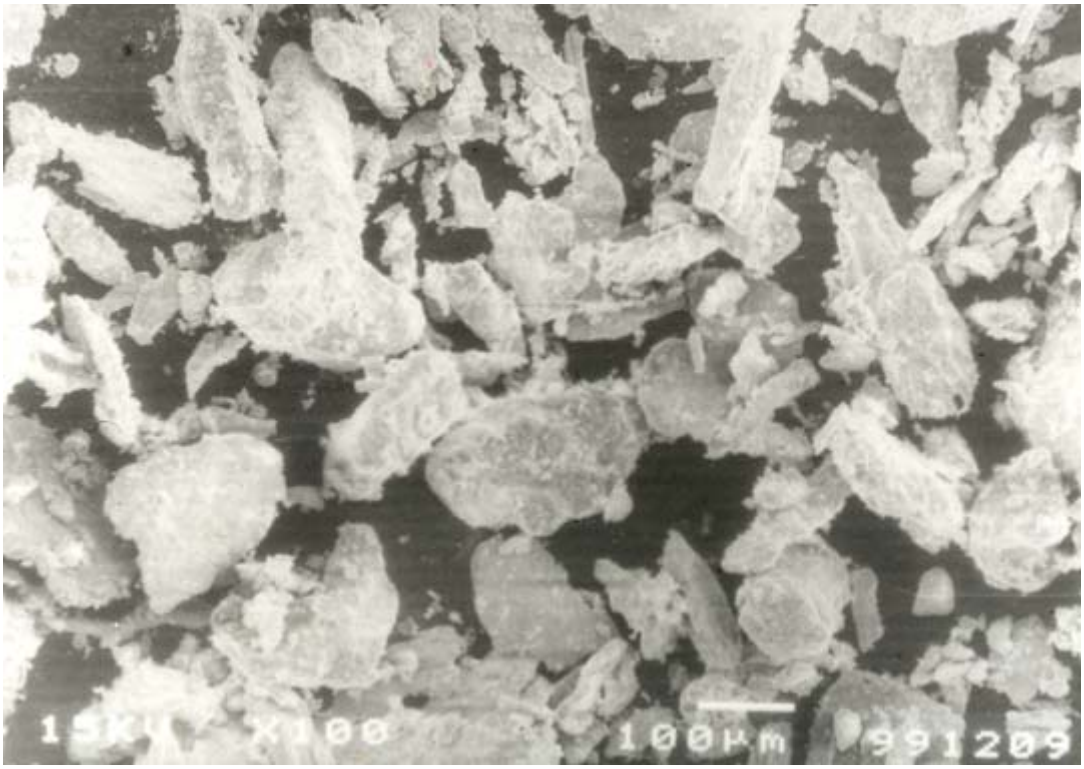

Fig. 4.16(a) Surface morphology (SEM micrograph) of Fe-Al powers, after ball milling.

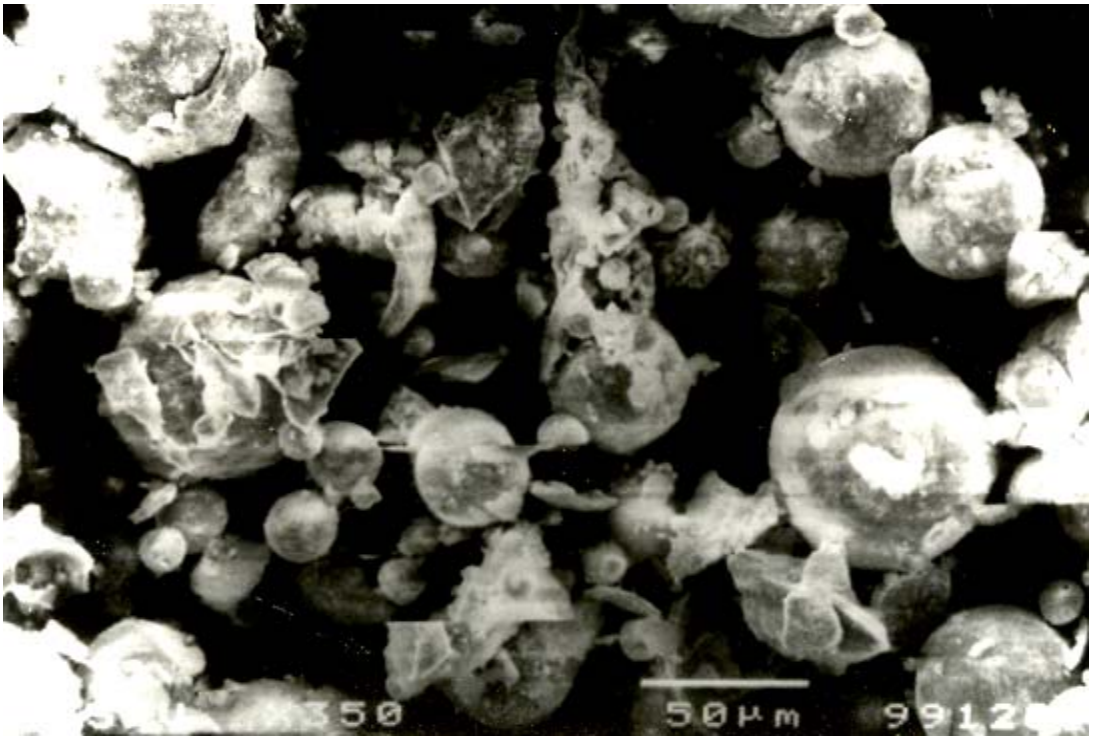

Fig. 4.16(b) Surface morphology (SEM micrograph) of Fe-Al spheroidised powders, processed at 10kW power level,100mm TBD.

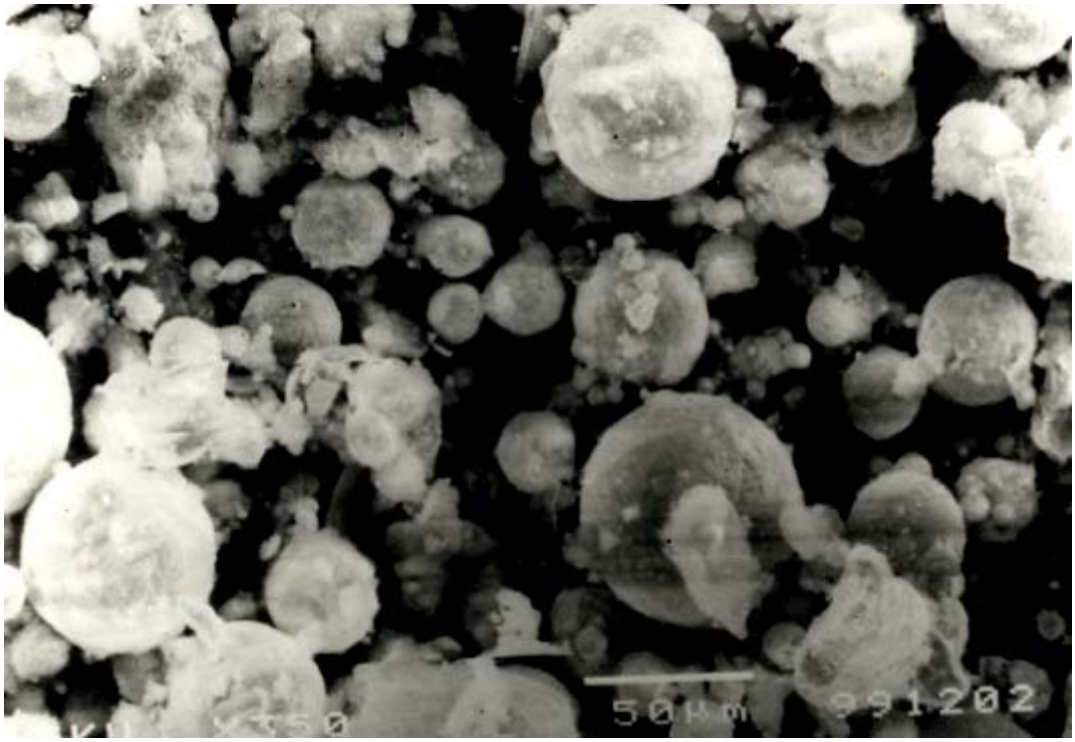

Fig. 4.16(c) Surface morphology (SEM micrograph) of Fe-Al spheroidised powders, processed at 10kW power level, 400mm TBD.

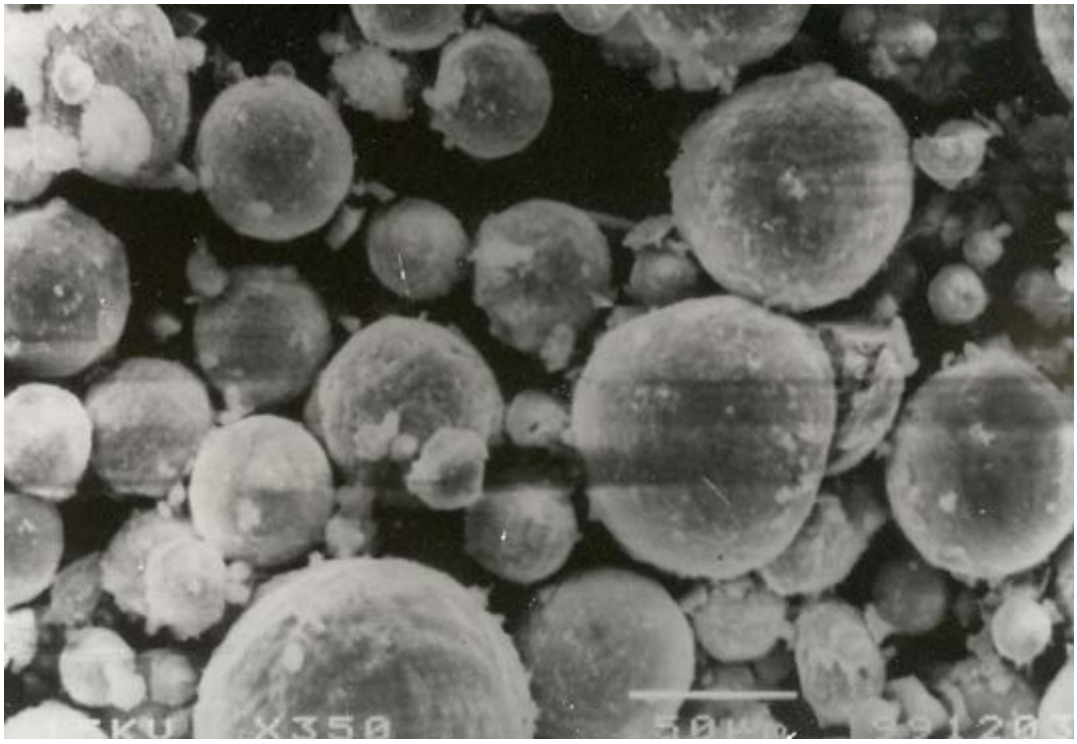

Fig. 4.16(d) Surface morphology (SEM micrograph) of Fe-Al spheroidised powders, processed at 16kW power level, 100mm TBD.

unmelted powder particles. When the standoff distance increased to 400mm, it exhibits a different morphology as shown in Figure 4.16(c).In this case almost all the particles are spherical in shape with varying diameters i.e. from ~ 20 μm to ~ 50 μm. When the Fe-Al ball milled powder, after being plasma processed at 16kW power, is collected at 100mm and 400mm standoff distances, there is a great change in particle shape and size as observed in the micrographs shown in Figures 4.16(d) and 4.16(e) respectively. Under this condition all the particles have attained spherical shape and appear to be solidified from fully molten state.

The micrograph of the other aluminide i.e. Ni-Al ball milled powder is shown in Figure 4.17(a). The variation in particle shape and size is observed, as it was in previous case, shown in Figure 4.13(a). The micrographs of the Ni-Al mix powders processed at 10kW power and collected separately at 100mm and 400mm standoff distances are shown in Figures 4.17(b) & 4.17(c) respectively. Comparing these two figures, it is envisaged that there is an appreciable change in shape and dimension of the particles. At lower standoff distance (i.e.100mm) although majority particles are of smaller size, but coagulation of particles are observed. Whereas, when collected at a larger standoff distance (i.e. 400mm), most of the particles are spheroidal in shape. The powder collected at 100mm standoff distance with higher magnification [Figure 4.17(d)] shows the tendency of deformation, may be towards increase in size by coagulation or to be fragmented. When Ni-Al mix powders processed at 16kW power and collected at 400mm standoff distance also bears different morphology as shown in figure 4.17(e). As compared to previous micrograph, here there is a great variation in particle size; shape, diameter etc. A particle with higher magnification [Figure 4.17(f)] implies that the surface melting has occurred and also a possibility for segregation. Comparing the micrograph of a particle collected at 100mm standoff distance [Figure 4.17(g)], do represent the crack

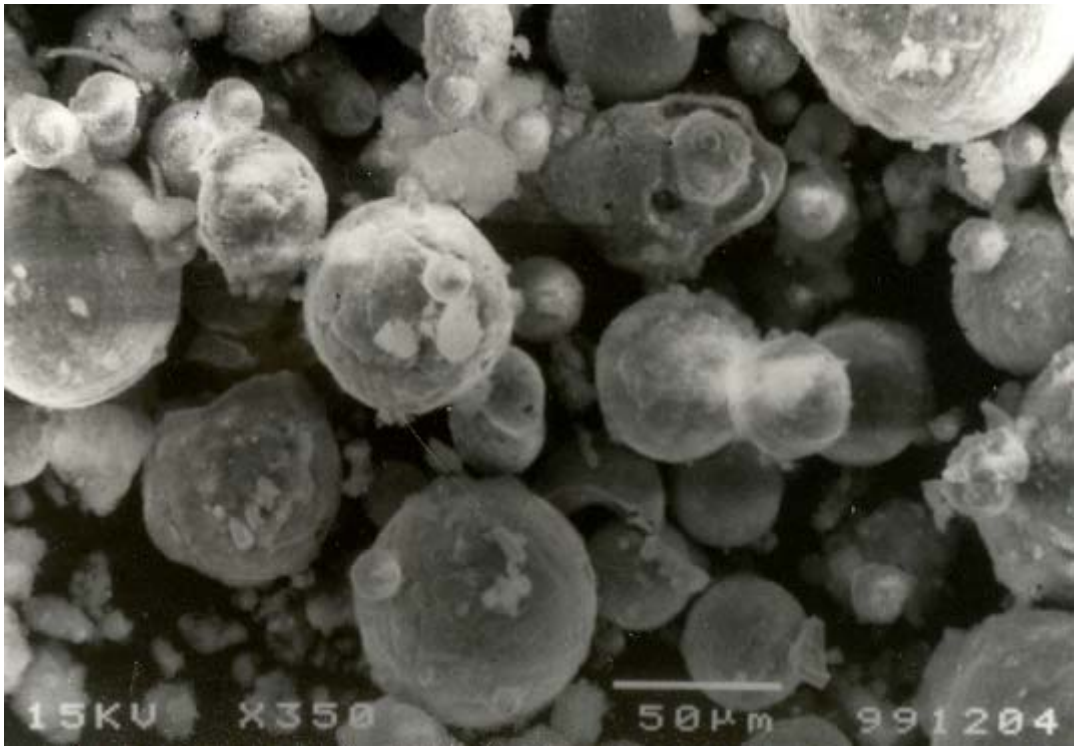

Fig. 4.16(e) Surface morphology (SEM micrograph) of Fe-Al spheroidised powders, processed at 16kW power level, 400mm TBD.

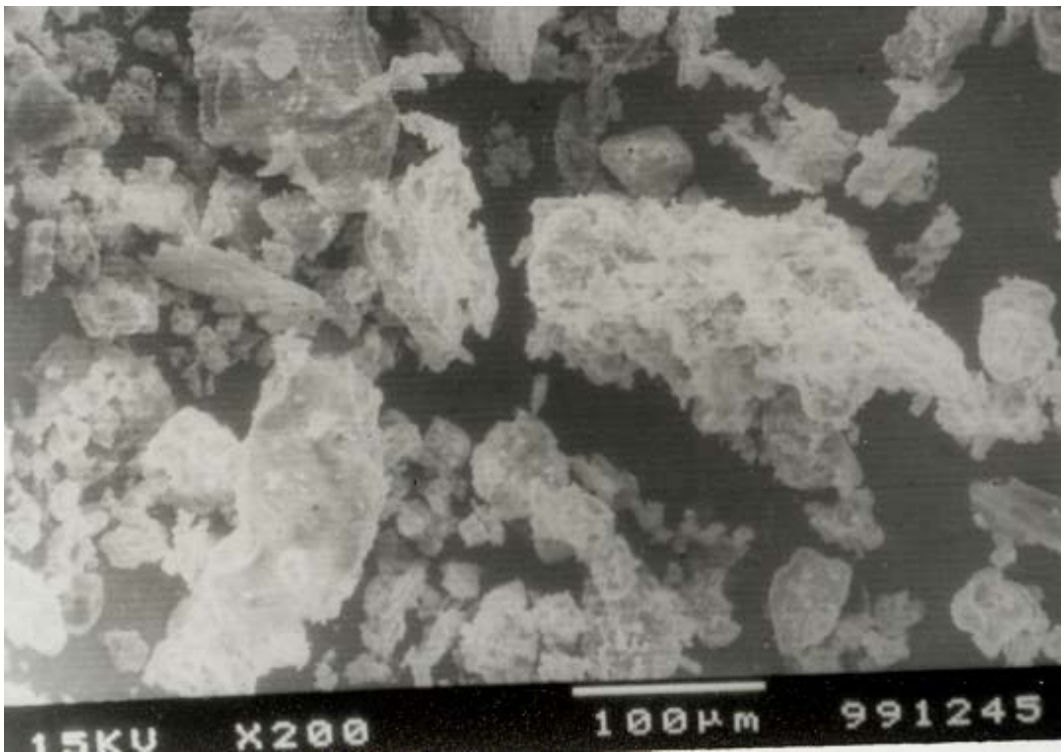

Fig. 4.17(a) Surface morphology (SEM micrograph) of Ni-Al powders, after ball Milling.

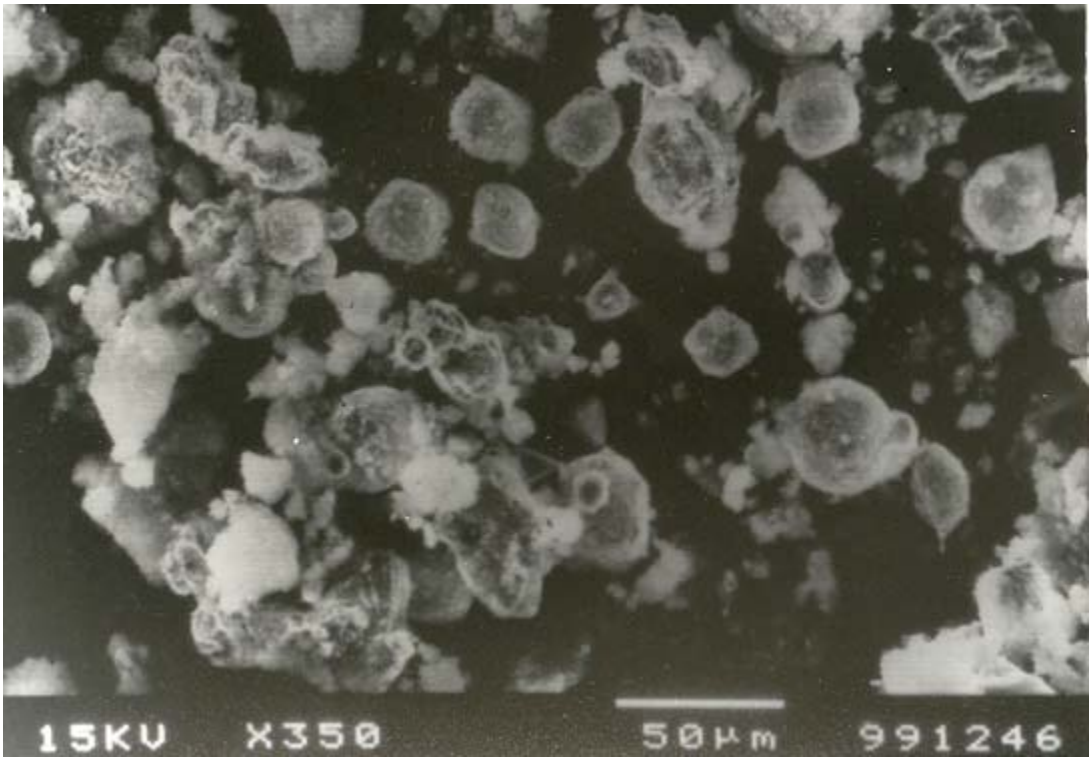

Fig. 4.17(b) Surface morphology (SEM micrograph) of Ni-Al spheroidised powders, Processed at 10kW power level, 100mmTBD.

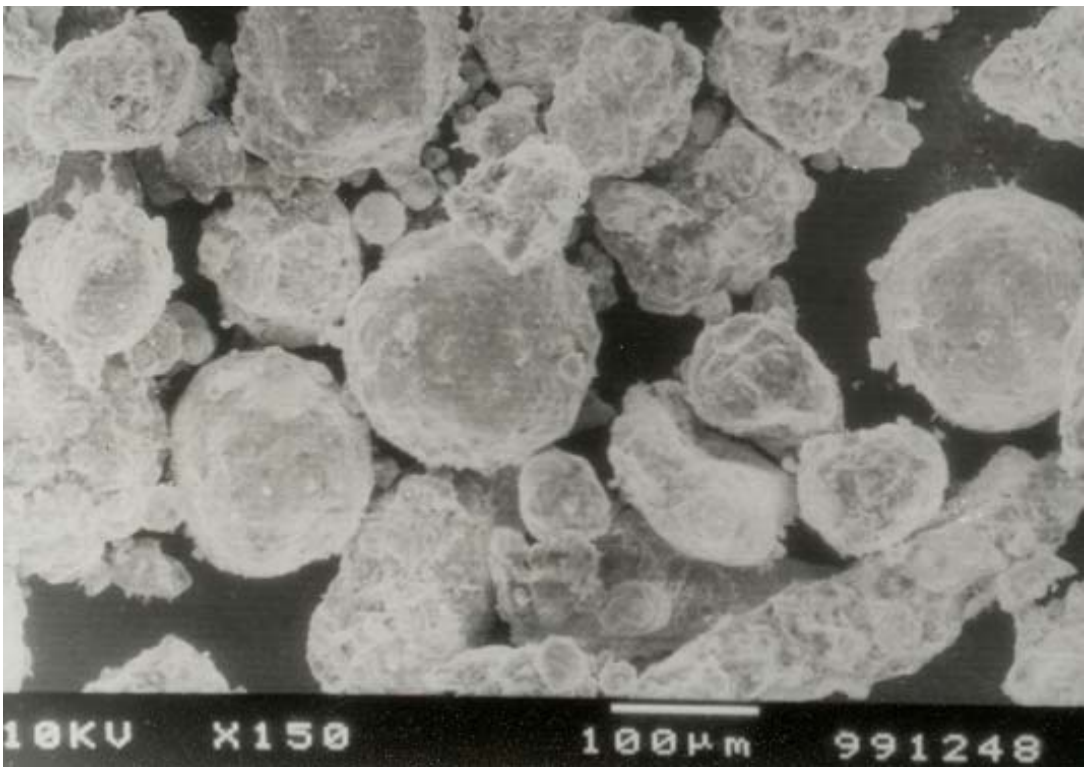

Fig. 4.17(c) Surface morphology (SEM micrograph) of Ni-Al spheroidised powders, processed at 10kW power level, 400mm TBD.

Fig. 4.17(d) Surface morphology (SEM micrograph) of Ni-Al spheroidised powders, processed at 10kW power level, 100mm TBD but with higher magnification(x1, 500).

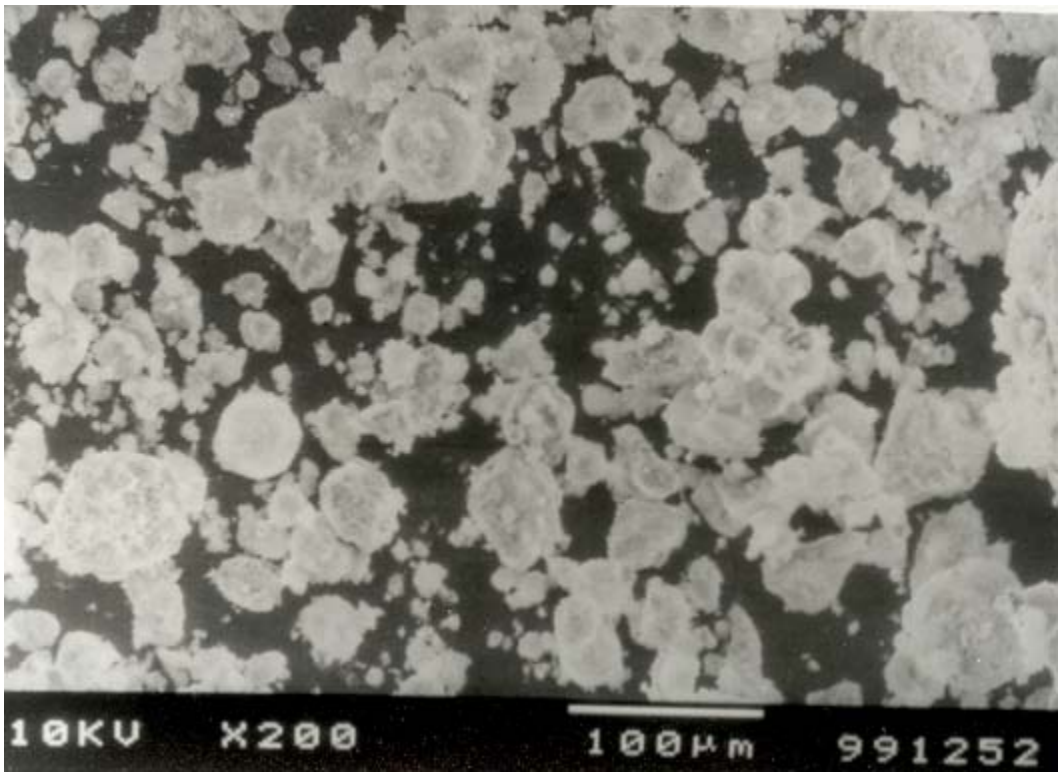

Fig. 4.17(e) Surface morphology (SEM micrograph) of Ni-Al spheroidised powders, processed at 16kW power level, 400mm TBD.

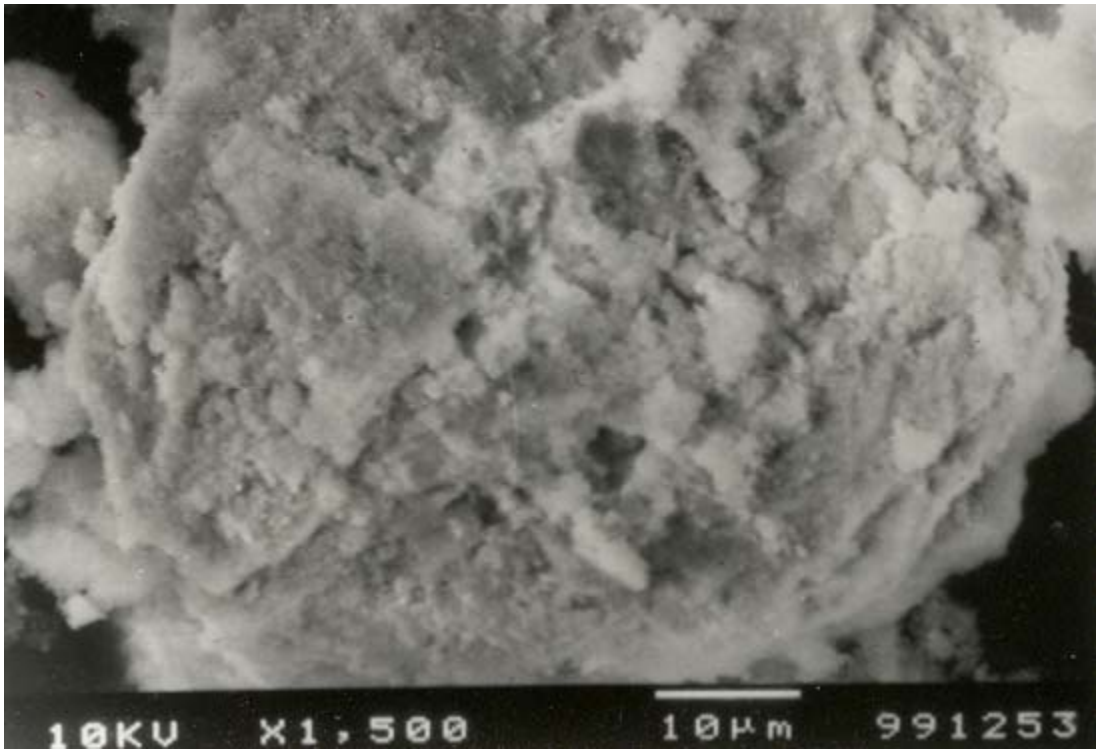

Fig. 4.17(f) Surface morphology (SEM micrograph) of Ni-Al spheroidised powders, processed at 16kW power level, 400mm TBD but with higher magnification(x1, 500).

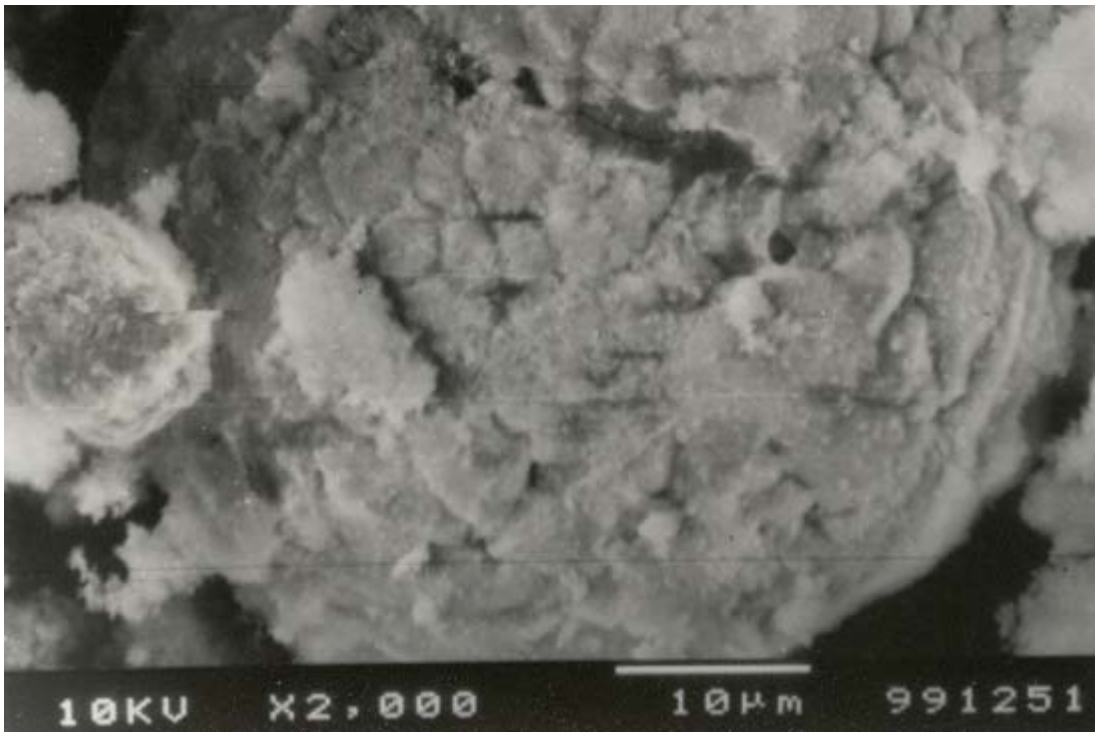

Fig. 4.17(g) Surface morphology (SEM micrograph) of Ni-Al spheroidised powders, processed at 16kW power level, 100mm TBD but with higher magnification.

propagation/origination; which would have subsequently lead to fragmentation of the particle. Different phase constituents are also observed in the micrograph of the particles.

4.6.2 Surface morphology of aluminide bond coats

The surface morphology of Fe-Al bond coat and Ni-Al bond coat are shown in Figure 4.18 and Figure 4.19 respectively.

Comparing Figures 4.18(a) and 4.18(b), it can be visualized that, the coating at 100mm standoff distance and at low power level (10kW) bears higher amount of porosity. With increase in standoff distance to 200mm, although inter particle bonding has enhanced but porosity is affected adversely. The surface morphology of the coating deposited at 16kW, with a standoff distance of 200mm (fig.4.18c) exhibits smaller particle dimension, homogeneity of particles but with localized cavitation.

The surface morphologies of Ni-Al bond coat deposited at 16kW power with different standoff distances namely, 100mm, 200mm and 400mm are shown in Figures 4.19(a), 4.19(b) and 4.19(c) respectively. It can be seen that at lower standoff distance (100mm) the particles are equi-axed type and distributed homogenously. Although some porosity is observed but is less in amount than that of the coating made at 200mm, Figure 4.19(b). When coating is deposited at higher standoff distance,[400mm, Figure 4.19(c)] cavity coalescence and propagation is well remarked. Also the particle phase dimensions are different as compared to the above two figures. From these observations the standoff distance 100mm is selected and preferred for deposition of further coatings.

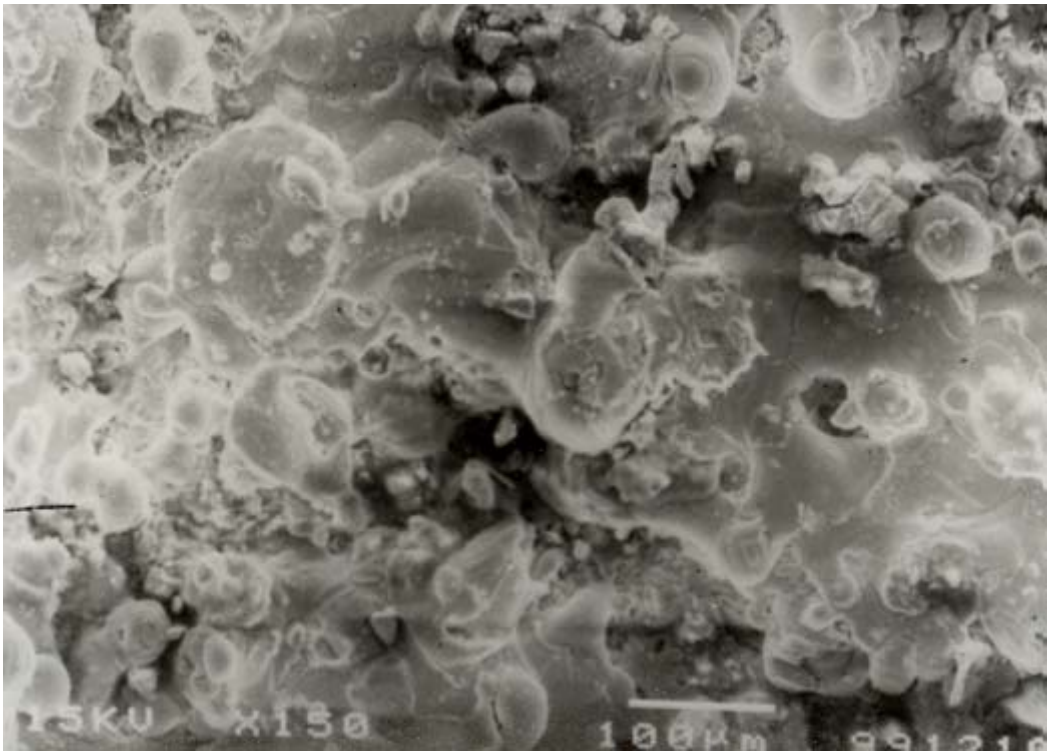

Fig. 4.18(a) Surface morphology (SEM micrograph) of Fe-Al bond coat, deposited at 10kW power level, 100mm TBD.

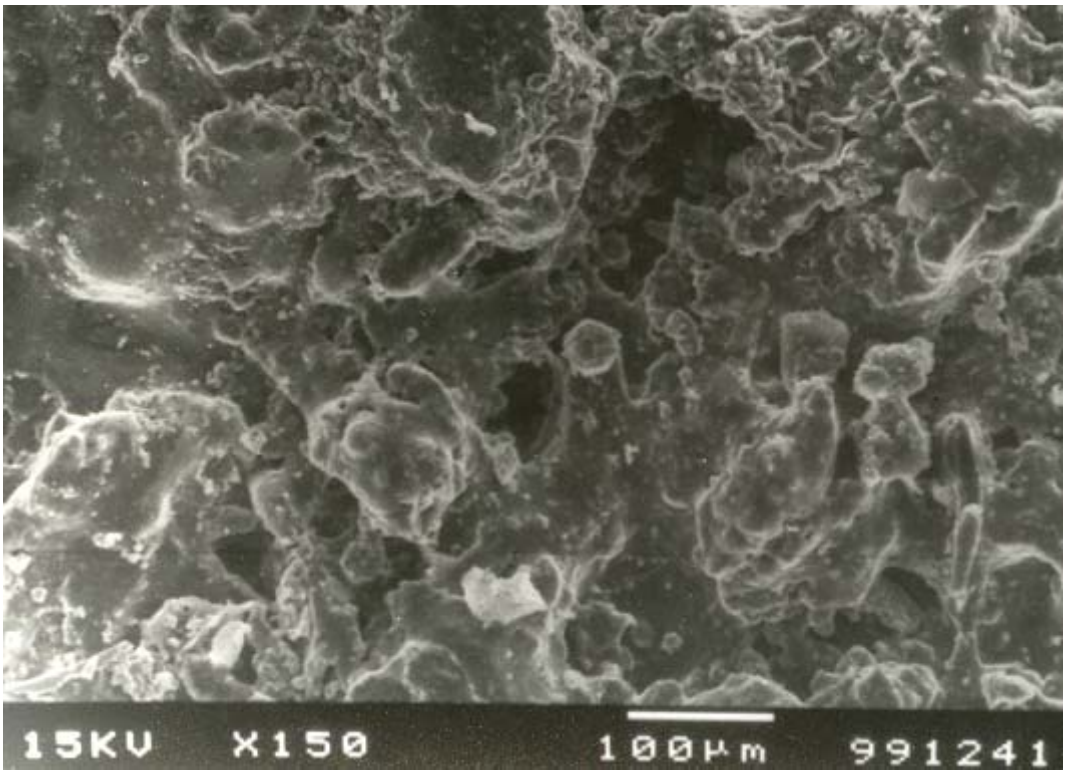

Fig. 4.18(b) Surface morphology (SEM micrograph) of Fe-Al bond coat, deposited at 10kW power level, 200mm TBD.

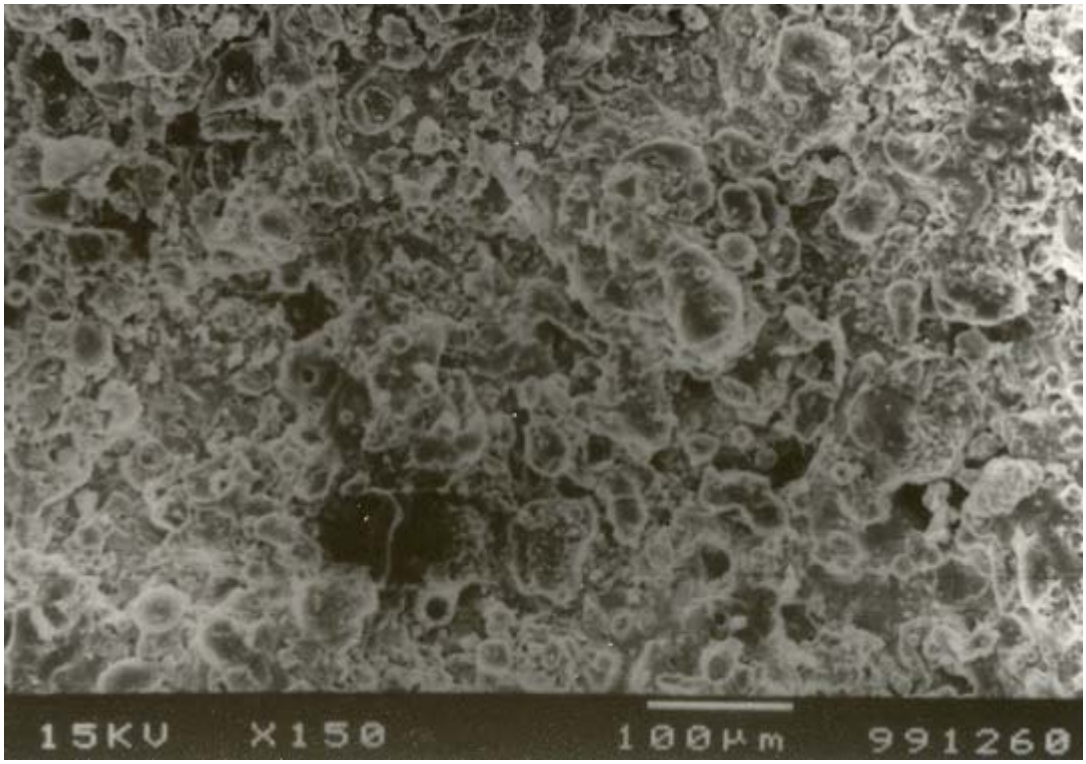

Fig. 4.18(c) Surface morphology (SEM micrograph) of Fe-Al bond coat, deposited at 16kW power level, 200mmTBD.

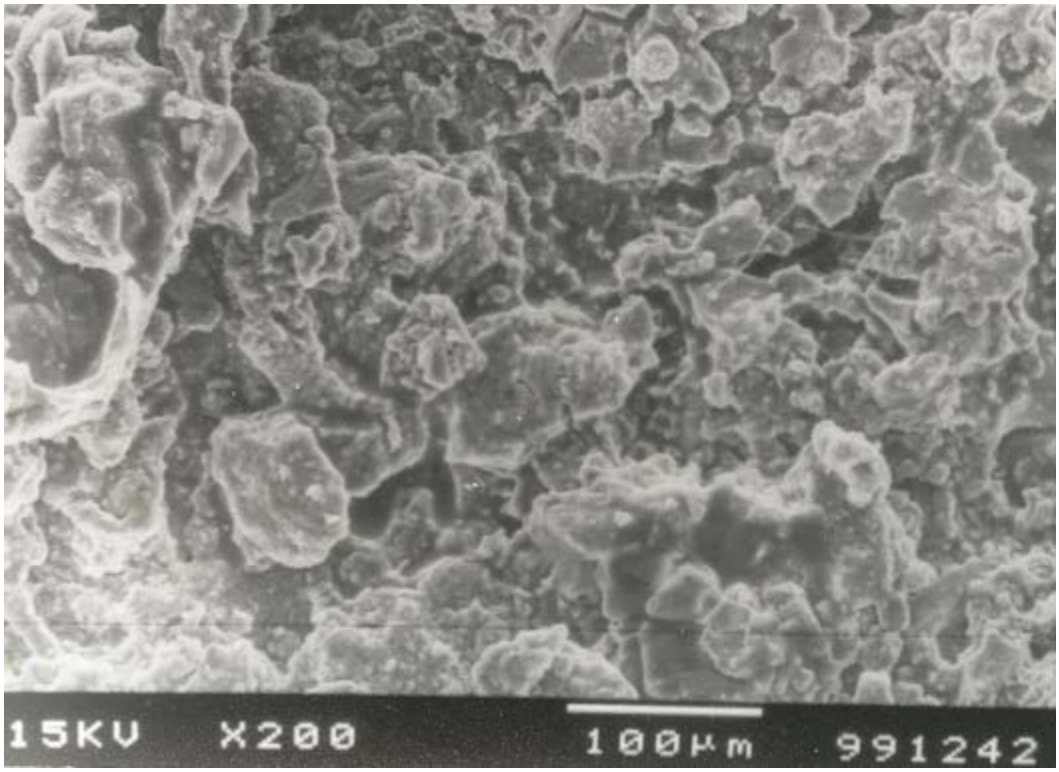

Fig. 4.19(a) Surface morphology (SEM micrograph) of Ni-Al bond coat, deposited at 16kW power level, 100mm TBD.

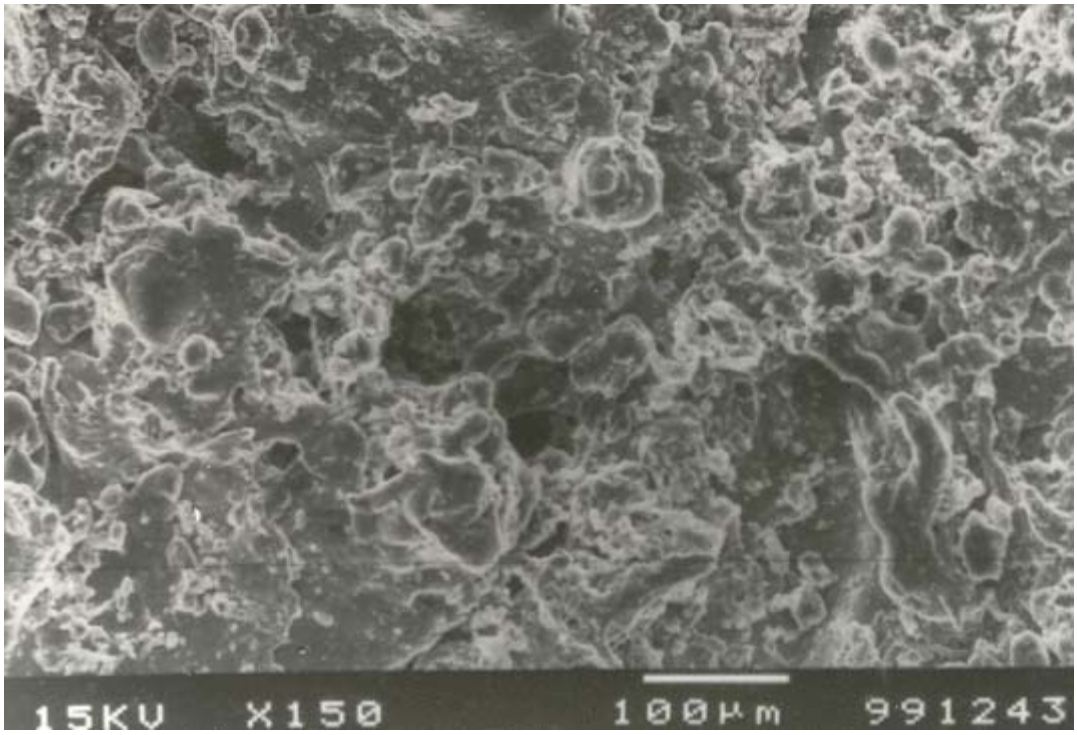

Fig. 4.19(b) Surface morphology (SEM micrograph) of Ni-Al bond coat, deposited at 16kW power level, 200mmTBD.

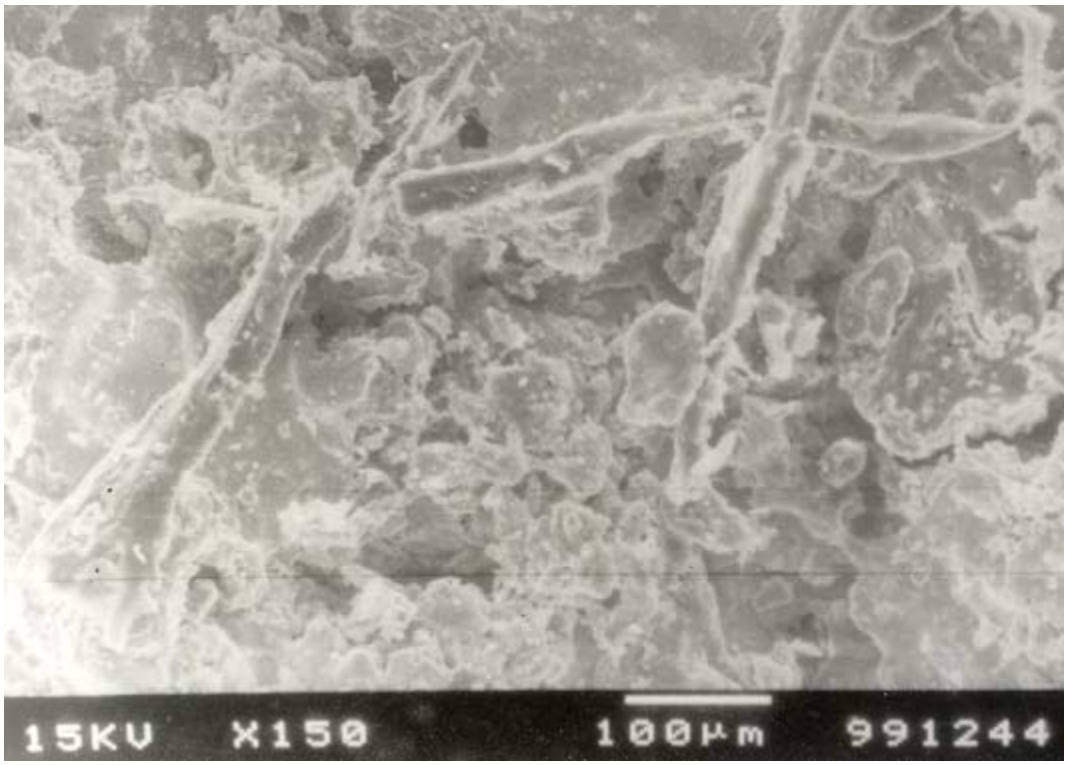

Fig. 4.19(c) Surface morphology (SEM micrograph) of Ni-Al bond coat, deposited at 16kW power level, 400mm TBD.

4.6.3. Interface morphology of the bond coats

The coating substrate interface with Ni+Al bond coat made on Cu and MS substrates are shown in fig.4.20 (a) & (b) respectively. In the bond coat region, the particle /phases are lamellar in shape for both the specimens. But in case of MS substrate the lamellae are joined to form long parallel structural view. This might be due to lower thermal conductivity of MS for which the molten/sprayed particles remain at higher temperature for longer time duration and have joined together to form long platelet type distribution.

The coating substrate interface with Fe+Al bond coat made on Cu and MS substrates are shown in fig.4.21 (a) & (b) respectively. For the coating deposited on MS substrate, the bond coat appears as thick layers joined together with some voids/porosity in-between them. Whereas, the bond coat is smoother in case of the coating made on Copper substrate. The interface morphology of the alumina coat is also different. These effects are, may be due to the rate of dissipation of heat from the substrate during spray operation. The cooling rate is faster for the substrate having higher thermal conductivity (i.e. Copper), so the particles solidify rapidly and remain smaller in size with less inter-particle diffusion.

4.6.4 Surface morphology of Al_2O_3 top coating

The surface morphology of the Alumina coating deposited at 16kW power level on Fe+Al bond coat and on Ni+Al bond coat are shown in fig.4.22 (a) & (b) respectively. It can be seen that, the coatings are dense but with a difference in particle size. The particles are smaller on Ni+Al bond coat than that of Fe+Al bond coat. This might be due to initial particle size of the sprayed powder and thermal conductivity of the bond coat.

Fig. 4.20(a) Coating interface of (alumina) over Ni+Al bond coat on Copper Substrate.

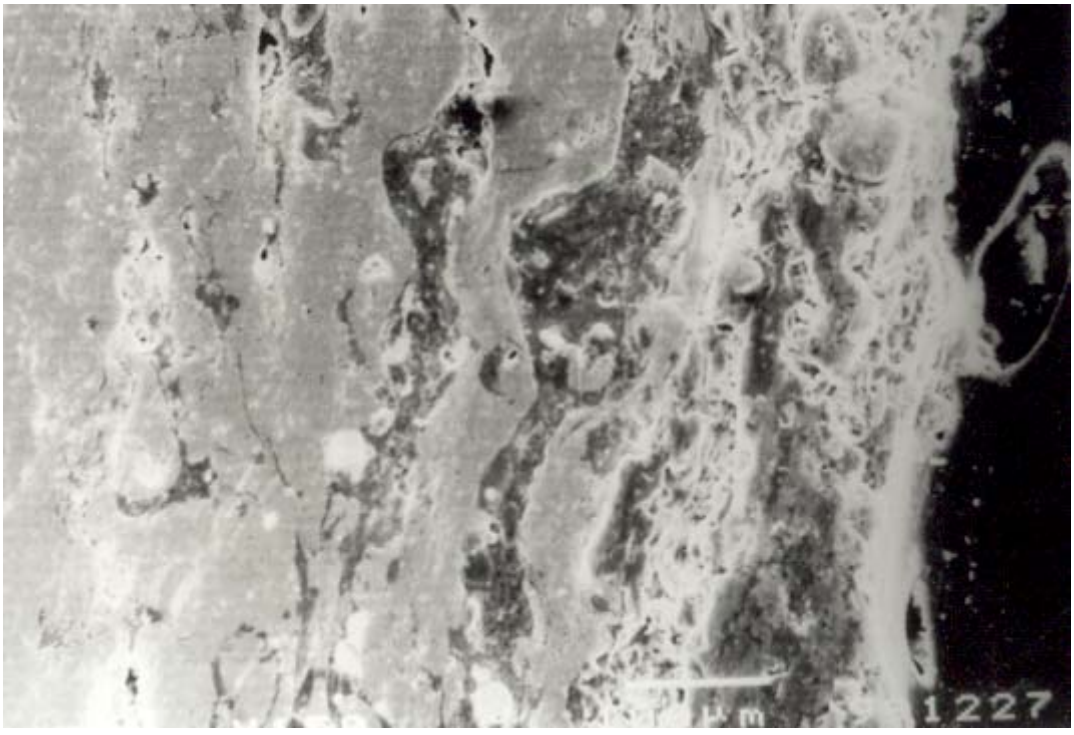

Fig. 4.20(b) Coating interface of (alumina) over Ni+Al bond coat on MS substrate.

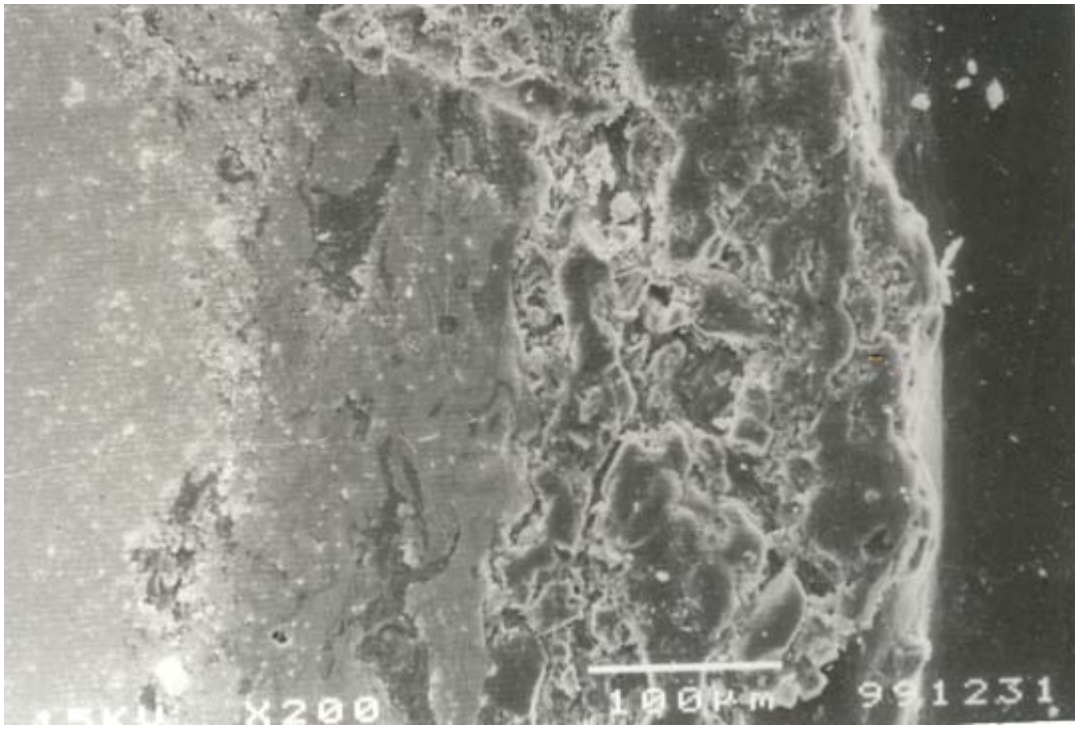

Fig. 4.21(a) Coating interface of (alumina) over Fe+Al bond coat on Copper substrate.

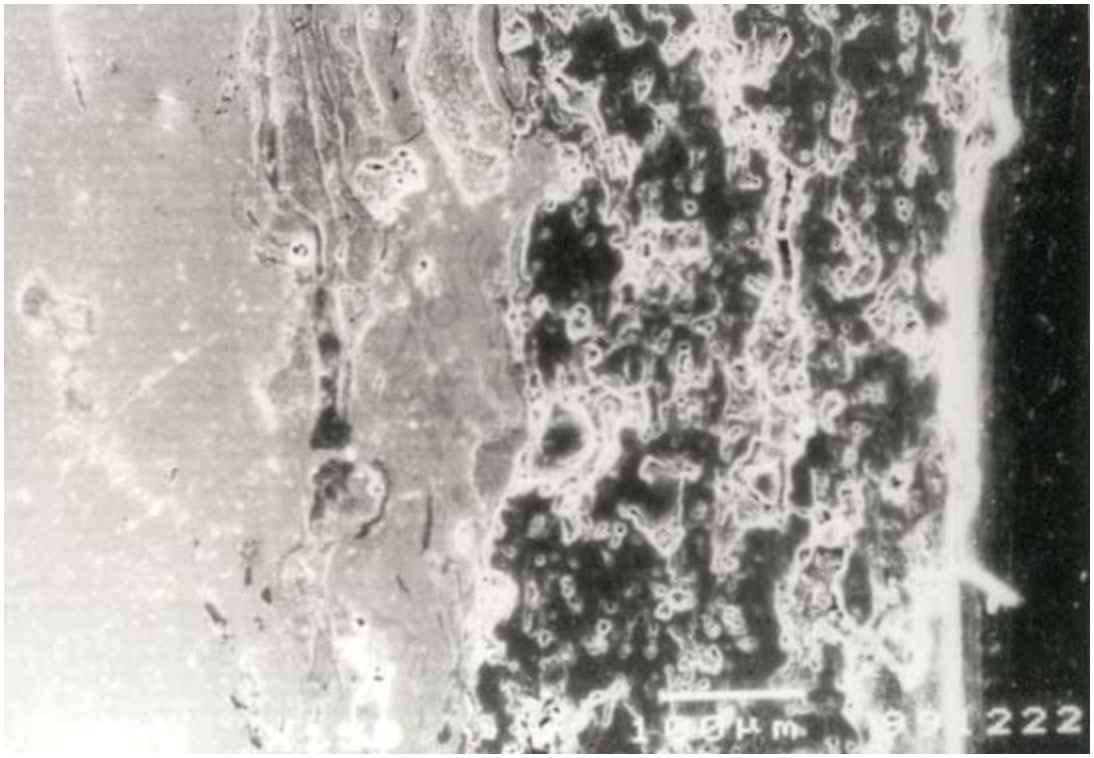

Fig. 4.21(b) Coating interface of (alumina) over Fe+Al bond coat on MS substrate.

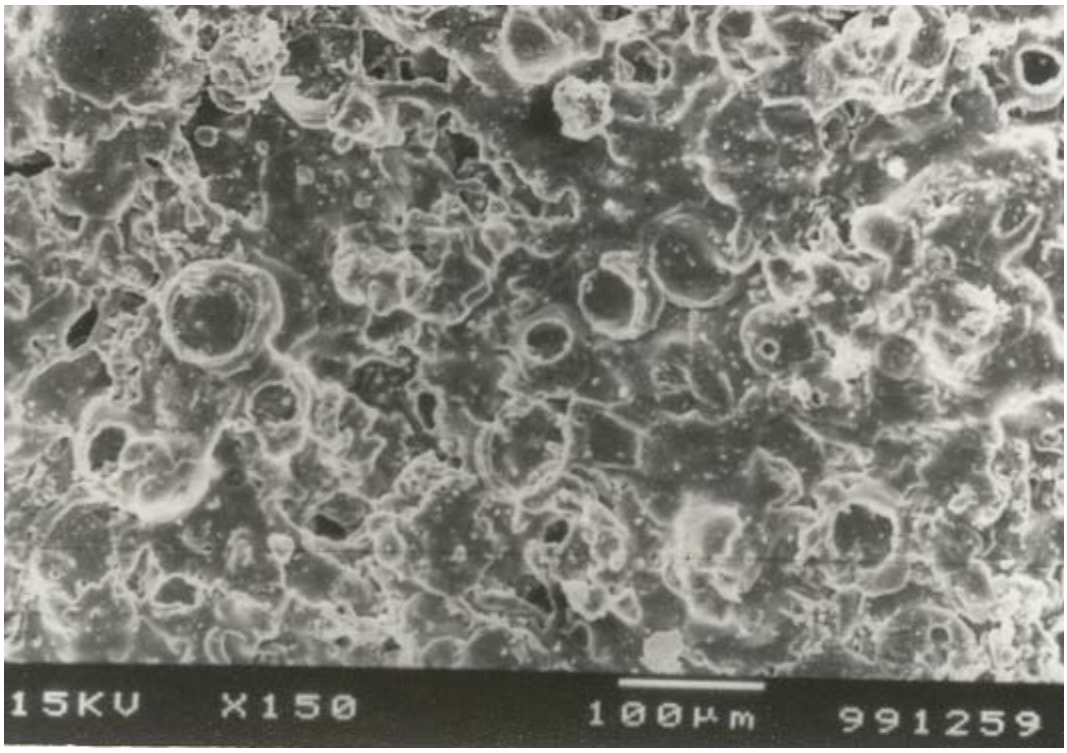

Fig. 4.22(a) Coating morphology of alumina over (Fe+Al) bond coat.

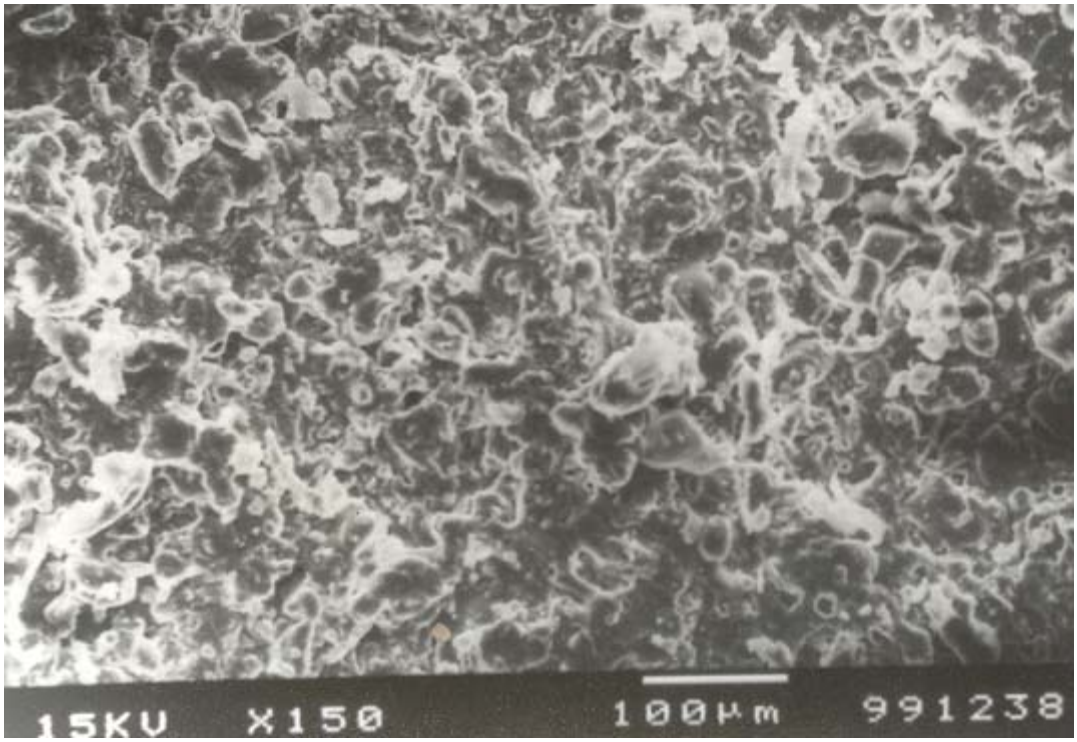

Fig. 4.22(b) Coating morphology of alumina over (Ni+Al) bond coat.

4.7 COATING POROSITY

Porosity measurement was done using the image analysis technique. The polished interfaces of various coatings were studied under optical microscope (Neomate) equipped with a CCD camera (JVC, TK 870E). From the digitized image obtained by this system, coating porosity was determined using VOIS image analysis software. The results are shown in fig.4.23. It is observed that porosity volume fraction of these coatings lie in the range of 3 to 6 % for Fe-Al, 3 to 5 % for Ni-Al and 9 to 14 % for Alumina. The amount of porosity is more in the case of coatings made at lower (10kW) and at higher (20kW) power levels. However; porosity is minimum at 16kW power for all coatings made under this study. It may be mentioned that in the conventional plasma sprayed ceramic coatings, porosity of about 3 – 10 % is generally observed [6]. Thus the values obtained in the coatings under study are found similar with previous observations.

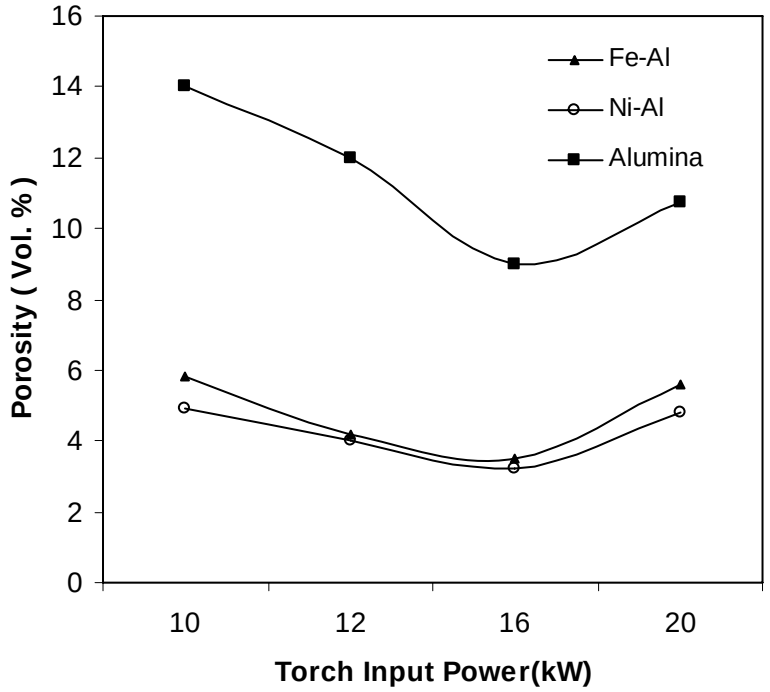

Fig. 4.23 Coating Porosity of Alumina & Aluminides Vs Power.

4.8 DISCUSSION

Thermal spraying is a highly complex deposition process with a large number of interrelated variables. Due to the high velocity and temperature gradients in the plasma plume, even small changes in the controllable or uncontrollable parameters can result in significant changes in the particle properties and thus in the microstructure of the coatings [7,8].

The adherence of the coating to the substrate is of major concern. The bonding mechanism operative between the coating and substrate can be classified into three categories: mechanical, physical and chemical. The molten particles striking a roughened surface conform to the surface topography. The mechanical interlocking between the coating and the protrusions on the substrate surface is termed mechanical adherence. Substrate-coating adherence by Vander-walls force is classified as physical bonding.

In majority of the situations encountered, adhesion is physical bonding of the coating to the substrate. The formation of an inter-diffusion zone or an intermediate compound between the coating and substrate is generally termed as chemical or metallurgical bonding. The specific mechanism operative between a coating and substrate depends primarily on the materials used and the physical condition of these material particles on impact.

In the present investigation it is noted that, invariably in all cases the interface bond strength increases with the input power of the torch up to a certain power level and then with further increase in torch input power does not improve the adhesion strength.

Variation of adhesion strength with TBD and input power to the plasma torch can be explained in terms of the thermal state of the particles as they strike the surface of the substrate. At lower power level, the plasma gas

temperature is not high enough to effect complete melting of all the particles entering the plasma jet. This results in partial melting of larger particles. It may also be possible that unmelted particles get embedded within the molten ones. This naturally leads to poor coating adhesion. When the input power to the plasma torch is increased, the average plasma temperature and heat transfer coefficient of the plasma increases, leading to complete melting of a large fraction of the injected powder particles. Therefore, there is better splashing and mechanical inter-locking of molten particles on the substrate surface leading to increase in adhesion strength. Thiyagarajan et al [9] has computed the temperature of the plasma at the nozzle exit for different input power to the plasma torch. The results are summarized in Table 4.4.It can be seen that as the input power increases, the plasma temperature at the nozzle exit as well as the mean flame temperature increases confirming the observed increase in adhesion strength. However, at much higher power level, the amount of fragmentation and vaporization of the particles increase.

The vapors and gaseous species of dissociated products can get entrapped in the coating and affect the porosity of the coatings. This can lead to a decrease in the adhesion value.

Table 4.4 Mean plasma temperature of Ar-N_2 plasma at nozzle exit for different operating power [9].

Input power (kW)	Plasma Temp. (K) at nozzle exit
8	**5939**
10	**6358**
12	**6678**
16	**9446**

The effect of coating adhesion on the torch-to-base distance (TBD) shows that adhesion decreases with increasing TBD. This is because as the TBD increases, the particle velocity and temperature decrease. The typical

velocity profile for alumina particles of different size, computed by Thiyagarajan et al [9] are shown in Figure 4.24. It is seen that the particle velocity increases with axial distance from the torch nozzle reaching a maximum and then falls off. A similar trend is also observed in the case of particle temperature. This has a direct bearing on the coating adhesion. At larger TBDs, the particles strike the substrate surface with lower velocities. This will result in lesser degree of flattening of the molten droplets and consequently the adhesion values decrease. Further, the particle temperature is also lower at larger distances from the nozzle a substantial fraction of the injected powder particles may solidify as they strike the substrate. This can result in inclusions of unmelted particles, which adversely affect the adhesion strength.

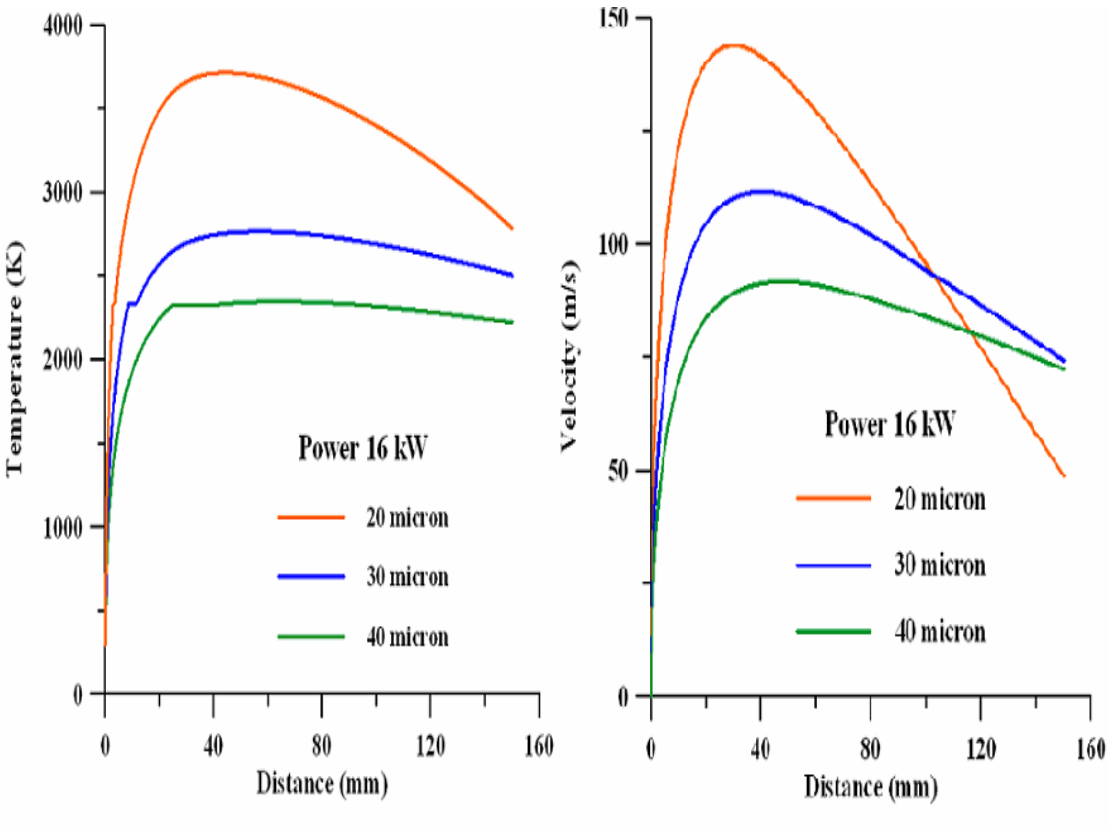

Fig.4.24 Temperature and Velocity Profile of alumina Particles in Plasma flame

The investigation on interface bond strength in case of ceramic coatings deposited with premixed metal powder was carried out by Lima et.al. [10] and Mishra et.al. [11].They has also reported an increase in coating adhesion strength of ceramics premixed with metal powders. Thus, the finding in the present study (i.e. greater adhesion strength of alumina along with the aluminides) is in concurrence with the study made by the above authors.

Bronco et.al. [12] reported that, the coating porosity influences the coating properties in three ways. Firstly it reduces the material strength against plastic deformation or chipping since the material at the edge of a void lacks mechanical support. Secondly, the concave surface inside a void that is not under the shadow of some void edge will see an impinging particle at an angle higher than the average target surface to impact angle (which is detrimental for brittle materials). And finally, pores can also impair strength by acting as stress concentrators and/or decreasing the load bearing surface.

The growth of voids along the oxide-metal interface during high temperature oxidation of simple aluminides (i.e.β-NiAl) and other intermetallics is a known mechanism for scale failure [13-15]. Hence, the coatings deposited at the higher and lower power levels are also due to microstructural conditions i.e. size, shape and distribution of particle phases, porosity/void etc. do attribute to the adhesion strength.

A thermal spray coating is built up and a microstructure is formed, when the individual (fully or partially molten) particles, traveling at a particular velocity, flatten, adhere and solidify on impact with the substrate [16, 17]. It has been reported that porosity is affected by the surface roughness of substrate, spray distance, substrate temperature and coating thickness [18]. Investigations also reveal that, the porosity and the surface roughness of coatings (as the characteristic of plasma spray process) are enhanced with the increasing surface roughness of substrate material and coating hardness is also

reduced relatively [19]. At shorter and longer spray distance, the particles remain unmelted or partially melted and surface roughness and porosity increases [20, 21]. Previous investigations also suggest that, the thicker topcoat is mechanically weakened with increasing pores and residual stresses. The higher hardness, lower porosity and lower surface roughness can be obtained at lower coating thickness. The increase of the porosity, results in decrease of the hardness of the coating [18-25].

Hence, in the present investigation the variation of coating properties are well supported by previous research evidences.

References

1. H.Chen,S.W.Lee,Hao Du,Chuan X Ding and Chul Ho Dho ; Materials Letter Vol.58, Issues 7-8,March **2004** pp.1241-1245,Influence of feed stock & spraying parameters on the dep.eff.and microhardness of plasma sprayed zirconia coatings.
2. G.Lalleman – Tallaron, Study of microstructure and adhesion of spinelles coatings formed by plasma spraying, Ph.D. Thesis No.96-58 (**1996**) E.C.Lyon, France.
3. J.L.Smialek and B.K.Tubbs.Metall.Trans.A.26A (**1995**), p. 427.
4. H.J.Grabke,G.Kurabtov and H.J.Schumtzler.Oxid.Met.43 (1/2)(**1995**),p. 97.
5. O.Sarikaya, Materials and design 26, **2005**, 53-57.
6. Lech Pawlowski – The Science and Engineering of Thermal Spray Coatings, JohnWiley & Sons, New York (**1995**) pp.218.
7. S. Sampath, Mater. Sci. Eng. A 167 (**1993**) 1.
8. R. Westergard, L.C. Erickson, N. Axen, H.M. Hawthorne, S. Hogmark, Tribol. Int. 31 (5) (**1998**) 271.

9. P.V. A. Padmanabhan, T.K.Thiyagarajan, K.P.Sreekumar, N.Venkatramani; Scripta Materialia, 50, **2004**, 143-147.
10. C.R.C.Lima, R.E.Trevisan, J.Thermal sprays Tech.62, **1997**, p.199.
11. S.C.Mishra,K.C.Rout,P.V.Ananthapadmanabhan and B.Mills; Plasma spray coating of fly ash premixed with Aluminum powder deposited on metal substrates,J.Material Processing Technology **2000**,102,1-3,pp.9-13.
12. Jose Roberto Tavares Branco,Robert Gansert,Sanjay Sampath,Christopher C.Berndt,Herbert Herman-Solid Particle Erosion of Plasma sprayed Ceramic Coatings- materials Research,Vol.7.No.1.147-153,**2004**
13. B.A.Pint. Oxid.Met. 48(**1977**),p.303
14. J.L.Smialek.Metall.Trans. 9A (**1978**), p.309.
15. M.W.Brumm and H,J.Grabke.Corr.Sci.34 (**1993**), p. 54
16. M. Friis, C. Persson, J. Wigren, Surf. Coat. Technol. 141 (**2001**) 115.
17. J. Matejicek, S. Sampath, Acta Mater. 49 (**2001**) 1993.
18. H.M. Choi, B.S. Kang, W.K. Choi, D.G. Choi, J. Mater. Sci. 33(**1998**)5895.
19. E. Celik, A.S. Demirkan, E. Avci, Surf. Coat. Technol. 116 – 119(**1999**) 1061.
20. T.J. Steeper, A.J. Rotolico, J.E. Nerz, Optimizing plasma sprayed alumina-titania coatings using statistical methods, Proceedings of the 1993 National Thermal Spray Conferance, Anaheim, CA, 7– 11, June **1993**.
21. Y. Li, K.A. Khor, Surf. Coat. Technol. 150 (**2002**) 125.
22. S. Sampath, X. Jiang, A. Kulkarni, J. Matejicek, D.L. Gilmore, R.A. Neiser, Mater. Sci. Eng. A A348 (**2003**) 54.
23. S. Sampath, X. Jiang, J. Matejicek, A.C. Leger, A. Vardelle, Mater. Sci. Eng. A A272 (**1999**) 181.
24. M.H. Staia, T. Valente, C. Bartuli, D.B. Lewis, Surf. Coat. Techno. 146–147 (**2001**) 563.

25. Kucuk, C.C. Berndt, U. Senturk, R.S. Lima, Mater. Sci. Eng. A 284 (**2000**) 41.

*****

Chapter 5

Conclusions

- Conclusions
- Scope for Future Work

Chapter V

CONCLUSIONS

5.1 CONCLUSIONS

From the present research work, the following conclusions are drawn.

- Alumina coatings are deposited on metal substrates with an intermediate bond coat of iron and nickel aluminides and these bond coatings exhibit desirable coating characteristics viz. adhesion strength etc.

- During plasma spray deposition, formation of aluminide phases of iron and nickel are observed. Maximum adhesion strength of ~ 40MPa is obtained in case of iron aluminide bond coat on copper substrate deposited at 16kW power level.

- The adhesion strength of iron aluminide bond coat is higher than that of the bond coat made with nickel aluminide. Also, the adhesion strength of alumina coating is found to be higher when iron aluminide bond coat is used.

- The adhesion strength of coatings is dependent on torch to substrate distance.

- The spherodisation studies on Fe + Al and Ni + Al powders clearly indicate the morphological changes on the particles. Almost all the particles attained molten state (at about 16kW power level), hence strongly adhere on impacting the substrate. Whereas at higher power

level, i.e. at ~20kW, partially cracked/ fragmented particles which give rise to more amount of void / porosity resulting lower adherence strength of the coating.

- Maximum deposition efficiency of ~60%, ~54% and of ~46% is observed in case of Fe + Al powder, Ni + Al powder and of alumina coating depositions respectively. So the bond coat with Fe + Al powder appears to be more suitable than that of bond coat made with Ni + Al powder for deposition of Al_2O_3 top coat on metals.

- The different aluminide phases observed in XRD studies corroborates to the observation of different hardness values for different optically distinguished phases.

- The microstructures of the coatings are dependent on operating power level of the plasma torch, the physical characteristics such as coating porosity, phase formation in the raw material during spraying and also the torch to substrate distance.

5.2 SCOPE FOR FUTURE WORK

The variation of amount of aluminide phases with operating power level is to be studied to find out the suitability of any particular phases of the aluminides if is responsible for increase in interface bonding of aluminides with a ceramic top coat. Addition of other alloying elements with Fe+Al and Ni+Al powder for deposition of bond coat to produce higher interface bond strength may be studied.

*****

Appendix

LIST OF PUBLICATIONS

1 **Thermal Plasma Processing of Nickel and Iron Aluminides–** S.Das, S.C.Mishra, P.V.Ananthapadmanabhan, K.P.Sreekumar, P.V.Ravindran – Power Beams and Materials Processing, published by Allied publishers Ltd., Mumbai, 2002, pp.702-705**.**

2 **Processing and Characterization of Al_2O_3-TiO_2 Coatings on steel -** S.C.Mishra, R.Mishra, K.R.Sriraman, S.Mishra, S.Das, K.P.Sreekumar, R.U.Satpute, P.V.A.Padmanabhan - Proceedings of DAE-BRNS National Symposium on Applications of Plasma, Lasers and Electron Beams in Advanced Materials Processing, Bhabha Atomic Research Centre, Mumbai; published by Allied publishers Ltd., Mumbai, 2002, pp.706-708**.**

3 **Study of Iron-Aluminide Deposition using Neural Computation –** Rojaleena Das, M.Chaithanya, S.Das, Anupama Sahu, A.Satapathy, S.C.Mishra, S.Naga Mahendra Babu, P.V.A.Padmanabhan, K.P.Shreekumar – National Symposium on Plasma Science & Technology, Malaviya National Institute of Technology, Jaipur;2006,pp141.

4 **Neural Network Analysis for Deposition of Nickel-Aluminide Coating on Steel by Plasma Spraying –** M.Chaithanya, Rojaleena Das, S.Das, Anupama Sahu, A.Satapathy, S.C.Mishra, P.V.A.Padmanabhan, K.P.Shreekumar – National Symposium on Plasma Science & Technology, Malaviya National Institute of Technology, Jaipur;2006,pp141-142.

5 **Thermal Plasma Processed Aluminides –** S.Das, S.C.Mishra, P.V.Ananthapadmanabhan, K.P.Sreekumar, P.V.Ravindran - Proceedings of the National conference on Developments in composites (Advanced, Infrastructural, Natural and Nano composites) National Institute of Technology,Rourkela;2007,pp 186-191.

6 **Microscopic Study and Erosion wear behaviour of Plasma Sprayed Iron-Aluminide Coatings -** Rojaleena Das, Anupama Sahu, S.Das, A.Satapathy, S.C.Mishra, P.V.A.Padmanabhan, K.P.Shreekumar – Proceedings of the National conference on Developments in composites (Advanced, Infrastructural, Natural and Nano composites) National Institute of Technology,Rourkela;2007,pp 102-111.

*****